Faculdade de Engenharia da Universidade do Porto

Immobilization of an antibiotic on a bone mimetic scaffold

Joana Sofia Almeida Dias

Dissertation for the Degree of Master in Bioengineering

Supervisor: Fernando Mendes Monteiro (INEB|i3S, Biocomposites group)

Co-supervisor: Susana R. Sousa (INEB|i3S, Biocomposites group)

September 2019

Abstract

Osteomyelitis is a bone infection caused by infecting microorganisms, that affects bone homeostasis. *Staphylococcus aureus* is the microorganism most frequently involved in most types of osteomyelitis. The standard treatment for osteomyelitis includes debridement of infected bone, systemic administration of antibiotics, to avoid post-operative infection, and subsequent bone reconstruction. Vancomycin is a common antibiotic used for the treatment of chronic osteomyelitis, but other antibiotics as gentamicin and tobramycin are also being used. The systemic route of administration is sometimes ineffective, demands monitoring of drug concentrations in serum to keep nontoxic levels and can be associated with severe side effects. A local controlled release of drugs is a viable alternative, with the use of antibiotic-impregnated bone void fillers, that also induce bone regeneration. Following the results obtained within the research group, the present work focused on making vancomycin available at the surface of the scaffold in a lyophilized manner, with evaluation of the subsequent release kinetics and antibacterial activity. The study also involved the study of gentamicin release and antibacterial activity, as well as the effect of sterilization by gamma radiation on the granules.

Heparinized nanoHA/collagen granules were obtained and after vancomycin adsorption they were lyophilized. Vancomycin release from lyophilized and non-lyophilized granules showed a high initial antibiotic concentration, followed by a sustained release for more than 15 days, always above MIC for methicillin resistant *Staphylococcus aureus* (MRSA). Non-lyophilized granules showed an initial antibiotic release higher than lyophilized, but lyophilized granules were able to release antibiotic for a longer period of time. Gentamicin release showed similar patterns. Also, the antibacterial activity was tested with vancomycin and gentamicin and it showed that both antibiotics could inhibit MRSA growth. Granules morphology and chemical composition were assessed by Scanning Electron Microscopy, Attenuated Total Reflectance Fourier transform infrared spectroscopy and Raman spectroscopy. The results obtained by these techniques showed that both the lyophilization process and the gamma irradiation do not seem to affect the material. Mass spectrometry was applied to lyophilized and non-lyophilized granules to detect the possibility of degradation products, but these were not detected.

Keywords: osteomyelitis, MRSA, vancomycin, gentamicin, hydroxyapatite, collagen, heparin, lyophilization, gamma irradiation

Resumo

A osteomielite é uma infeção óssea provocada por microrganismos que afeta a homeostasia óssea. *Staphylococcus aureus* é o microorganismo mais frequentemente associado a uma grande parte dos diferentes tipos de osteomielite. O tratamento convencional para osteomielite inclui o desbridamento do osso infetado, administração sistémica de antibióticos, e posteriormente a sua reconstrução. A vancomicina é um dos antibióticos mais frequentemente usados no tratamento da osteomielite crónica, assim como, a gentamicina e a tobramicina. A via de administração sistémica de antibiótico é a forma de tratamento convencional para a osteomielite, mas por vezes é ineficaz, e requer uma monitorização cuidada das concentrações séricas do fármaco para manter níveis não tóxicos sob o risco de provocar efeitos secundários graves. A libertação local controlada de fármacos com o uso de *fillers* de cavidades ósseas impregnados com antibióticos é uma alternativa viável, que também permite a indução da regeneração óssea. Seguindo os resultados obtidos dentro do grupo de investigação Biocomposites do INEB, o presente trabalho tem como objetivo a libertação de vancomicina liofilizada da superfície de um scaffold, com consequente avaliação da cinética de libertação e da atividade antimicrobial. O estudo também envolveu o estudo da libertação controlada de gentamicina e a sua atividade antimicrobial, bem como o efeito da esterilização por radiação gama sobre os grânulos.

Foram produzidos grânulos de nanoHA/colagénio heparinizados, procedeu-se à adsorção de vancomicina seguida de liofilização. A libertação de vancomicina de grânulos liofilizados e não-liofilizados mostrou uma elevada concentração inicial de antibióticos, seguida de uma libertação sustentada durante mais de 15 dias, sempre acima do MIC para *Staphylococcus aureus* resistente à meticilina (MRSA). Os grânulos não liofilizados mostraram uma libertação inicial de antibióticos superior aos liofilizados, mas os grânulos liofilizados foram capazes de libertar antibiótico por um período de tempo mais longo. A libertação de gentamicina mostrou resultados semelhantes. Além disso, a atividade antibacteriana foi testada usando vancomicina e gentamicina e ambos os antibióticos foram capazes de inibir o crescimento de MRSA. A morfologia e composição química dos grânulos foi avaliada por Microscopia Eletrónica de Varrimento, Espectroscopia IV por transformada de Fourier com Reflexão Total Atenuada e espectroscopia Raman. Os resultados obtidos por estas técnicas parecem mostrar que, tanto o processo de liofilização como o de esterilização por radiação gama, não parecem afetar o material. Espetrometria de massa foi aplicada em grânulos liofilizados e não liofilizados para deteção de possíveis produtos de degradação da vancomicina, mas estes não foram encontrados.

Keywords: osteomyelitis, MRSA, vancomycin, gentamicin, hydroxyapatite, collagen, heparin, lyophilization, gamma irradiation

Acknowledgements

Com os melhores e mais cordeias cumprimentos, quero agradecer a todas as pessoas que contribuíram para a concretização desta dissertação, do meu percurso académico, e para a etapa em que a minha vida está neste momento.

Primeiramente, quero agradecer aos meus orientadores, ao Professor Doutor Fernando Jorge Monteiro e à professora Doutora Susana Sousa por me terem aceite neste projeto, por todo o acompanhamento e apoio que demonstraram aquando da realização do presente trabalho, e pela paciência, compreensão e prontidão na resolução de todas as adversidades encontradas.

Gostaria de agradecer a todos os elementos do grupo de investigação Biocomposites no qual estive inserida, por toda a ajuda, apoio, dicas, almoços, lanches, cafés e chocolates partilhados que se tornaram indispensáveis para o trabalho desenvolvido. Um especial agradecimento à Tatiana Padrão pela "não obrigação" que teve para comigo, pela paciência, apoio, disponibilidade e autocolantes fofos motivacionais, sem ela não teria sido possível a realização deste trabalho. A todas as pessoas de outros grupos de investigação que chateei, um muito obrigada e espero não ter incomodado muito.

Quero também agradecer a todos os técnicos e pessoas de várias entidades que se mostraram sempre prestáveis e contribuíram para a realização desta dissertação: ao Ricardo Vidal (i3S), que sempre se mostrou disponível para ajudar com as técnicas e equipamentos; ao senhor Carlos por me ter ajudado a resolver o problema do Turrax; à Daniela Silva (CEMUP) por todos os momentos de paciência durante as sessões super interessantes de SEM; e também ao Rui Rocha (CEMUP) porque em sensivelmente 10 minutos comigo foi perspicaz para dizer "És demasiado exigente e perfecionista, mas dá gozo picar contigo porque tu respondes" (definição da minha vida!!); vou ter saudades de dizerem "Já não te vida há algum tempo!" quando só estive duas semanas ausente, por isso obrigada Fátima Fonseca (IBMC), por me ensinares a ser independente no "teu" laboratório (001S1A).

Aos meus pais por sempre me proporcionarem todos os meios para alcançar os meus sonhos, pelo apoio incondicional, por me guiarem na direção correta (sim, fiz bem em não continuar em Anatomia), por todos os momentos de paciência, quando eu não tinha paciência, peço desculpa por ser reles. Obrigada por me ensinarem a dar valor às coisas importantes da vida, sou a pessoa que sou graças a vocês.

Aos meus irmãos, eu sei que sou uma pessoa complicada e não muito afetuosa e carinhosa e que não o demonstro, mas eu gosto muito de vocês, obrigada por sempre me aturarem.

A todos os amigos que a faculdade me deu e se tornaram amigos para a vida, por todas as experiências, ridículas por vezes (se fosse agora, não tornava a invocar o diabo, e não sei se me tornava Aragog). Obrigada às Levianas da Araucária, Filipa Leal, Helena Teixeira e Cláudia Leão, por me acolherem em Vila Real, me acompanharem no percurso na FEUP, pelas casas, histórias e refeições partilhadas. À Filipa, ao Gabriel Lopes e ao Marco Miguel por todas as gargalhadas, palavras sinceras, aleatórias e desprovidas de nexo, pelos almoços, cafés e jantares (que acabam sempre em francesinha). À Filipa (again) por me ter acompanhado em todo o meu percurso, ser a pessoa que me juntou às Levianas, e se tornar ridiculamente importante na minha vida, obrigada por todo o apoio académico e principalmente pessoal e psicológico. À Rita Gouveia por se tornar das pessoas mais importantes que conheci na FEUP, obrigada por todo o apoio que me deste, não só enquanto estive de Erasmus mas durante estes três anos, por todas as saídas tolas e por todas as discussões que espero que não tenhamos mais. E obrigada a todos os colegas, alguns dos quais evoluíram para amigos, que bioengenharia e metalurgia me deu, procrastinar é vida.

Aos amigos Lisboetas que fiz enquanto estive de Erasmus em Pisa, obrigada por todos os momentos partilhados, todos os jantares realizados e visitas feitas. De futuro, espero que ganhemos dinheiro suficiente para não precisarmos de ficar num hostel como o de Roma.

Às Survivors, Joana Lobato Costa e Cláudia Leite, um muito obrigada por 23 anos de existência conjunta, mas principalmente um "Thank you!" e um doggo para a minha BBF Joana Lobato, a paciência não tem limites.

Às Sextas Loucas, chegaram mais tarde, mas não deixam de ser igualmente importantes. "Café este fim de semana ? Sexta ou sábado ?".

E a todos que passaram pela minha vida e acrescentaram, de forma positiva ou negativa, algo para a pessoa que sou hoje, não sou a mesma que fui há 5 minutos atrás e obrigada por isso.

"Success is falling nine times and getting up ten."

Jon Bon Jovi

Index

List of figures

List of tables

Abbreviations and Symbols

3D	3 Dimensions
AIDS	Acquired Immune Deficiency Syndrome
ALP	Alkaline Phosphatase
ATR	Attenuated Total Reflectance
Au	Gold
BMP	Bone Morphogenetic Proteins
$Ca_{10}(PO_4)_6(OH)_2$	Hydroxyapatite
CaP	Calcium-phosphate
CFU	Colony Forming Units
CS	Tricalcium Sulphate
DBM	Demineralized Bone Matrix
DDS	Drug Delivery System
DNA	Desoxyribonucleic Acid
ECM	Extracellular Matrix
EDC	N-(3-dimetilaminopropil)-N'-etilcarbodiimida
EDS	Energy Dispersive X-Ray Spectroscopy
ESI	Electrospray Ionization
FAB	Fast-atom bombardment
FTIR	Fourier-transform infrared
HA	Hydroxyapatite
HAColHep	Heparinized nanoHA/collagen granules
HAColHep_L	Heparinized nanoHA/collagen granules that were Lyophilized
HCl	Hydrochloric acid
HIV	Human Immunodeficiency Virus
KBr	Potassium Bromide
LC	Liquid Chromatography
M	Molar
m/z	mass-to-charge ratio
MALDI	Matrix-Assisted Laser Desorption/Ionization
MES	2-mofpholinoethane sulfonic acid buffer

MIC	Minimal inhibitory concentration
MRSA	Methicillin-resistant *S. aureus*
MS	Mass Spectrometry
NaCl	Sodium Chloride
nanoHA	Nanohydroxyapatite
NHS	N-hidroxisuccinimida
OH^-	Hydroxide
PBS	Phosphate-Buffered Saline
PCL	Poly(-caprolactone)
Pd	Palladium
PGA	Poly(glycolic acid)
PLA	Poly(lactic acid)
PLGA	Poly(lactic-co-glycolic acid)
PMMA	Polymethylmethacrylate
RNA	Ribonucleic Acid
rpm	Revolutions per minute
RT	Room Temperature
SEM	Scanning Electron Microscope
S. aureus	*Staphylococcus aureus*
S. epidermis	*Staphylococcus epidermis*
S. pneumoniae	*Staphylococcus pneumoniae*
S. pyogenes	*Staphylococcus pyogenes*
T_c	Critical temperature of the formulation
TCP	Tricalcium phosphate
T_{eu}	Eutectic temperature
$T_{g'}$	Glass transition temperature in the frozen state
TSA	Tryptic Soy Broth with Agar
TSB	Tryptic Soy Broth
V_0.25h	Heparinized nanoHA/collagen granules with Vancomycin adsorbed for 0.25 h
V_0.5h	Heparinized nanoHA/collagen granules with Vancomycin adsorbed for 0.5 h
V_2h	Heparinized nanoHA/collagen granules with Vancomycin adsorbed for 2 h
VHAColHep	Heparinized nanoHA/collagen granules with Vancomycin adsorbed and Lyophilized
VL_0.5h	Heparinized nanoHA/collagen granules with Vancomycin adsorbed for 0.5 h and Lyophilized
VL_24h	Heparinized nanoHA/collagen granules with Vancomycin adsorbed for 24 h and Lyophilized
VL_2h	Heparinized nanoHA/collagen granules with Vancomycin adsorbed for 2 h and Lyophilized

Chapter 1

Introduction

1.1. Bone Tissue

Bone is a connective tissue that protects and gives support to the internal organs, contributing to the structural integrity of the body. Bone is an enervated and vascularized tissue. Its constant remodelling acts as the calcium and other ions reservoir of the body [1]. Bone is constituted by an organic part, mainly collagen, and an inorganic part, calcium phosphate (apatite) crystals located within the collagen matrix. Bone is composed by osteoprogenitor cells of mesenchymal origin (osteoblasts and osteocytes), bone-resorptive cells of hematopoietic origin (osteoclasts), and bone lining cells, that regulate bone homeostasis [1, 2]. Bone remodelling is performed by the equilibrium between bone formation (performed by the osteoblasts) and resorption (performed by osteoclasts). This equilibrium is also important for healing, bone regeneration and to maintain the structural integrity of the tissue [1]. With age, bone density decreases because osteoblasts become progressively less productive in making new bone and repairing microcracks [3].

1.2. Bone Infections

1.2.1. Pathophysiology

Osteomyelitis is an infection, mainly bacterial, that can occur in bone and bone marrow and results in a painful process with local bone destruction and necrosis [4, 5]. The infection may involve a single portion of the bone or several regions, like marrow, cortex, periosteum, and the surrounding soft tissue, but it rarely is multifocal. If it affects only cortical bone, the infection is designed *osteitis*; if the cortex and medulla are involved, the condition is osteomyelitis [6, 7].

Classification of osteomyelitis is not easy, since it depends on the age of the patient, the chronicity of the infection (acute, subacute or chronic – Figure 1), the causative organism (pyogenic

or mycobacterial), spread manner (hematogenous versus contiguous focus or direct inoculation), as well as the immune and vascular status of the patient and affected region [8].

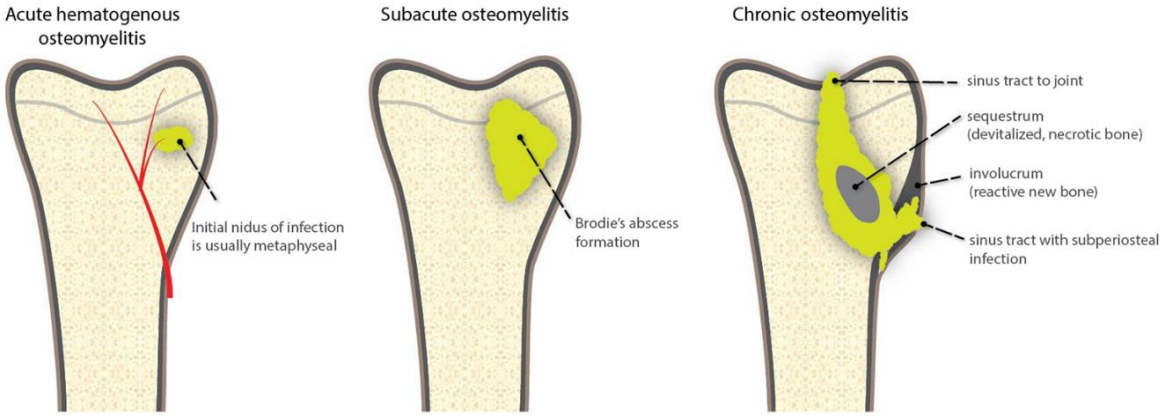

Figure 1 - Illustration of acute, subacute and chronic osteomyelitis [8].

Haematogenous osteomyelitis implies the blood as the carrier of bacteria from a focus of infection elsewhere in the body. Normal healthy bones are very resistant to infection: it may be seen mostly in pre-pubertal children due to an abundant blood supply needed for the growing bone, and in elderly patients. It is less common in adults, in which case the spine is most generally affected. Contiguous infection involves an initial infection that can reach the bone: it is mostly seen with direct contamination of bacteria in open fractures or joint replacement surgery with an orthopaedic implant, skin ulcer and pressure sore. It can occur at any age, it can involve any bone, and implies trauma, bone surgery, or joint replacement. If it manifests itself within days after an injury or operation, is classified as acute; if it involves a greater bone extension and manifests itself for weeks to months, it is classified as chronic. Contiguous osteomyelitis always affects soft tissues and can cause death of the cortical bone before medullary infection; in the case of hematogenous osteomyelitis, this is no longer true. Osteomyelitis provoked by direct inoculation is the main entrance door for infections in adults, induced by trauma, either accidental or surgical. Bacteria are seeded into the bone by contamination of open trauma or surgery or by exposure of the bone in an infected or colonised ulcer [1, 3, 4].

Acute haematogenous osteomyelitis has a fast onset of symptoms, with localized pain, fever, chills and malaise, and local clinical signs as redness, swelling, warmth, and tenderness. The infection occurs mostly in the metaphysis of the long bone (distal femur and proximal tibia), starting in the medulla but easily reaches the cortex along with sinus formation, subperiosteal abscess formation and, soft-tissue extension. If the infection has a periosteal stripping spread it causes local ischaemia, microvascular thrombosis and, tissue death. The acute phase ends with the appearance of dead bone signals [7, 9].

Brodie's abscess is a medullary form of haematogenous osteomyelitis with a sub-acute appearance. The signs and symptoms of acute osteomyelitis, such as fever and onset pains, are typically absent [7, 8].

Chronic osteomyelitis may begin as acute haematogenous or contiguous disease. The key feature of chronicity is the development of bone necrosis. When bone tissue is infected, the bacteria induce an acute inflammatory reaction. The bacteria and inflammation affect the periosteum and spread within bone causing bone necrosis. Absorption of small areas of dead bone or even revascularization can occur, but inflammatory macrophages can induce a separation of larger dead bone fragments or *sequestra*, a lifting in the periosteum, that can cause a compression and obliteration of vascular channels, and a reduction in bone circulation, resulting in a segment of devascularized bone. This provides a safe harbour for bacteria that is inaccessible to antibiotics. Sequestrum may be surrounded by new bone, known as in involucrum, which acts as a shield to isolate the sequestrum from the bloodstream [4, 5, 7, 8].

Abscess and sequestrum formation, merge together can act as a barrier that prevents the access of antibiotics and immune cells to the infecting organisms, allowing the infection to become chronic. Another barrier to the host defence, that can induce chronicity, is the biofilm formation. Biofilm has been defined as an aggregation of microbial cells that is irreversibly associated to a devitalized bone or surface of implants and confined in an extracellular polysaccharide matrix (glycocalyx) and has been shown to let the organisms to transfer resistance plasmids, to deceive the host immune system and reduced susceptibility to antimicrobial agents. The combination of sequestrum, abscess and biofilm, may allow infecting organisms to evade host defences and treatment, delaying the treatment [5, 9, 10].

Pyogenic vertebral osteomyelitis is associated with diabetes, renal insufficiency, catheters, intravascular devices, and a wider variety of organisms, being the most predominate *Staphylococcus aureus* (*S. aureus*) and Methicillin-resistant *Staphylococcus aureus* (MRSA). But Coagulase negative *staphylococci*, *Escherichia coli*, *Enterococcus faecalis*, *Pseudomonas aeruginosa*, among others, can also be found [5].

S. aureus is a Gram-positive, non-motile, coagulase-positive coccoid bacterium, and when the cutaneous and mucosal barriers are disrupted, due for example surgical interventions, it can gain access to the underlying tissues of the bloodstream and cause infection. *S. aureus* has the ability to acquire resistance to any antibiotic, hindering current and future treatments. A recent study found that 75% of culture positive cases were caused by *S. aureus*, with an increasing incidence of resistant organisms with a 9% incidence of methicillin-resistant *S. aureus* [5, 10, 11].

MRSA is a *S. aureus* clone that suffers a gene transfer of staphylococcal cassette chromosome, which provide resistance to methicillin and to most ß-lactam antibiotics. Individuals with MRSA colonization or carriage have a higher risk of subsequent infection and are an critical source of person-to-person transmission [11].

Mycobacterial osteomyelitis is mainly caused by *Mycobacterium tuberculosis*, but nontuberculous mycobacterial infection expanded with the increase of HIV/AIDS. Besides, this form of immunosuppression may also be associated with direct inoculation by injury or propagation of mycobacterial disease. Atypically, mycobacterial osteomyelitis may be caused by *Mycobacterium xenopi*, *Mycobacterium fortuitum*, *Mycobacterium marinum*, among others [5].

As the treatment of acute haematogenous osteomyelitis has been improving, and the incidence decreasing, the incidence of chronic osteomyelitis should also decrease, leading to a reduction of chronic osteomyelitis incidence. Nevertheless, there is a rising in the incidence of infection due to contiguous spread and direct inoculation, because of the increasing prevalence of diabetic foot infections and peripheral vascular disease, leading to an increasing incidence of chronic osteomyelitis. Diabetes results from an increase in the concentration of free radicals in the surrounding tissues making the environment more acidic, activating the osteoclasts that resorb the bone matrix, causing loss of bone tissue. As the population becomes older and have simultaneously more than one medical condition, the incidence of chronic osteomyelitis is likely to increase [1, 5, 12].

1.2.2. Antibiotics

All cases of osteomyelitis should consider an antimicrobial therapy and a surgical approach: acute and chronic osteomyelitis may require surgical debridement and is almost always needed in chronic infection since the presence of dead bone colonized by bacteria prevents eradication by antibiotics alone. Haematogenous osteomyelitis generally does not require surgery; on the order hand, in an infected fracture, cure can be achieved combining bone removal with antibiotic treatment. Antimicrobial therapy requires strict surveillance and treatment with appropriate antibiotics. Surgery may be needed if a postoperative infection is diagnosed. Complex fractures where extensive soft-tissue is damaged require a more extensive antibiotic therapy over a longer period of time. Normally, a single-agent antimicrobial therapy should be sufficient, except in cases related to prosthetic joints and chronic osteomyelitis. The surgery requires adequate drainage, thorough debridement of all involved soft tissue and bone until bleeding healthy tissue is encountered. If the surgical debridement does not remove all the infected soft tissue and necrotic bone, a recurrence of infection can occur. Regarding antibiotic therapy, if after a week the infection does not disappear, possible complications should be considered, such as the presence of a subcutaneous, subperiosteal, or intramedullary abscess, the formation of sequestra, or the presence of foreign material. A surgical intervention should solve this problem more efficiently than to change to another antibiotic [5, 6, 7, 9].

Antibiotics are designed in such a way that they should be able to inhibit/kill the infecting organisms [13]. In the treatment of bacterial infections using antibiotics, there are essentially five antibacterial steps that are usually followed. As schematized in Figure 2 [14], these include inhibition of peptidoglycan/cell wall biosynthesis, target by antibiotics such as the β-lactams and the vancomycin-type glycopeptides. The second step is the inhibition of bacterial protein synthesis, with most antibiotics targeting the ribosome. The third step is the blockage of DNA replication and

transcription to RNA, by targeting DNA gyrase and RNA polymerase. The fourth step is inhibition of folate biosynthesis: the carbon unit that would be released is no longer available and the DNA synthesis is blocked. The final step is the disruption of membrane integrity [14].

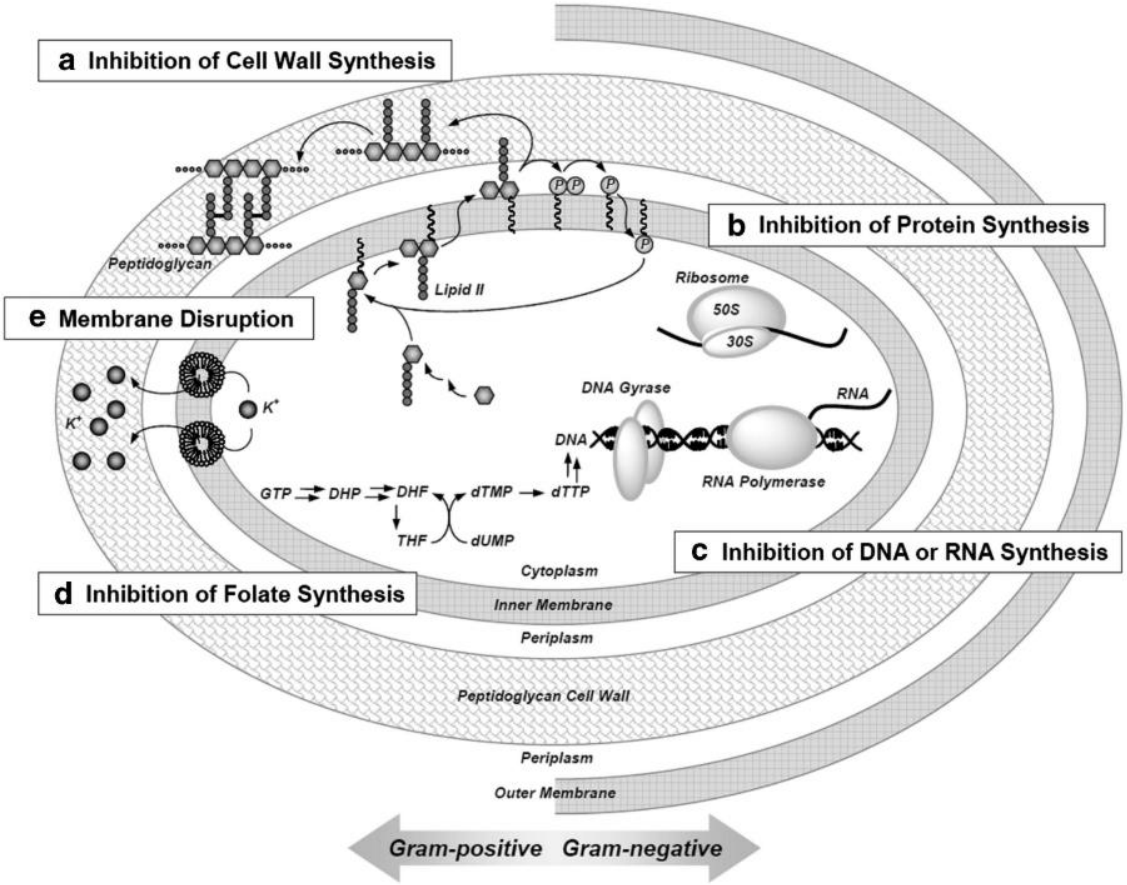

Figure 2 - The five main clinically validated antibacterial targets/pathways [14].

The choice of the adequate antibiotic should be determined, if possible, by microbial cultures and susceptibility results to antibiotics. If clinically possible, delaying antibiotics is recommended until results are available. If not clinically possible, broad-spectrum, empiric antibiotics should be administered [12]. The treatment currently recommended for osteomyelitis caused by *S. aureus* is a parenterally administered semisynthetic penicillin or vancomycin [6], amoxicillin, cephalexin, sulfamethoxazole, ciprofloxacin have also been proved to be useful for local treatment [15]. To treat most MRSA infections, glycopeptides antibiotics as vancomycin and teicoplanin remain the standards [16, 17], but rifampin [18], daptomycin, linezolid [17, 19], and gentamicin in combination with vancomycin [20, 21] can also be used. Regarding infected open fractures, vancomycin and gentamicin are recommended in the treatment, since their combination is effective against a broad range of Gram positive and Gram negative bacteria [22].

Vancomycin is a tricyclic glycopeptide antibiotic produced by *Streptococcus orientalis* [23], active against plenty of Gram-positive cocci and bacilli [24]. It is usually prescribed to fight infections caused

by Gram-positive bacteria as it inhibits the bacterial cell wall synthesis with the formation of stable complex murein pentapeptides, thus causing inhibition of further peptidoglycan biosynthesis [23, 25]. It is also indicated for patients who are allergic to penicillins and cephalosporins. Generally, it is effective against *S. aureus*, *S. epidermis*, *S. pyogenes*, *S. pneumoniae* amount others. Despite this, some Gram-negative bacilli, mycobacteria and fungi are resistant to vancomycin [23]. A treatment with heparin and vancomycin, applied in patients with septic thrombophlebitis showed that heparin causes vancomycin precipitation when administered using the same tubing, leading to subtherapeutic concentrations of vancomycin, and persistent bacteremia [26]. Vancomycin has a slow killing mechanism and is negatively affected by biofilm formation, large bacterial inoculates, and anaerobic growth conditions [25]. Vancomycin has become more relevant with the emergence of MRSA and penicillin-resistant pneumococcal infection [23].

Gentamicin is a basic, water-soluble, aminoglycoside antibiotic isolated from two species of microorganisms belonging to the genus *Micromonospora* [27], and is active against most Gram-negative bacilli and many Gram-positive cocci [24]. Is a bactericidal component that causes bacterial polypeptide synthesis by binding to specific receptor sites on the 30S ribosome; this affected ribosome is removed from the protein-producing pool. Aminoglycosides cause cell death and only need contact with the cell for enough time for the compound to enter the bacterium and bind to the ribosome [28]. Gentamicin is active against both *S. aureus* and *S. epidermis*. It is particularly useful in the treatment of Gram-negative bacillary infections. The antibiotic inhibited both *Pseudomonas*, *Proteus* and *Enterobacteriaceae* organisms among the common Gram-negative bacilli; it also inhibited *Staphylococci* and was active against Aerobacter and coliform bacteria. Against most other Gram-positive cocci, gentamicin shows poor activity and is useful only in combination with penicillin to achieve synergy. Synergistically, penicillin will induce damage to the cell wall allowing the entry of aminoglycosides [28, 29, 30]. Gentamicin consists of two closely related isomeric pseudo-oligosaccharides, which have essentially identical polarities. Belongs to the same category of antibiotics as kanamycin, neomycin, streptomycin, colistimethate and polymyxin B, and is distinguished from them by its paper chromatographic behaviour in a variety of solvent systems. When choosing the most appropriate therapeutic regimen, the potential toxicity must be evaluated [21, 25]. Like most antibiotics and their metabolites, gentamicin is excreted mainly through urine, and since it is an aminoglycoside, a high dose can cause alterations in kidney function [31].

An optimal therapy should eradicate the bacterial infection and stabilize bone, promoting biological repair of the skeletal defects. Intravenous antibiotics therapy with several antibiotics requires careful monitoring of serum drug concentrations to maintain non-toxic systemic levels, and their efficacy may be limited due to the impaired blood supply and a low penetration rate at the site of infection. Because of the altered structure of tissue surrounding an infected site, the diffusion of antibiotics into the central part of the infected region may require high serum concentrations of the therapeutic agents. In addition, long-term treatment and high doses are associated with severe side effects, such as myelosuppression, renal failure, and hepatitis. Antibiotic-impregnated bone void

fillers or cements can act as local anti-infective drug release systems, allowing to fill-up the dead space after surgical debridement and also deliver high antibiotic concentrations at the site of potential infection, without increasing serum antibiotic levels. Therefore, the interest in local administration of antibiotics has been increasing [16, 32, 33].

1.3. Drug Delivery Systems (DDS)

By impregnating antibiotics into carrier vehicles, it is possible to increase their local concentration, without systemic toxicity [33, 34] which should also allow a prolonged release of the antibiotic in time. Because of the poor blood circulation in the osseous defect sites, a level of drugs, such as antibiotics, antimicrobials, and growth factors, need to reach the affected regions. In patients with chronic osteomyelitis, in the necrotic bone region, occurs an alteration in blood flow, which can trigger a suppression in the bioavailability of systemically administrated antibiotics [35]. In order to be effective as a DDS, the carrier needs to fulfil the requirements of safety, greater efficacy, predictable therapeutic response, and controlled and prolonged release period [36]. Rand *et al*. [22] confirmed that local delivery of antibiotics into an infected bone defect is more effective than systemic antibiotics alone in reducing bacteria contamination.

The benefits of DDS by comparing with intravenous antibiotics are higher levels of antibiotic concentration in the affected area, with lower risks of systemic toxicity, pharmacokinetic advantages, the ability to overcome the possibility of resistant pathogens, shorter hospital admission, cost-effectiveness, and, in cases of biodegradable material, avoidance of further surgical procedures [35, 37].

1.3.1. Bone substitutes

Bone defects can have different origins, like infections, tumours or surgeries, so it is essential to replace the missing bone with a material that can fill the bone defects [38]. To be considered as ideal, a bone substitute should have properties of osteoconduction, osteoinduction, osseointegration and/or osteogenesis. Osteoinduction is a biologic stimulation that induces proliferation of osteoblastic progenitors and their differentiation to express an osteoblastic phenotype: initially, cells are undifferentiated, but are stimulated to evolve into cells of bone-forming lineage. Some proteins are good examples of an osteoinductive agent, like BMP. Osteoconduction refers to a property of the scaffold to facilitate migration of cells transplanted in the graft or arising from the neighbouring tissue, and bone growth onto a permissive surface. Bioactive calcium phosphate based ceramics are an example of osteoconductive agents and represent a scaffold that may promote cellular migration, vascular invasion, and bone growth. Osseointegration refers to direct contact between bone and an implant without a fibrous interface as intermediate, reinforcing the stability of the implant in load-bearing fixation. Osteogenesis is the process of bone formation with no reference of cellular origin [33, 34].

1.3.1.1. Features

A bone substitute should simulate the structure and properties of the natural bone extracellular matrix (ECM) and grant the occurrence of the necessary biological triggers found in natural bone. Currently, the goal is to create 3D-scaffolds using biomaterials and cells that can mimic the ECM, support the formation of new tissue/bone, and desintegrate as new bone is formed. The optimal properties that a scaffold must have are related to the strength, rate of degradation, porosity, microstructure, and shape and sizes of the scaffold [1].

To be used efficiently in bone tissue engineering, the scaffold should be biocompatible; must promote cell adhesion, allowing the adhesion and proliferation of osteogenic cells to the scaffold, promote their differentiation and the synthesis of mineralizing bone matrix; must promote vascularization, the supply of nutrients and oxygen to the cells and removal of metabolites, and support normal cellular activity including bioactive molecules, which direct osteogenic differentiation of adherent cells; and after implantation, the scaffold should only trigger a limited and controlled inflammatory response [1, 39]. The degradation rate of the scaffold must provide the necessary support and allow the body cells to replace the implant, the biomaterial must undergo resorption as new bone is formed: the rate of formation of the new bone tissue should be proportional to the rate of degradation of the biomaterial (between a few months and about 2 years), and its degradation products must not cause inflammation or toxicity in surrounding tissues or the entire system of the host, and exit the body without interference with other organs. The scaffold should be easy to fabricate into 3D-structure and should possess well interconnected pores and high porosity. The ease of processing may determine the choice of biomaterial, due to conformation and whether or not it can be injected [1, 3]. Porosity causes the scaffold to have a much higher surface area, thus providing good mechanical fixation and sites on the surface that allow chemical bonding between the bioceramics and bones: pore sizes provide surface and space for cell adhesion and bone ingrowth, facilitating bone formation, without being disturbed by high circulation body fluid or mechanical stress due to implant movement; interconnected pores provide pathways for cell infiltration and nutrient exchange, as well as *in vivo* blood vessel formation suitable for sustaining *denovo* bone tissue formation and possibly remodelling [3]. Cells firstly interact with the scaffold via proteins and chemical groups or ligands on the material surface. These ligands are present in the form of Arg-Gly-Asp (RGD) binding sequences in scaffolds synthesized from natural extracellular materials, but scaffolds made from synthetic materials may require deliberate incorporation of these ligands through, for example, protein adsorption. The density of ligands is influenced by the available pore surface to which the cells can adhere. The mechanical properties should be consistent with the anatomical site into which it is to be implanted and must be strong enough to allow surgical handling during implantation. The scaffold should maintain enough mechanical properties until newly formed bone can assume a structured role [1]. Table 1 show some of the features that a scaffold to be used in a bone tissue engineering should have, withdrawn according to what has been said along this paragraph.

Table 1 - Features that a scaffold to be used in bone tissue engineering should possess.

Requirements
• Biocompatibility; • Promote cell adhesion and vascularization; • Biodegradability, not promoting inflammatory response; • Degradation rate similar to bone; • Easy to fabricate; • Flexibility; • Scaffold architecture, high porosity and interconnected pores; • Mechanical properties similar to pre-existing tissue at the implantation site.

An ideal bone void filler to be used in the treatment of osteomyelitis should have the attributes referred above and mostly, should be able to elute high levels of antibiotic locally [34]. If this is added to the final ceramic solid then its release is governed by diffusion alone, decreasing the elution time; if it is added before the ceramic has set, then a proportion of the antibiotic may be trapped within the ceramic and only become available for release on the dissolution of the carrier, which takes much longer time [34]. A study performed by Rathbone *et al.* [40] allowed to investigate the *in vitro* effect of various antibiotics on human osteoblast cell numbers and activity by measuring osteoblast DNA and alkaline phosphatase (ALP) levels after 10-14 days of antibiotic exposure. Among all antibiotics used, gentamicin was one of those showing the greatest decrease, while vancomycin was one of the least cytotoxic and did not appreciably affect cell numbers and activity until very high concentrations were used. The study also allowed to observe that at very high doses, all antibiotics presented a suppressive effect on osteoblast numbers. The negative effects should be considered when choosing the ideal antibiotic and dose. The goal is bone recovery, but the initial priority is the clearance of infection [34].

1.3.2. Antibiotic Carriers

Since it was discovered that bone cement mixed with antibiotics was effective in the treatment of infection in total hip replacement, there was an increased interest in developing carriers of local antibiotics. Several biodegradable and nonbiodegradable substances have been used as vehicles for delivery, attempting to locally provide high antibiotics concentration [37]. However, the use of non-biodegradable carriers can attract glycocalyx-producing bacteria despite the presence of local antibiotics. The resulting biofilm acts as a foreign body and a surface of bacterial colonisation, leading

to secondary infection and the need to remove the implant. The use of biodegradable carriers is seen as an advantage due to its potential to reduce the risk of secondary infection and does not need to be removed [41].

Several biomaterials are used for local antibiotic delivery such as synthetic polymers as polymethylmethacrylate (PMMA), poly(glycolic acid) (PGA), poly(lactic acid) (PLA), and poly-co-glycolic acid (PLGA); ceramics, such as hydroxyapatite (HA) and tricalcium sulphate (CS); acellular tissue matrices as bladder submucosa and small intestinal submucosa; natural derived materials such as collagen and alginate; and composites [35, 42]. These materials are used to locally deliver vancomycin or gentamicin, but also kanamycin, tobramycin, teicoplanin, rifampin, among others [35, 37]. A bone substitute made of hydroxyapatite and tricalcium sulphate was impregnated with gentamicin and proved to decrease the rate of infection and increase new bone growth, comparing to the bone substitute without antibiotic and no use of a void filler in a debridement osteomyelitic environment [43].

Synthetic polymers are able to control the release kinetics and predictability/quality, the degradation rates and the mechanical properties [35]. They can be easily synthesized with reproducible quality and purity and fabricated into various shapes with desired bulk and surface properties [42]. These materials degenerate through non-enzymatic hydrolysis of the ester linkages in a bulk erosion process, and their nontoxic degradation products are eliminated from the body in the form of carbon dioxide and water [35, 42]. The diffusion of the polymers and the hydrolytic degradation of the bulk regulate the antibiotic release, allowing for sustained release profiles for weeks or months, depending on the formulation. The degradation rate of these polymers can be controlled by altering their crystallinity, initial molecular weight, and the copolymer ratio of lactide and glycolide [42]. A reduction in the pH can stimulate the hydrolytic erosion process, giving rise to an autocatalytic degradation of the polymer and accelerate the release of drugs, depending on the degradation rate and the local fluid exchange rate. If the polymer erodes very easily it can motivate an acidic environment that induces a host inflammatory response and may lead to a reducing of the functional efficacy of the delivered antibiotics. Another type of synthetic polymers that degrade through surface erosion are polyanhydrides. This type of erosion enables a constant release rate of antibiotics over time. They are biocompatible, but some studies showed an extreme inflammatory reaction with sebacic acid-based-polymers [35].

PMMA beads are the major representative of nonbiodegradable carrier systems, but they require surgical removal upon completion of drug release [37], since PMMA could affect healing of the debrided bone defect [35]. PMMA has been the most widely used bone cement in staged surgical treatment of chronic osteomyelitis, for prophylaxis and local therapy, but it has reduced biocompatibility with bone, short duration of antibiotic release, a very low release rate and thermal damage of the antibiotic [33, 35]. PMMA bone cements containing either gentamicin or tobramycin at low doses are sufficient for prophylaxis, but not for therapeutic applications in established osteomyelitis. Various antibiotics can be mixed with PMMA, but the most frequent are gentamicin,

tobramycin, vancomycin, or cephalosporins. Antibiotics that are heat-liabile cannot withstand the exothermic polymerization reaction, making them incompatible with PMMA. Others, like rifampin, are able to remove free radicals, making them incompatible since it can affect the PMMA polymerization. The mixing procedure and the additives used alter the porosity of the PMMA spacer, but those, in combination with the type of antibiotic used, influence the elution kinetics of the antibiotic from the PMMA. The *in vitro* elution of antibiotics can be more efficient if they are combined in the PMMA, rather than incorporated alone. Tobramycin and vancomycin are a combination of antibiotics that shows better results. Reports show that PMMA provides an additional substratum for bacterial colonization. To solve the problems related to the high rate of re-infections, the bactericidal efficiency needs to be improved; using a different biomaterial can solve the limitations related to the choice of the antibiotic; and by using a biodegradable, osteoconductive or osteoinductive material, rather than PMMA, or any other non-biodegradable material, the surgery to remove the material is no longer needed [35]. Therefore, there is a need to develop of biomaterials for local antibiotic delivery, focused on biodegradable solutions.

Ceramic-based bone substitutes include calcium phosphate (CaP)-based products (biphasic CaP, tricalcium phosphate, and synthetic and natural hydroxyapatite), calcium sulphate and bioactive glass (silica-based products) [44]. Semi-hydrate form of calcium sulphate, commonly known as plaster of Paris, can be applied as a local DDS, and was used for decades to fill bone cavities resulting from disease, trauma, or surgery until it starts being used as a DDS [37]. Calcium sulphate is a slow drug release carrier that is affordable, is readily available, it is easy to sterilize, biocompatible and radio opaque. It can temporarily fill bone defect, leaving no space for bacteria to grow while at the same time it can provide an osteoconductive structure for bone ingrowth [45]. It has a short degradation time (30 - 60 days) causing a rapid loss in mechanical properties, limiting its use in load-bearing environments [44]. Being resorbed by the body, natural bone can simultaneously replace the material. The problem related to the use of pure calcium sulphate is that it can delay wound healing and osteolytic processes during resorption by pH lowering [45]. Another disadvantage of these products is related to serous drainage during the degradation process [44]. Antibiotic-loaded CS has been employed in the treatment of patients with osteomyelitis: these calcium-based antibiotic-delivery systems show leverages over PMMA, due to a wider range of antibiotics that can be impregnated and do not need a second surgery to remove them [35].

Bioactive glass, collagen implants, calcium phosphates, demineralized bone matrix and allograft bone are other types of biomaterials that have been clinically used for local administration of antibiotics [35]. Allografts are used as a bone graft (structural allograft and cancellous allograft) and as allograft-based bone substitutes (demineralized bone matrix). Due to the risk of disease transmission and potential for immunogenicity, allografts require pre-treatments such as radiation and/or freeze-drying prior to use, in order to alter the grafts mechanical and biologic properties, including reductions in osteoinductive and osteoconductive properties, when compared to autografts. In addition, radiation reduces incorporation rates, increasing the potential for structural failure. In

order to preserve some of the osteoinductive properties of allograft, demineralized bone matrix (DBM), a composite of noncollagenous proteins, growth factors, and collagen, was created by acid extraction of the mineralized phase of bone [44]. PMMA beads show comparable rates of infections clearance when compared to biodegradable materials, but they required more subsequent surgeries. More clinical trials are vital to better understand the efficacy of biodegradable materials over the PMMA beads in the treatment of infections, as the only apparent leverage seems to be the reduced number of follow-up surgeries [35].

Regarding natural polymers, collagen, fibrin, chitosan and alginate, have been used in a diversity of drug delivery applications. Fibrin is a biopolymer that participates in blood coating: is obtained from the polymerization of fibrinogen cleavage by the protease thrombin. Since it is a natural constituent in the healing process, surgeons employ fibrin as a sealant for general wound homeostasis. Fibrin sealants have also been applied for infection prophylaxis by adding powdered antibiotic to the polymerization fibrin gel at the site of wound closure [35, 42].

Chitosan is a polycationic biopolymer originated through deacetylation of chitin, which is often obtained from the exoskeletons of crustaceans, and that readily forms hydrogels [35]. Alginate has been used as a hydrogel for cell encapsulation, drug delivery and tissue engineering [42].

Several carriers have been developed to encapsulate drugs, such as biodegradable polymers (synthetic or natural) and bioactive ceramics, in the forms of particulates, membranes and porous matrix. New antibiotic bone substitution materials/bone void fillers are based on biodegradable or resorbable materials such as polylactic acid, chitosan or new combinations based on calcium sulphate. These implantable materials, unlike non-biodegradable ones, do not have to be removed after a time. By using antibiotic-impregnated bone substitutes, the need for systemic antibiotic could be potentially reduced [32, 36].

1.4. Commercially Available Local Osteomyelitis Treatments

1.4.1. Bone Substitutes

Commercially available bone grafts and bone substitutes can be classified as allograft-based, ceramic-based, growth factor-based, and polymer-based graft substitutes [44]. Since this study uses a hydroxyapatite scaffold, we will focus on ceramic-based bone substitutes.

HA is the main component of the mineral phase of native bone, leading to the origin of CaP compounds as bone substitutes. Due to its osteoconductive properties and biocompatibility, a lot of commercial products are based on CaP: Vitoss® (Tricalcium phosphate – Stryker), ProOsteon® (coral-based HA matrix - Biomet), Norian SRS® (injectable moldable tricalcium phosphate - Synthes) [44], all showed in Table 2.

Table 2 - Summary of selected bone graft substitutes commercially available for use.

Class	*Commercial Product (Company)*	*Composition*	*Claimed mechanism of Action*	*Formulations*	*References*
Ceramic Based	***Norian SRS® (Synthes)***	Calcium Phosphate	Osteoconduction Bioresorbable	Injectable paste	[44]
	Vitoss® (Stryker)	Beta-TCP and bioactive glass	Osteoconduction Osteoinductive with bone marrow aspirate Bioresorbable	Putty, Strips, Injectable, Morsels, Shapes	[3, 44, 46]
	ProOsteon® (Biomet)	HA and calcium carbonate	Osteoconduction Bioresorbable	Injectable granules or block	[44, 47]
	BonePlast® (Biomet)	Calcium sulfate	Osteoconduction Bioresorbable	Paste	[44]
	Calcibon® (Biomet)	Alpha-TCP, dicalcium phosphate calcium carbonate and HA	Osteoconduction	Paste, Granules	[46, 48]
Composite	***Collagraft® (Zimmer)***	Type I Collagen and HA with TCP	Osteoconduction	Granules	[47, 49]

1.4.2. Antibiotic Carriers

The current work focus on combining ceramics with antibiotics, since ceramics are biocompatible and osteoconductive, are cable of carrying a wider range of antibiotics and do not need a second surgery to remove them. Osteoset® T, Herafill® G, PerOssal®, Stimulan® and Cerament®, are commercially available antibiotic carriers licensed for the treatment of osteomyelitis. PerOssal® and Stimulan® do not contain antibiotics, they are mixed with antibiotics at the time of implantation [34]. A study comparing Osteoset® T, Septocoll® E and Cerament® G showed that Cerament® G had fewer prolonged wound leaks, a lower fracture rate and a lower recurrence rate [50]. In Table 3 a selection of some antibiotic carriers commercially available for use are presented.

Table 3 - Some antibiotic carriers commercially available.

Commercial Product (Company)	*Composition*	*Antibiotic*	*Formulations*	*References*
Osteoset® T (Wright Medical)	Calcium sulphate	Tobramycin	Pellets	[32, 34, 44, 51, 52]
Herafill® G (Heraeus)	Calcium sulphate + Calcium carbonate + Triglyceride	Gentamicin	Pellets	[32, 34, 37, 53]
PerOssal® (aap)	Nanocrystalline Hydroxyapatite + Calcium sulphate	--	Pellets	[34, 54]
Stimulan® (Biocomposites)	Calcium sulphate	--	Pellets or injectable paste	[34, 52]
Cerament® G (BoneSupport)	Calcium sulphate + Hydroxyapatite (40wt%)	Gentamicin	Injectable Cement	[34, 50, 51]
Palacos® (Heraeus)	PMMA	Gentamicin	Beads, cement	[37, 55]
Septopal® (Merck)	PMMA	Gentamicin	Beads, injection	[35, 45, 46, 52, 56]
Septocoll® E (Biomet)	Type I Collagen	Gentamicin	Fleece	[50, 52, 57]
Genta-coll® (Resorba)	Collagen	Gentamicin	Sponge	[58]
Vancogenx® (Tecres)	PMMA	Vancomycin + Gentamicin	Pellets	[46, 59]

1.5. Biocomposite

1.5.1. Nanohydroxyapatite

Bioceramics are needed to alleviate pain and restore function to diseased or damaged calcified tissues (bones and teeth) of the body. Calcium orthophosphates have a chemical similarity to the mineral component of mammalian bones and teeth. Besides being non-toxic, they are biocompatible, not recognized as foreign materials in the body, exhibit bioactive behaviour, and integrate into living tissue by the same processes active in remodelling healthy bone. This leads to osteointegration, a physicochemical bond between the implants and bone. Calcium orthophosphates are also known to be osteoconductive and support osteoblast adhesion and proliferation. In biomedical applications, calcium orthophosphates are used in the production of non-load-beating implants, filling of bone defects in oral and orthopaedic surgery, and coatings of dental implants and metallic prosthesis, due to being brittle and having poor fatigue resistance [3].

Ceramics are defined as refractory, inorganic, and non-metallic materials. They are hard, brittle, heat- and corrosion-resistant materials made by shaping and then firing a non-metallic mineral at a high temperature [39]. Ceramics such as HA, tricalcium phosphate (TCP), bioactive glasses and glass-ceramic are commonly used as bone graft substitutes due to their biocompatibility and osteoconductive properties: they are either biodegradable or resorbable by osteoclasts and can be incorporated into newly forming bone [35]. They have been shown to have osteoconductivity, high

compressive strength and good bone integration [1], thus being used for filling bone defects and bone graft substitutes.

The bigger challenge regarding medical applications of bioceramics is to replace the old damaged bone with a material that can function during the remaining years of the patient's life. Because the average life span of humans is now 80+ years and the major need for spare parts begins at about age 60, the implanted bioceramics need to last for at least 20 years [3]. The ability of reabsorbable ceramics to promote regeneration of tissue depends on how fast the ceramic dissolves and how quickly it is replaced by the host tissue. A small initial pore size confers high mechanical strength, but as it dissolves, it becomes more porous, allowing the ingrowth of tissue [41].

Crystals of calcium-phosphate have been used as a delivery system because of their physical and chemical properties, high surface interaction properties and their biocompatibility [60]. HA is a calcium phosphate with an hexagonal structure and the formula $Ca_{10}(PO_4)_6(OH)_2$, and with a chemical and crystallographic similarity to the human bone and teeth, exhibiting good bioactivity and biocompatibility [61, 62]. HA, when compared with other biodegradable carriers, has a very slow absorption rate [61]: is slowly replaced by new-forming bone, reducing the need for additional forms of reconstruction; has a greater antibiotic absorption and a more prolonged antibacterial activity, in addiction to inherent osteogenic properties [41]. However, a study showed that, in the presence of HA, the proliferation and differentiation of osteoblasts were very low [61]. Any antibiotic can be placed in calcium hydroxyapatite ceramic as there is no thermal damage to the drug [33]. HA is easily incorporated into bone and is osteoconductive but not osteoinductive [39]. For this reason, and because it is biocompatible, it may show a high interest as a drug delivery system, and can be used to deliver steroids, antibiotics, proteins, hormones, among others [60]. HA porous forms have been used in biomedical applications as bone scaffolds to enhance the adhesion between bone and an apatite implant, improving bone ingrowth and osseointegration, but the brittleness and low strength limit applications in hard tissue implants [36, 63]. In order to be able to withstand large loads efficiently, the mechanical properties of the HA porous body should be improved. As a DDS, the pore structure of the scaffold needs to be controlled in terms of porosity and pore size, since porosity is a factor that allows substances to adhere [36, 63]. Other factors like the surface functional groups, acidity and basicity, surface charge and hydrophilicity also contribute to the incorporation of functional groups on the HA surface [63]. Drugs should be entrapped efficiently to be released for a prolonged period [36].

Results showed that antibiotic-impregnated HA treated osteomyelitis in a rabbit model, as it could clear infection of S. aureus in 72.7 % of cases. When implanted into a dead space after debridement for MRSA, HA impregnated with vancomycin showed a better success rate when compared to PMMA beads impregnated with vancomycin [41].

Considering that bone is a nanocomposite of minerals and proteins, when it comes to choosing a substitute that mimics the natural bone, it is preferable to choose a nanostructured biomaterial [64], thus making it an area with great interest in regenerative medicine [65]. Peter *et al.* [66] produced

chitosan-gelatin/nanoHA composite scaffolds, where the addition of nanoHA lead to a decrease in biodegradability, with an improved protein adsorption, cell attachment, and biological and mechanical properties.

Nanosized HA shows different hydrophilicity, wettability, surface area, and surface roughness, when compared to micro-sized HA, enhancing osteoblast adhesion and improved osteoconductivity and bonding properties to host bone [65]. Nanohydroxyapatite has a great surface-to-volume ratio and a higher surface reactivity when compared to micro-sized HA [67, 68]. Laranjeira *et al*. [68] showed that nanostructured-HA granules enabled to obtain a highly porous material with a high surface area, promoting cell adhesion and migration. A DDS in a nanoscale level can enhance therapeutic efficacy of a drug by allow to monitor release kinetics, to regulate biodistribution and to minimize toxic side effect [65]. Ferraz *et al*. [69] produced nanoHA microspheres capable of provide a sustained release profile of amoxicillin, amoxicillin + clavulanic acid, and erythromycin, with an inhibitory effect on bacteria, capable of enhancing bone regeneration while treating periodontitis.

As a drug delivery system, the HA scaffold alone seems insufficient to keep drugs at the site and entrap them, resulting in a drug release in an uncontrolled way [36].

1.5.2. Collagen

Structural proteins such as collagen, laminin, elastin, and fibronectin have been used as naturally derived materials for tissue engineering and as a vehicles for cell delivery [42]. It is a macromolecule composed of several amino acids that, by a condensation reaction, form a polymer chain [70]. Collagen types I, II, III, V and IX are known to form fibers out of the 29 different types of collagen identified so far [1]. Structurally, every collagen type consists of three polypeptide chains with each alpha chain composed of repeating units of Gly-X-Y, with Gly standing for glycine, and X and Y being resides of proline or 4-hydroxyproline. These three α-like helices are organized together to form the characteristic triple helix structure of collagens, resulting in a fiber-like structure [1, 70, 71]. This allows the collagen to produce a highly interconnected network all over the ECM, providing structural integrity and biochemical properties to the connective tissue [70]. Collagen is capable of self-aggregation and cross-linking, forming fibers with extra strength and stability. The fibers are the final quaternary structure of the collagen protein [72]. Through the crosslinking process, the mechanical and degradation properties of collagen can be tailored [73].

Collagen is the most extensively utilized natural protein in orthopaedic applications, as a biomaterial, due to its biological properties, as high biocompatibility, matrix mimicking and non-toxicity [1, 35]. Type I collagen is the most abundant structural protein in the human body and is a critical component of bone extracellular matrix [35]. It plays a significant role in the formation of tissues and organs and is involved in several functional expression of cells [72]. It is a major component of connective tissue and the main structural protein of all organs [41]. It has been used in bone tissue engineering due to a lack of immune reactivity associated with its use [73]. Collagen is a good surface-active agent, exhibits biodegradability, antigenicity and high compatibility when compared with other

natural polymers, such as albumin and gelatine [72]. If not adequately cross-linked it may degrade off quite quickly when implanted in the target site [1].

Collagen can support cell adhesion, assuming an important role in tissue remodelling [74]. It can attract and stimulate the proliferation of osteoblasts, promoting mineralization and production of collagenous callus tissue, which aids the formation of new bone [72].

Moreover, collagen-based systems have some disadvantages, regarding their poor mechanical strength, ineffectiveness in the management of infected sites and difficulty of assuring adequate supplies [72]. A list of advantages as disadvantages are presented in Table 4 [72].

Table 4 - Advantages and disadvantages of collagen as a biomaterial [72].

Advantages	*Disadvantages*
• Available in abundance and easily purified from living organisms • Non-antigenic • Biodegradable and bioreabsorbable • Non-toxic and biocompatible • Synergic with bioactive components • Biological plastic due to high tensile strength and stability • Promotes blood coagulation • Formulated in several different forms • Biodegradability can be regulated by cross-linking • Easily modifiable to produce materials as desired by utilizing its functional groups • Compatible with synthetic polymers	• Excessive cost of pure type I collagen • Variability of isolated collagen • Hydrophilicity which leads to swelling and more rapid release • Variability in enzymatic degradation rate as compared with hydrolytic degradation • Complex handling properties • Side effects, such as BSF and mineralization

Collagen is much used in drug delivery systems since it can be extracted into an aqueous solution and molded into various forms of delivery systems. Some of its applications are in shields in ophthalmology, sponges for wounds and burns, controlling material for transdermal delivery, nanoparticles for gene delivery, a replacement/substitute for artificial blood vessels and valves, among others. It is easily absorbable in the body, has very low antigenicity, a high tensile strength and high affinity with water. It is also non-toxic, biocompatible and biodegradable [72]. A combination of collagen with other polymers can enhance attachment and proliferation of fibroblasts and support growth of cells [74].

Antibiotics are mostly incorporated into collagen products by soaking the material in the antibiotic solution and allowing absorption by the hydrophilic matrix [35]. A study performed by Phinney *et al*. [24] showed that an impregnated collagen shield, as a contact lens, is capable of delivery high levels of gentamicin and vancomycin. Collagen fleece is a reliable and biodegradable method of delivering antibiotics locally. Gentamicin-loaded collagen fleece treated patients with post-traumatic and post-operative osteomyelitis. This was combined with intravenous antibiotics, and the results suggest that antibiotic-loaded collagen fleece is useful as an adjunct to systemic antibiotic treatment. It was also showed that gentamicin-loaded collagen fleece had a superior pharmacokinetic profile with complete elution of the antibiotic when compared to a PMMA setting [41].

Three-dimensional collagen scaffolds, being biodegradable *in vivo* and with a large surface area for cell attachment, can support vascularization processes and be used as artificial blood vessels, heart valves or cell transplant devices.

1.5.3. Composite

Individually, all biomaterials have limitations, related to the mechanical properties, drug elution kinetics, or the ability to contribute to tissue regeneration [35]. The production of hybrids of biodegradable carriers systems is increasing, since the combination of properties of different components, as synthetic or natural polymers with a ceramic bone substitute, can improve the release of antibiotics from an osteoconductive carrier [41]. Also, they are able to stimulate the formation of new bone and provide a scaffold. Ceramics and cements alone can provide high compressive strength and structural support, but they have limitations in tissue engineering due to their brittleness, difficulty of shaping for implantation and biodegradability. By combining natural biomolecules with synthetic polymers or with ceramics or by using biocomposite materials, scaffold properties can be improved, like tissue interaction (controlling degradation), the biocompatibility in tissue engineering applications, and the biological performance, by enhancing cellular interaction [1, 35]. Since HA is the major component of bone in weight and collagen is the most abundant protein in bone, they are frequently combined in composite scaffolds [73]. The association of HA and collagen is the one that better simulates natural bone, regarding composition, nanostructure, and biological response [67]. Heparin is a glycosaminoglycan present in the extracellular matrix of different tissues and know to interact with several biomolecules, like growth factors and collagen [67]. The inclusion of heparin in nanoHA/collagen granules was proved to improve vancomycin release, in a more controlled and sustainable way [67]. With the improved composite formulations and their higher functional points, composites may be the best solutions to treat infections, followed by bone regeneration. Table 5, adapted from [35], shows a combination of natural or synthetic polymers with ceramic bone substitutes that were previously used.

Table 5 - Composites already used for local antibiotic delivery.

Materials	***Antibiotic***
Calcium phosphate + PLGA	Vancomycin + Rifampin
PLA + bioactive glass	Ciprofloxacin
Borate bioactive glass + Chitosan gel	Teicoplanin
Borate bioactive glass + Chitosan gel	Vancomycin
PLA + HA/TCP	Ciprofloxacin
Cellulose + nanoHA + chitosan gel	Gentamicin
PMMA BaSO4 + β-TCP	Gentamicin + Vancomycin
Chitosan coated $CaSO_4$	Daptomycin

1.6. Lyophilization

1.6.1. Principle

Lyophilization, by freeze drying, is a technique often used for food products, biological materials and drug delivery systems. It is a dehydration technique based on the removal of water/solvent from the frozen solution by sublimation under vacuum, at low pressure, leading to an anhydrous or almost anhydrous structure [1]. It is a multi-stage process, represented in Figure 3, in which water is frozen, followed by its removal from the sample, initially by sublimation (primary drying) then desorption (secondary drying) and finally storage, resulting in a dry material [75].

Lyophilization is being used to remove water from products, mostly of biological origin, without damaging them, so they can be preserved easily, with improved stability, in a permanently storable stage easily transportable and that can be reconstituted just by adding water [75, 76]. Antibiotics, vaccines, drugs and protein-containing products are some example of freeze-dried products [75].

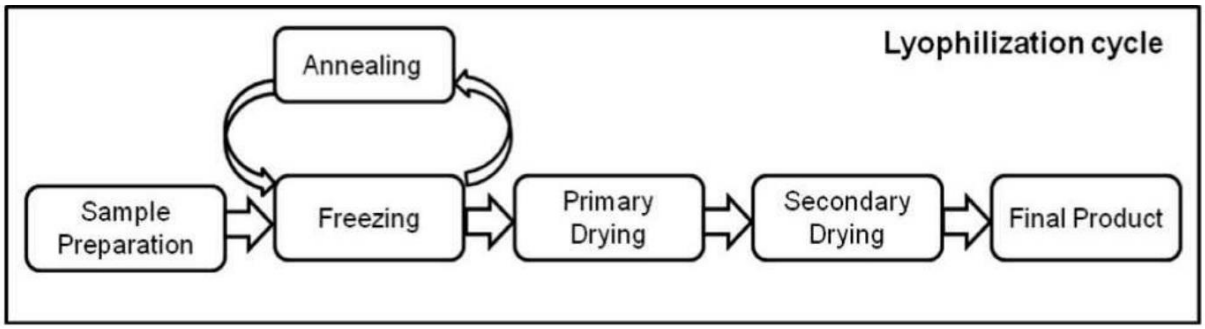

Figure 3 - Steps involved in lyophilization [75].

The main principle is sublimation, where water passes directly from solid to the vapor without passing through the liquid state. The process is performed at temperature and pressure below the triple point (low temperature and pressure), to enable sublimation of ice (Figure 4, extracted from [75]). The material to be dried first has to be frozen and then subjected under a high vacuum to heat (by conduction, radiation or both) so that frozen liquid sublimes leaving only solid, dried components of the original liquid. During primary drying, the water vapor pressure increases with increasing temperature, to accelerate sublimation: temperature should be kept as high as possible, but below the critical temperature of the formulation (T_c), to avoid a loss of the "cake structure" [75]; T_c is the temperature above which the freeze-dried product loses macroscopic structure and collapses during the process [76]. During freezing, the vaporized solvent is removed from the vacuum chamber by converting it back to a solid, and ice crystals start separating out until the solution becomes maximally concentrated. The resulting product have a very large surface area thus promoting rapid dissolution

of dried product. The concentration gradient of water vapor between the drying front and the condenser is the driving force for removal of water during lyophilization [75].

Annealing is an optional step, used to crystallize the formulation component. It is a thermal treatment performed after the initial freezing step if the formulations contain a crystalline bulking agent [77]. It is necessary to determine a temperature, that depends on whether the solute is crystalline or amorphous. If the solute separates into crystalline form, this temperature should be above the eutectic temperature (T_{eu}); if it generates an amorphous form, then the temperature should be above the glass transition temperature ($T_{g'}$). After annealing, the temperature is again decreased to completely freeze the system [75, 77].

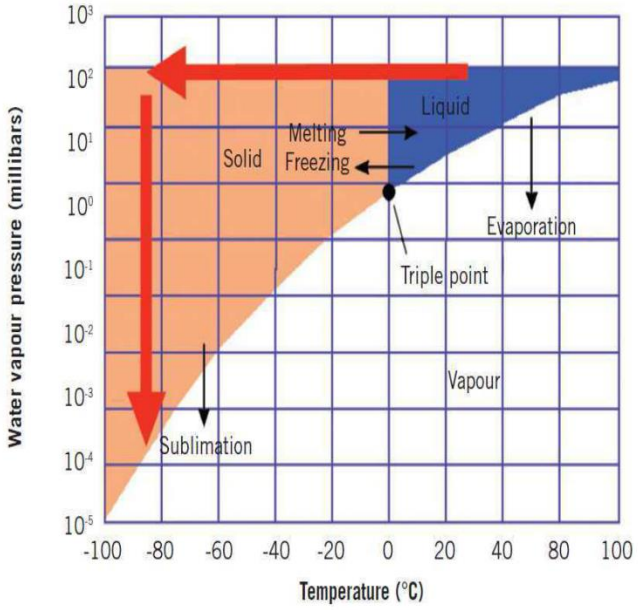

Figure 4 - Freeze drying process with phase diagram showing triple point of water at 0.01°C, 0.00603 atm. [75]

The most significant advantage of freeze drying is that the process is carried out at low operating temperature with the absence of air resulting in prolonged and superior quality products by preventing deteriorations caused by oxidation or chemical modification, enhancing product stability in a dry state, and giving unstable chemical solutions a long lifetime when they are stored at room temperature. It also allows the elimination of bacterial growth and enzyme action, which normally occur in aqueous preparations; does not cause de-naturation of many proteins; and provides excellent solubility characteristics to the final product, allowing rapid reconstitution. Freeze drying is the most suitable technique for dehydration of almost all heat sensitive substances such as natural oils, drugs and water-soluble components. However, freeze drying technique has some drawbacks such as increased handling and processing time, high capital and operating costs in comparison to other methods. Also, volatile compounds may be removed by vacuum, and there is a need to use sterile diluents upon reconstitution. The porous structure of freeze dried powders due to the ice sublimation during the process may in some cases also be one of the major limitations [75, 78].

1.7. Sterilization

1.7.1. Principle

Sterilization is a technique that kills or destroys transmissible agents like bacteria from any surface, medications or equipment, and can be achieved by different ways: ionizing radiation, elevated temperature, chemical liquids and gases [79].

Sterilization is crucial in scaffold production both at laboratory and industrial level [3], since implantable drug delivery systems should be sterile [80]. Gamma irradiation is the most used technique for sterilization of pharmaceuticals raw materials and drugs, due to the high penetrating ability [79]. It is capable of reaching 10^{-6} probability of microbial survival without excessive heating of the product or exposure to toxic chemicals but may cause radiolytic degradation of the incorporated drug and polymer matrix [80]. It is also used because it is easy to control, reliable, fast and the final product has no harmful effect on the environment [79]. The recommended dose to sterilize health care products is 25 kGy [81], but lower or higher doses are acceptable [79]. In medical applications, bone allografts are constantly sterilized with gamma radiation to minimize the spread of diseases [82], but a dose of 25 kGy is not sufficient to ensure sterility of human tissue grafts [81].

Sterilization can cause modifications in collagen-based materials and in biological materials in general, leading to an alteration on their biomedical and clinical performance [83]. Sterilization by UV radiation can cause collagen degradation [84]. Collagen is usually sterilized by ionising radiations, like beta/E-beam and gamma, and gas sterilization by ethylene oxide, which involves a chemical process like alkylation [83]. Currently, the most used method to sterilized collagenous materials is by gamma sterilization, with doses between 5 and 25 kGy [83]. Gamma-radiation induce chain scissions in collagen molecules, when the sample is dry, leading to a decrease in the mechanical strength of the sample. It also causes an increase in the susceptibility concerning enzymatic degradation [83].

Sarıgöl *et al.* [80] develop PCL microspheres containing vancomycin HCl and evaluated the effect of gamma irradiation: morphologically there were no alteration; the drug release patterns were similar before and after irradiation; and the antimicrobial activity also did not showed any differences.

Ethylene oxide and other gas sterilization methods are not desirable for vancomycin sterilization due to the risk of reaction with the components of the matrix modifying the mechanism of drug release and possible producing toxic residues [85]. Also, it has been show that a gamma irradiation of 25 kGy did not affect the properties of minitablets containing gentamicin sulphate and vancomycin [86].

Chapter 2

Materials and Methods

2.1 Materials Preparation

2.1.1. Production of nanoHA granules

To produce the nanoHA granules, scaffolds were prepared using polyurethane sponge impregnation method, previously described elsewhere [67]: polyurethane sponge (SupreCell AR 4234 BR, Euroespuma, Portugal) was cut into cubes with approximately 1cm^3, the cubes were impregnated with nanoHA slurry and compressed repeatedly until most of the air bubbles were removed. Then, the excess suspension was removed by squeezing the foam after being dipped into the suspension. The slurry was prepared using a ratio of 5:4.4:0.2, respectively, of nanoHA powder (g) (nanoXIM Hap202, Fluidinova SA, Portugal), with an average particle size of 5.0 ± 1.0 μm, ultrapure water (mL), and dispersive agent Dolapix CE64 (mL) (Zschimmer & Schwartz, German). The impregnated sponges were dried in the oven at 37ºC for 1-2 h and then heat-treated in a sintering furnace (Termolab). The heat treatment cycle used was as follows: heating rate of 1 ºC/min till 600 ºC with 1h dwelling time, followed by a heating rate of 4 ºC/min till 1050 ºC with 1 h dwelling time. Afterwards, the samples were naturally cooled inside the furnace. After sintering, the scaffolds were crushed and sieved to obtain nanoHA granules with sizes between 2.00 – 3.35 mm.

2.1.2. Collagen crosslinking within nanoHA granules and heparin immobilization

Collagen inclusion and crosslinking within nanoHA granules, and heparin immobilization was done as previously described by Coelho et *al*. [67]. A 0.5 % (w/v) collagen solution was prepared by dissolving type I collagen (bovine Achilles tendon, Sigma-Aldrich) in HCl (0.01 M, pH = 2) at 4 ºC overnight. The solution was then homogenized using an Ultra Turrax (T25 D, IKA®) at 10000 rpm for 3 h on ice. Then it was diluted to a 0.05% solution and a single drop of collagen was added into each nanoHA granule. Afterwards, the nanoHA granules were placed in a vacuum oven (Binder, Germany) at room temperature (RT, 25 ºC) for 48 h to allow collagen to pass through the granules.

Collagen was chemically crosslinked with *N*-(3-dimethylaminopropyl)-*N*'-ethylcarbodiimide (EDC) (Aldrich) and *N*-hydroxysuccinimide (NHS) (Fluka), in a 2-mofpholinoethane sulfonic acid buffer (MES) (0.05 M, pH=5.4, Sigma). Regarding heparin immobilization, heparin (Sigma) was added to the previous solution. Collagen crosslinking and heparin immobilization reaction was carried out at 4 ºC for 2 h. Afterwards, the granules were placed in a phosphate-buffered saline (PBS) solution (pH = 7.4) for 2 h to stop heparin immobilization. PBS was then removed and a washing procedure with NaCl and ultrapure water was applied: 6 times with NaCl 2 M for 4 h, followed by 4 times with NaCl 4 M for 6 h and 3 times with ultrapure water for 8 h [87]. In the end, the granules were dried for 24 h in the vacuum oven at room temperature, resulting in heparinized nanoHA/collagen granules (HAColHep).

2.2 Granules Characterization

2.2.1. Scanning electron microscopy

Scanning electron microscopy (SEM) and energy-dispersive X-ray spectroscopy (EDS) were performed to analyse the granules morphology, collagen distribution, semiquantitative elemental chemical composition, the presence of vancomycin after lyophilization, and the effect of gamma radiation on the collagen mesh present on the surface of the granules. The analysis was achieved using a high-resolution environmental scanning electron microscope with X-ray microanalysis and electron backscattered diffraction analysis (FEI Quanta 400 FEG ESEM/EDAX Genesis X4M). The samples were previously fixed with Araldite on the aluminium samples holder and sputter coated with Au/Pd for 100 seconds and with a 15 mA current, using the SPI Module Sputter Coater equipment, resulting in a thin film, which grant them electrical conductivity.

2.2.2. Fourier transform infrared spectroscopy

Fourier transformed infrared (FTIR) spectroscopy was used to assess the chemical composition of nanoHA, heparinized nanoHA/collagen granules, heparinized nanoHA granules loaded with vancomycin and lyophilized, and gamma radiation sterilized heparinized nanoHA/collagen granules. FTIR spectroscopy is based on the absorption of infrared radiation, a characteristic present in all materials [88]. The location of the adsorption bands is related with the vibrational transitions in covalent bonds of specific functional groups of the biomolecules present [71, 88]. The Attenuated Total Reflection (ATR) represents a more critical way of acquiring the spectra due to difficulties in obtaining a good contact between the sample and the crystal, but is more suitable for a surface analysis (up to a depth of 0.5 - 5μm) [88, 89]. It is based on the multiple internal reflection of the beam incident on the sample [88]. KBr disks were made in order to perform the analysis in the transmission mode [89], the most used with materials which can be prepared in transparent samples [88]. In this technique, the beam passes through the sample and the transmitted energy is collected in the detector [88].

A FTIR spectrometer (Perkin Elmer 2000, Perkin Elmer) was used with a resolution of 4 cm^{-1} and a frequency region from 400 to 4000 cm^{-1}, and 100 scans were accumulated per sample. To make the KBr disks, a mortar was used to crush 2 mg of granules and 200 mg of KBr. Then, the powder was compressed with a hydraulic press. Regarding the ATR-FTIR analysis, an accessory (Universal ATR, Perkin Elmer) with a silicon hemispherical crystal was coupled to FTIR.

2.2.3. Confocal Raman spectroscopy

In order to complement the results obtained with FTIR analysis, Raman spectroscopy was also performed. Also, for symmetrical molecules, there are certain vibrational modes that are active and detectable with Raman spectroscopy but not with FTIR [70]. This technique detects changes in the polarization of the molecule, is also based on the vibrational motion of functional groups [88], allows to obtain a molecular fingerprint of biological samples [84] and has the advantage of not being affected by water, which is not possible in FTIR [70, 88]. By increasing the electron density, the bond strength will increase and so the bond length will decrease, leading to a decrease in the polarizability of the molecule [88]. When a monochromatic beam of high intensity radiation is irradiated in a sample, a portion of the radiation is scattered and the shifts produced with respect to the wavelength of the incident beam depend on the chemical structure of the molecules [88]. However, a longer exposure of the sample to the incident beam can lead to an increase in the temperature of the sample, affecting its nature and particular characteristics [70].

Raman spectra were collected with a Confocal Raman Microscope (LabRAM HR800 UV, Horiba Jobin-Yvon). A 633 nm laser diode was used as an excitation source. The incident laser beam was focused on the sample using a 100x objective lens. The signal was collected through a confocal pinhole of 100 µm. The samples were scattered on a spectral range from 400 to 4000 cm^{-1} with a spectral resolution of 0.2 cm^{-1}. The software for data acquisition and analysis was LabSpec 5.

2.3 Vancomycin release kinetics

Vancomycin loading was performed by immersing 20 mg of granules in Eppendorf tubes with 1 mL of vancomycin solution (HIKMA Farmacêutica, S.A.) with a concentration of 50 mg/mL. To perform antibiotic adsorption onto granules, the tubes were placed in an orbital shaker (KS 4000 IC, IKA®) at 37 ºC and 120 rpm and different times of adsorption were studied. Regarding the freeze-drying process, after the antibiotic adsorption, the granules were transferred to new Eppendorf's, frozen at -80 ºC for 4 h and lyophilized for 24 h (FreeZone Plus 2.5 Liter, U.S.).

After adsorption, the supernatant was removed, and the granules were transferred to new Eppendorf tubes, and 1 mL of PBS was added. The tubes were placed in the orbital shaker at 37 ºC and 120 rpm to begin the vancomycin release from the granules. To determine the vancomycin release from the granules, 200 µL of solution was withdrawn and replaced with fresh PBS solution every 24 h. The removed solution was centrifuged at 14000 rpm for 5 minutes to avoid particles in suspension. All tests were performed in triplicate.

Vancomycin concentration was determined by molecular absorption spectroscopy using a spectrophotometer UV-Vis (NanoDrop ND - 1000) at 280 nm, value which represents the maximum adsorption of vancomycin [15, 90].

2.4 Mass Spectrometry

Mass spectrometry is a technique to characterize various biomolecules like proteins, nucleic acids, and carbohydrates [91]. To measure biomolecules, their molecular mass must be known, or the masses of various components of the original molecule [91]. It is a technique with high sensitivity, high mass accuracy and structural information [91], that comprises four steps: first, the molecules of the sample are ionized, then ions are separated according to their mass-to-charge ratio (m/z), their abundance

is measured and the signal is converted into a form suitable for study [92]. The ion sources commonly used are fast-atom bombardment (FAB), electrospray ionization (ESI) and matrix-assisted laser desorption/ionization (MALDI) [91]. In this case, since vancomycin is a polar compound, it was applied positive electrospray ionization [93]. The use of mass spectrometry coupled with liquid chromatography (LC) has been used in the evaluation of drug safety [94].

The analysis was performed using a LC-MS Orbitrap technique to quantity the vancomycin released from both lyophilized and non-lyophilized nanoHA/collagen granules and to see if any degradation products of vancomycin were detected.

The LC-MS combines an Ultimate 3000 liquid chromatography system coupled to a Q-Exactive Hybrid Quadrupole-Orbitrap mass spectrometer (Thermo Scientific, Bremen, Germany) with an electrospray ionization source. Acquisition was performed in positive mode. The conditions of the analysis were optimized for vancomycin using a standard solution of the antibiotic in the mobile phase, injected in a C18 column using an auto-sampler and separated by a water/acetonitrile gradient. Full scan analysis was performed in the range *m/z* 400-1500, with a total chromatographic run time of 7.50 min. Regarding the peak analysis, it was considered the monoisotopic peak for the extraction ion chromatogram procedure (XIC).

2.5 Antibacterial Activity of Vancomycin

Vancomycin bioactivity was assessed by putting the granules in contact with bacterial suspension. For that, methicillin-resistant *S. aureus* (MRSA) ATCC 33591 was used, and the quantification of the suspended bacteria was obtained through the counting of the CFU's.

In order to prepare the materials for the incubation with the bacteria, they were first disinfected with ethanol 70 % for 30 min and then washed 3 times with NaCl. Then, for the antibiotic adsorption, the material was immersed in 400 µL of vancomycin solution. After antibiotic adsorption, the granules were transferred to a well plate, with replicates for each sample.

Firstly, the bacteria were grown on Tryptic Soy Broth (TSB) liquid medium for 24 h at 37 ºC and 150 rpm. The next day, that bacterial suspension was spread on a petri dish with TSB with Agar (TSA) and put in an incubator at 37 ºC overnight. From the Petri dish containing the bacteria, an inoculum was taken and incubated in TSB liquid medium for 3 h at 37 ºC and 150 rpm, corresponding to the exponential growth phase. The concentration of the bacterial suspension was adjusted to 10^8 CFU/mL and 400 mL of that suspension was added to each well containing 20 mg of granules. The materials were incubated with the bacterial suspension at 37 ºC for 24 h and 150 rpm. After incubation, successive dilutions of the bacterial suspension were made in NaCl, plated in TSA and incubated at 37 ºC for 18 h. Then, the number of colonies present on the plates were counted and the number of CFU/mL determined.

2.6 *MRSA* adhesion to granules

The adherent MRSA on granules surfaces was assessed using SEM. For that, granules with MRSA were washed with a saline solution and fixed using 1.5% (v/v) glutaraldehyde (Agar) in cacodylate buffer (0.14 M, Merk) for 10 min. Then the samples were dehydrated in increased concentrations of ethanol solutions for 10 min. The samples were dried overnight at RT. The adherent MRSA on the surface of the granules were visualized using SEM as previously described in Section 2.2.1.

2.7 Gentamicin release kinetics

The adsorption and release procedure used was identical to the one used for the vancomycin.

Briefly, gentamicin loading was performed by immersing 20 mg of granules in Eppendorf tubes with 1 mL of gentamicin sulphate solution (LABESFAL, Laboratórios Almiro, S.A.) with a concentration of 40 mg/mL [95, 96].

Gentamicin concentration was assessed by molecular absorption spectroscopy using a spectrophotometer UV-Vis (NanoDrop ND - 1000) at 280 nm (Figure A1, ANNEX).

2.8 Antibacterial Activity of Gentamicin

Gentamicin bioactivity was assessed by putting the granules in contact with bacterial suspension, as it was described previously for the vancomycin antibacterial activity (Section 2.5).

2.9 Sterilization Procedure

Granules were put on Falcon tubes and packed on a box filled with polystyrene and treated with 25 kGy γ-irradiation (Aragogamma, Spain), to evaluate if this sterilization process induces changes on the material, mainly on collagen.

2.10 Statistical Analysis

The statistical analysis was performed using one-way analysis of variance (One-Way ANOVA) followed by a *post hoc* Tukey's test with a significance level of $p < 0.05$. The results are expressed as the arithmetic mean ± standard deviation. The data analysis was performed using GraphPad Software.

Chapter 3

Results

3.1 Granules Characterization

3.1.1. Granules Morphology

SEM analysis was performed to observe the collagen distribution and if granules morphology obtained in previous studies was maintained. Moreover, it also allowed to detect if the freeze-drying process induced some changes in the granule's morphology as well as the presence of vancomycin after adsorption and lyophilization.

Figure 5 illustrates the presence of interconnective macroporosity (A and B), as well as microporosity (C, D, E and F), before (A, C and E) and after vancomycin adsorption and lyophilization (B, D and F). It is also possible to see in Figure 6 that the collagen is distributed heterogeneously and in a grid-like shape. This way, we can prove that the freeze-drying process does not induce changes in the nanoHA granule's morphology and on collagen distribution. Figure 7 depicts that the vancomycin, after being adsorbed and lyophilized, forms a film on the surface of the granules, covering the pores (A). In larger magnifications it is possible to notice that the vancomycin layer presents some discontinuities in its surface that allow the visualization the interior appearance of the vancomycin layer (B). The characteristic granular appearance of the granules (C, D and E) is also noted as well as the presence of microporosity (E, F and G).

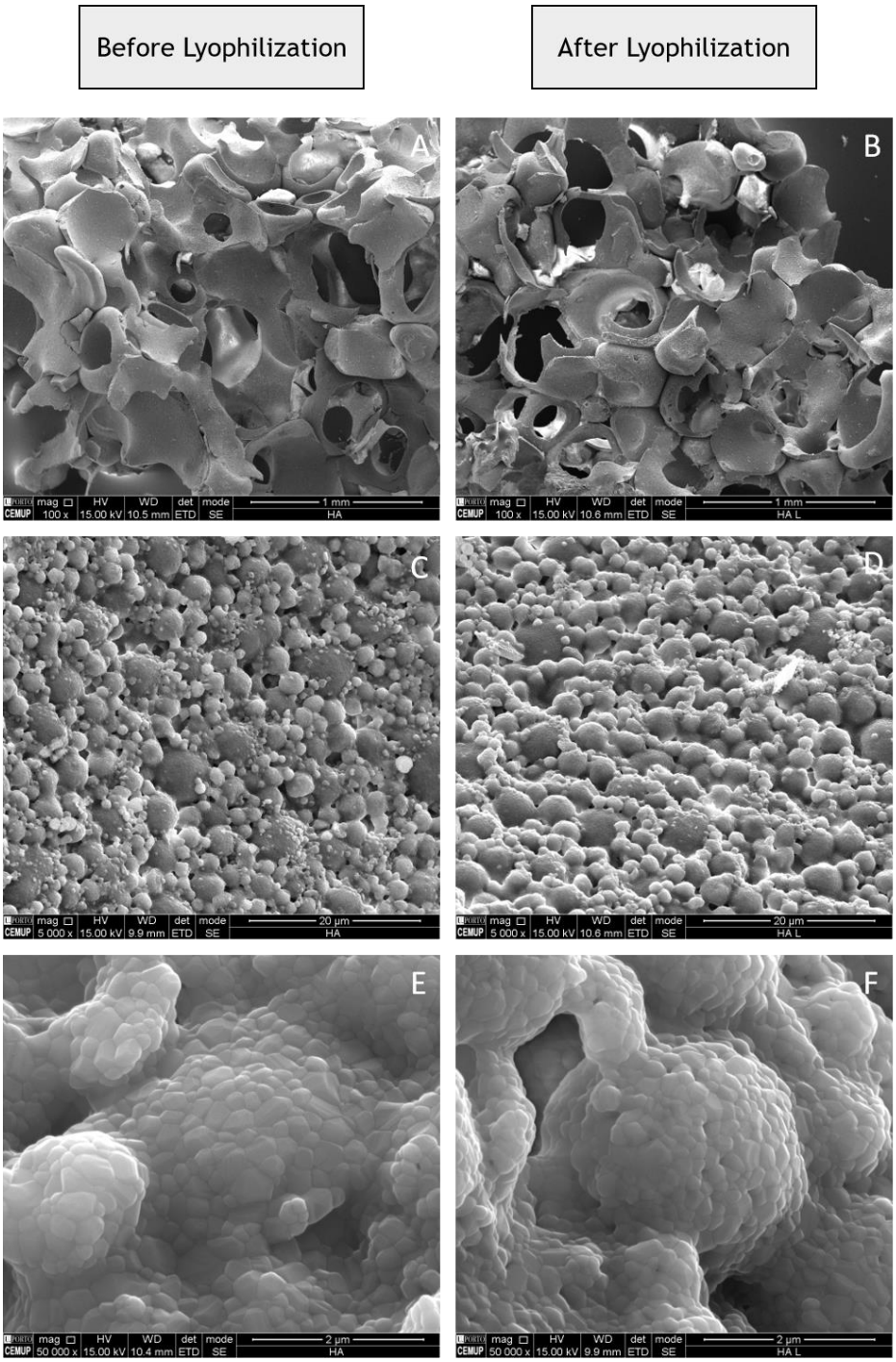

Figure 5 - NanoHA granules morphology before (A, C and E) and after lyophilization (B, D and F). A, B: Presence of interconnective macroporosity. C - F: Presence of microporosity.

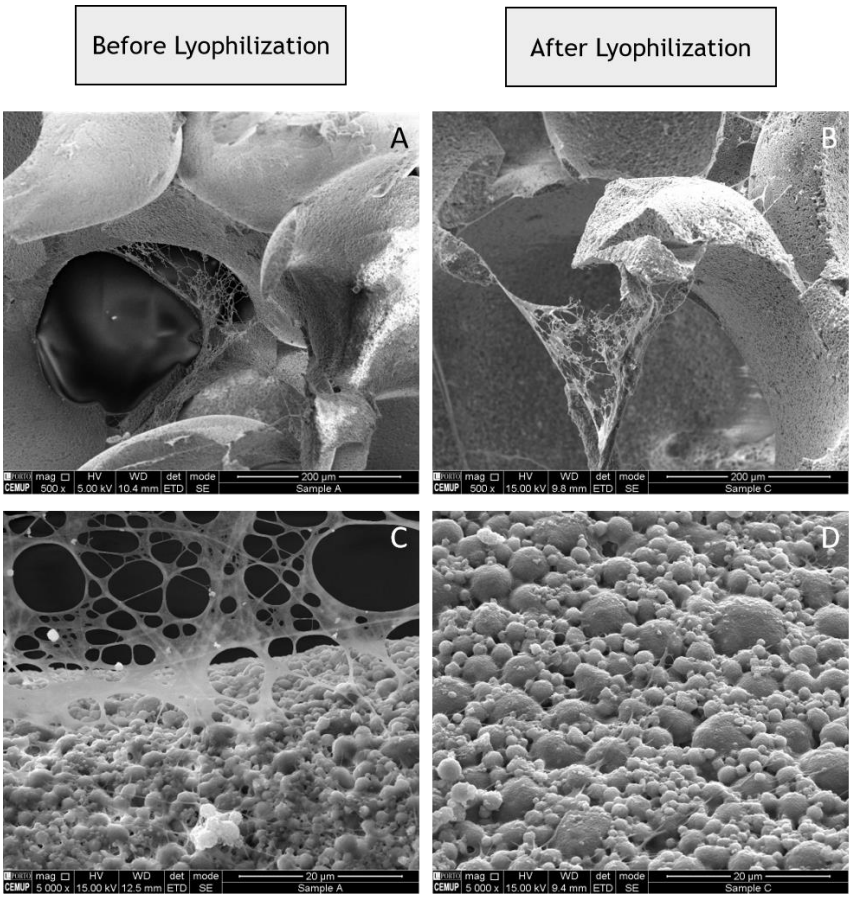

Figure 6 - Collagen distribution on heparinized nanoHA/collagen granules (A and C) and heparinized nanoHA/collagen granules that were lyophilized (B and D).

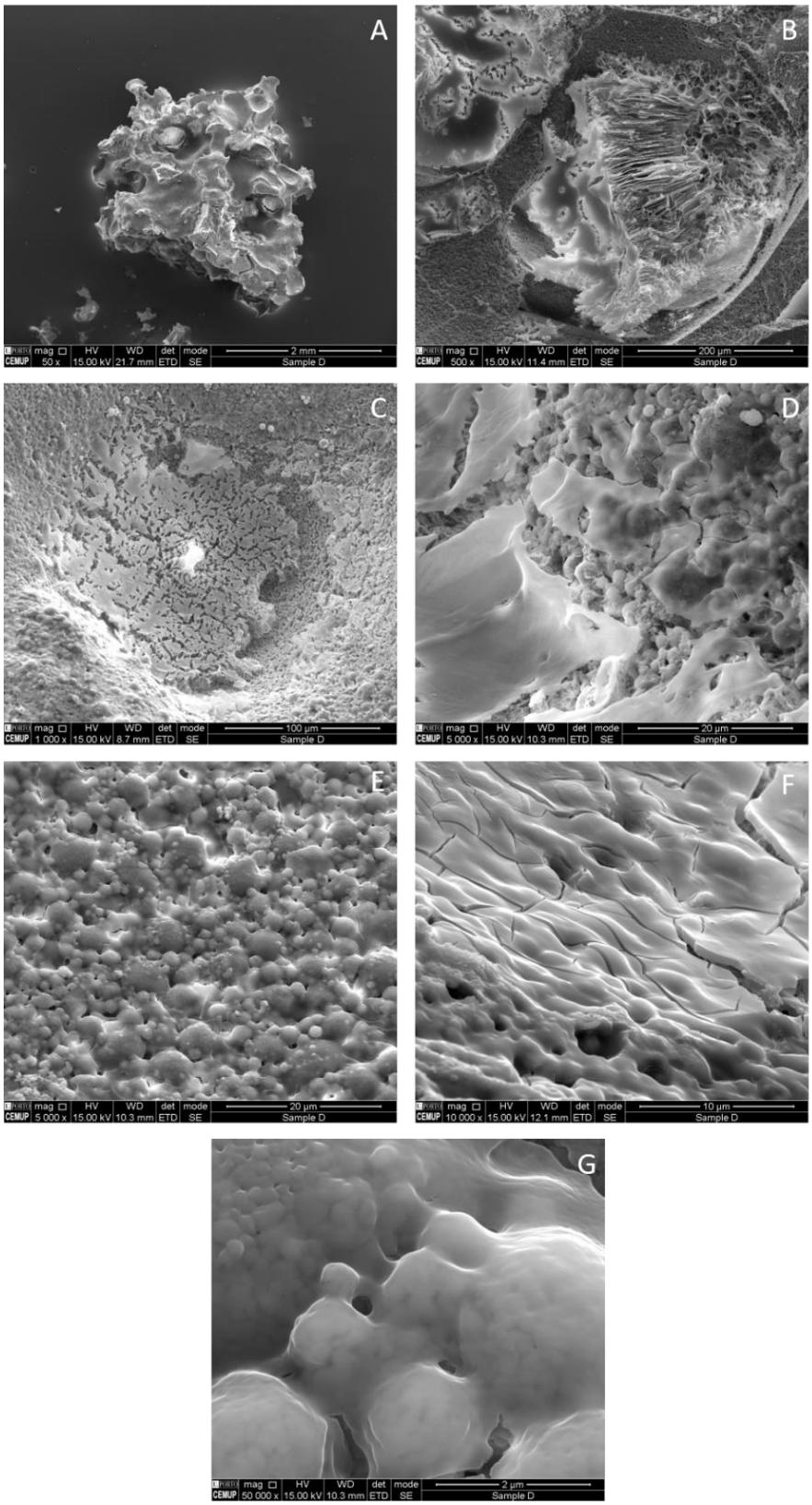

Figure 7 - NanoHA granules with vancomycin lyophilized. A: Vancomycin layer covers the macropores. B: The inside of the vancomycin layer. C - G: Vancomycin layer with cracks. D - G: Presence of microporosity.

The semiquantitative elemental chemical composition was assessed by EDS. In Figure 8 it is possible to observe a SEM image of a heparinized nanoHA/collagen granule, where two areas are represented. In zone Z2 it is possible to observe the presence of an agglomerate of collagen, confirmed by the detection of the representative elements of its chemical composition: C, N and O; the presence of Ca and P from nanoHA is also detected (Figure 8 (C)). In the spectrum of zone Z1 (Figure 8 (B)) it is possible to identify Ca and P but also C and O.

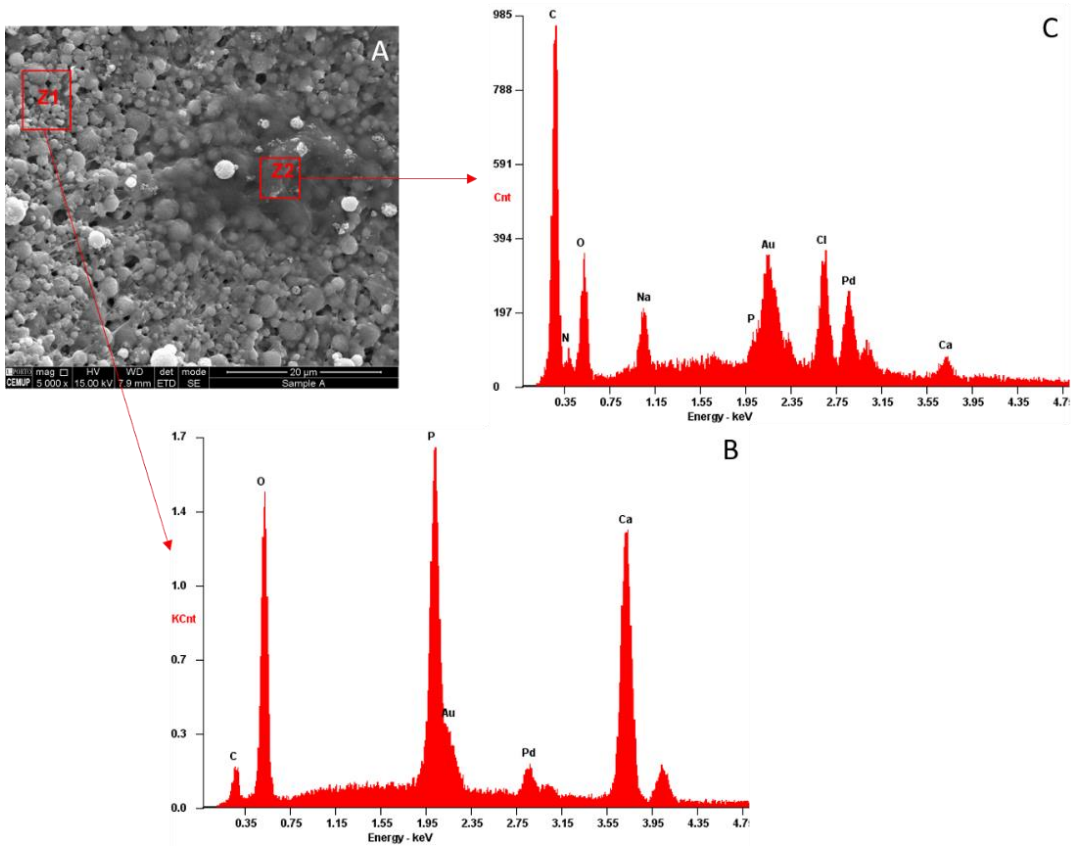

Figure 8 - EDS spectra of heparinized nanoHA/collagen granules. Z2 corresponds to an area with a larger agglomerate of collagen, compared to Z1. B: Spectrum of area Z1; C: Spectrum of area Z2

Figure 9 represents a SEM image of heparinized nanoHA/collagen granules that was lyophilized, where Z3 represents an area with a collagen layer, and Z4 an area with a lower amount of collagen, as it is possible to see on the respective spectrum: the spectrum of zone Z3 detects the presence of C and N, besides Ca, P and O; Z4 spectrum shows the presence of Ca, P, O, and C, and does not detect N.

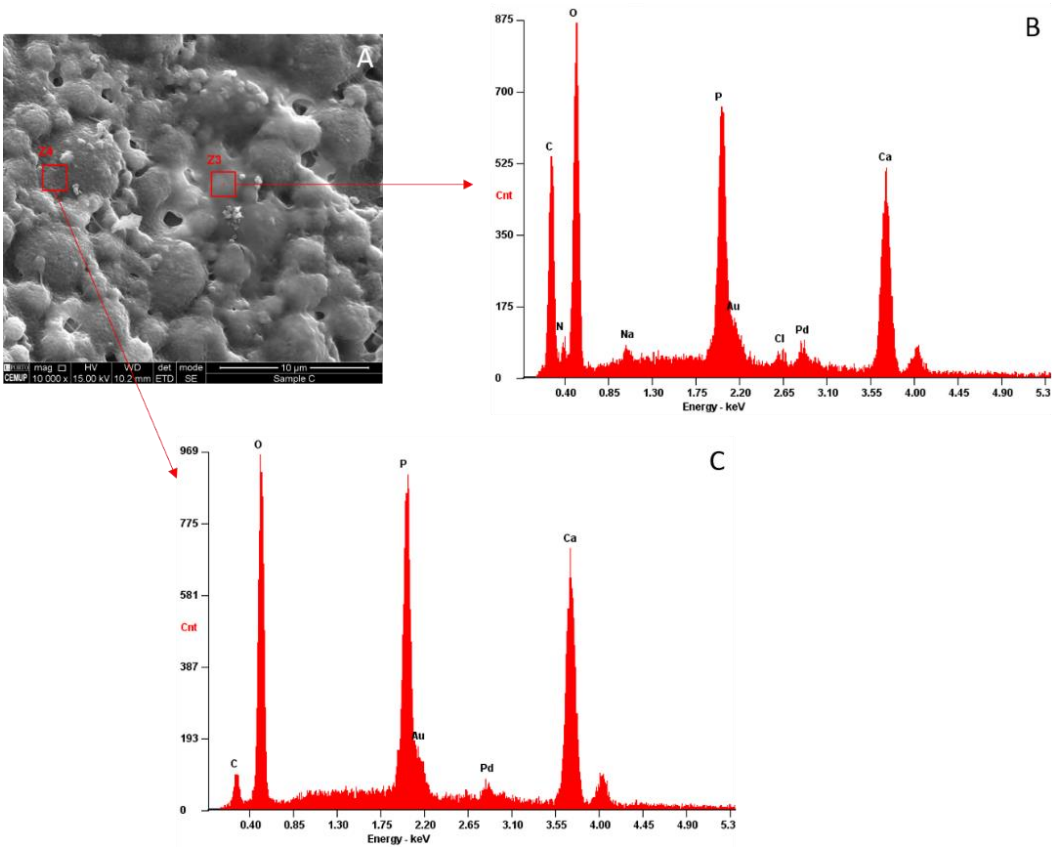

Figure 9 - EDS spectra of heparinized nanoHA/collagen granules that were lyophilized. Z3 corresponds to an area with a larger amount of collagen, compared to Z4. B: Spectrum of area Z3; C: Spectrum of area Z4.

In Figure 10 it is possible to observe a SEM image of a heparinized nanoHA/collagen granule with vancomycin adsorption and lyophilization, with two areas of the vancomycin layer, one focused on an apparently thicker area (Z2) than another. In zone Z1 (Figure 10 (B)) is possible to identify C, N and O, representative elements of vancomycin. In zone Z2 (Figure 10 (C)) these elements are present, as well as Cl, also representative of vancomycin but not detected in Z1.

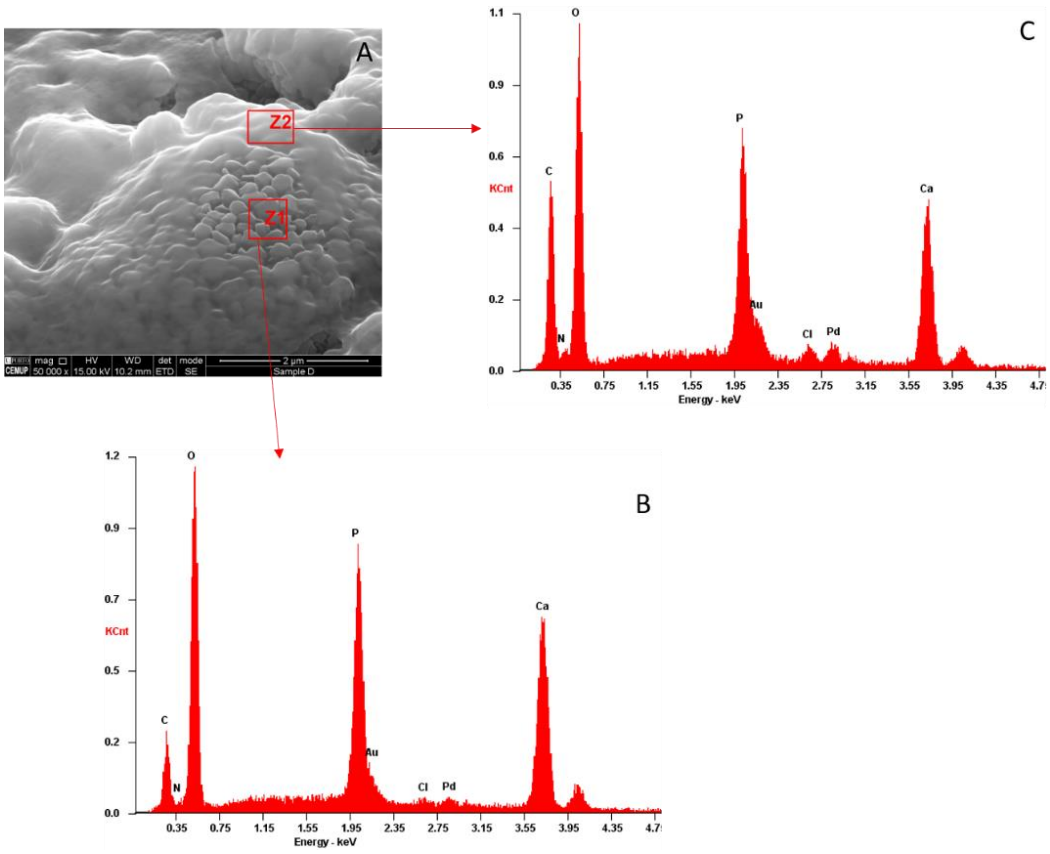

Figure 10 - EDS spectra of granules with lyophilized vancomycin. Both zones are of the vancomycin layer, but Z2 is a denser area. B: Spectrum of area Z1; C: Spectrum of area Z2.

3.1.2. Chemical Composition

Regarding the chemical composition of the granules, infrared and Raman spectroscopy were used to provide complementary information. Although functional groups adsorb radiation in a small frequency range, the position of a band may change due to interactions with the surrounding atoms [88].

3.1.2.1. Infrared Spectroscopy

The ATR-FTIR analysis was performed on granules of HA, nanoHA/collagen (HAColHep), HA lyophilized, nanoHA/collagen that were lyophilized (HAColHep_L), and also with vancomycin adsorbed to the surface and lyophilized (VHAColHep), revealing the spectra obtained in Figure 11. This analysis made it possible to determine whether the lyophilization process affected the chemical composition not only of nanoHA, but also of collagen. It also allowed the detection of characteristic vancomycin peaks.

Considering the sample of HA, the characteristic peaks of the phosphate group were obtained at 473, 562, 599, 961, 1023 and 1087 cm^{-1} [67, 68, 97, 98, 99], where the band at 473 cm^{-1} corresponds to vibrational mode $\upsilon 2$, the bands at 562 and 599 cm^{-1} are referred to mode $\upsilon 4$, 961 cm^{-1} represents the $\upsilon 1$ mode, and 1023 and 1087 cm^{-1} are relative to mode $\upsilon 3$. Peaks associated to hydroxyl (OH^-) were detected at 630 and 3572 cm^{-1} which corresponds to OH^- vibrational and stretching modes, respectably [67, 68, 98]. This analysis confirmed that, even after being lyophilized, HA maintains its typical peaks, and no additional peaks corresponding to new functional groups were originated. These peaks are also present in the remaining samples, thus confirming the presence of HA in all of them.

Considering the sample with vancomycin (VHAColHep), the peaks found at 1652, 1587, 1504 and 1230 cm^{-1} represent an amide I, amide II, an aromatic ring and a phenol group, respectively [100, 101, 102, 103, 104]. Other peaks characteristic of vancomycin where found at 3283, 1424 and 707 cm^{-1} [103]. In Figure A4 of the ANNEX it is possible to see the spectrum with a higher magnification.

Regarding the samples with collagen, the characteristic peaks of collagen were not detected, so it's presence cannot be confirmed, neither if it has changed.

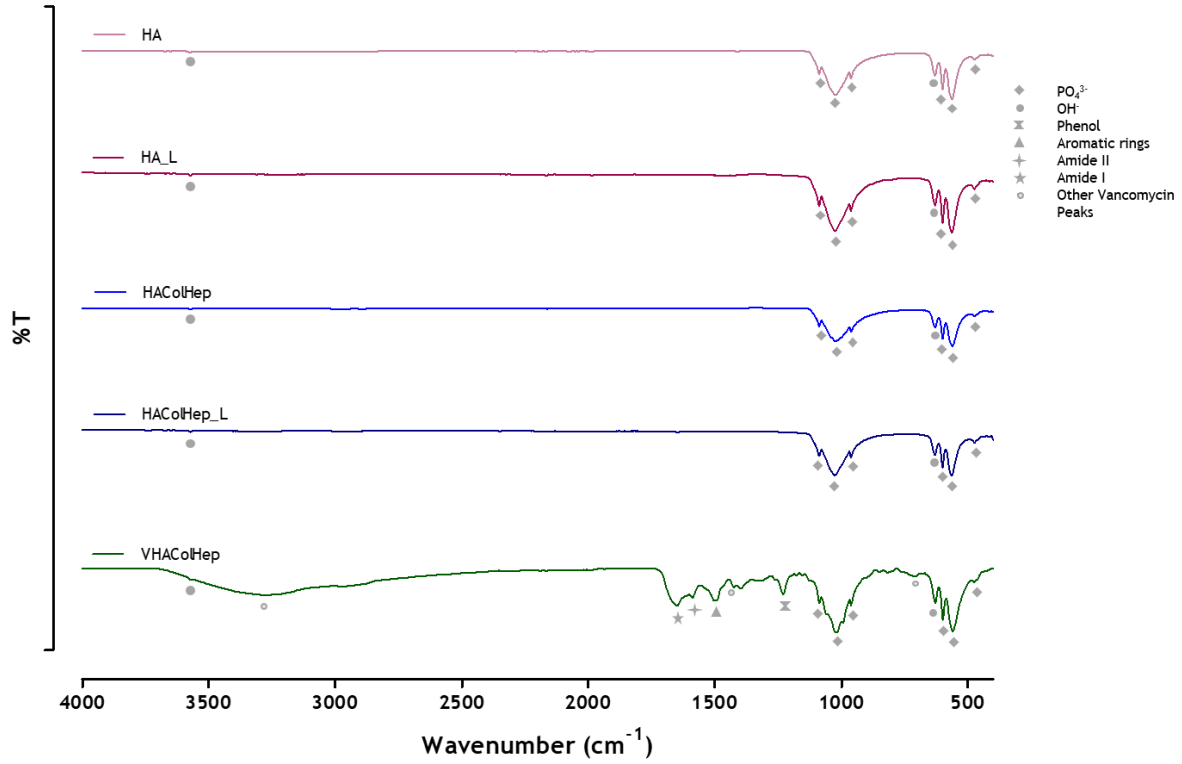

Figure 11 - ATR-FTIR spectra of HA, HA lyophilized (HA_L), nanoHA/collagen (HAColHep), lyophilized HAColHep (HAColHep_L) and HAColHep with vancomycin lyophilized (VHAColHep).

3.1.2.2. Raman Spectroscopy

Raman Spectroscopy was performed on granules of HA, nanoHA/collagen (HAColHep), HA lyophilized, nanoHA/collagen that were lyophilized (HAColHep_L), and also with vancomycin adsorbed to the surface and lyophilized (VHAColHep). Figure 12 shows the spectra of the referred samples.

Considering the sample of HA, the characteristic peaks of the phosphate group were obtained at 431, 447, 580, 592, 608, 616, 962, 1028, 1047, 1054, 1062 and 1076 cm^{-1} [105, 106], where the peaks at 431 and 447 cm^{-1} are relative to doubly degenerated bending mode ($\upsilon 2$) of the PO_4^{3-} group, peaks at 580, 592, 608 and 616 cm^{-1} are referred to triply degenerated bending mode ($\upsilon 3$) of PO4, 962 cm^{-1} represents a totally symmetric stretching mode ($\upsilon 1$) of the tetrahedral PO4, and 1028, 1047, 1054 and 1076 cm^{-1} are characteristic peaks of a triply degenerated asymmetric stretching mode ($\upsilon 3$) of the phosphate group. The peak found at 1062 cm^{-1} could be due to a C-C stretching [107]. Since all peaks are present in all samples, this analysis confirmed that the lyophilization process did not alter the granules composition.

Considering the sample with vancomycin peaks were found at 587, 1235, 1609, 2909, 2937, 2948 and 3056 cm^{-1} [107, 108, 109]. The peak found at 1609 cm^{-1} is relative to cytosine (NH_2); 1235 cm^{-1} corresponds to amide III; 587 cm^{-1} could be a free OH, out of plane bending; 2909 cm^{-1} could be an asymmetric stretch (range 2889 - 2908 cm^{-1} [107]); and 2937 cm^{-1} may be a chain end CH_3 symmetric band (~ 2935 cm-1 [107]).

Similarly to FTIR, it was not possible to identify the presence of collagen.

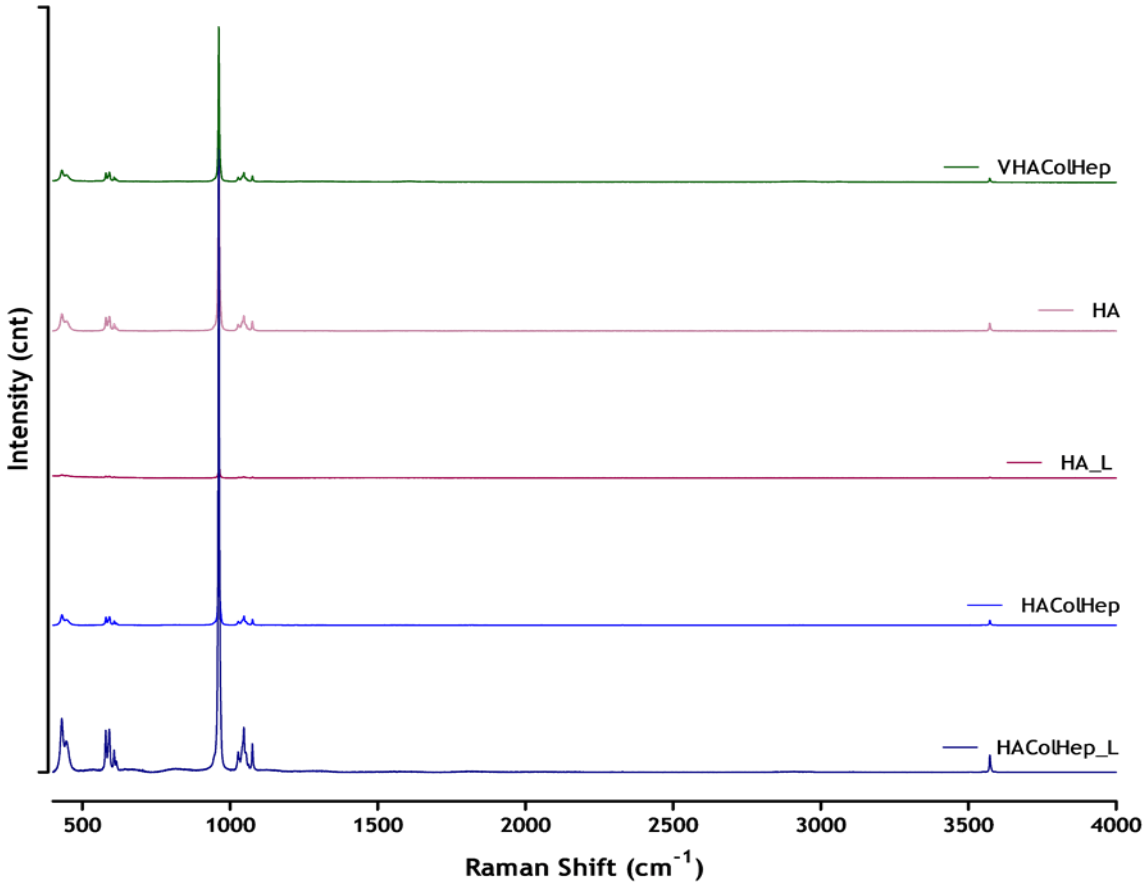

Figure 12 - Raman spectra of HA, HA lyophilized (HA_L), nanoHA/collagen (HAColHep), lyophilized HAColHep (HAColHep_L) and HAColHep with vancomycin lyophilized (VHAColHep).

3.2 Vancomycin release kinetics

The vancomycin release from heparinized nanoHA/collagen granules was studied for adsorption times of 0.25, 0.5 and 2 h (Figure 13). It is possible to verify that the release of antibiotic was possible during 23 days for granules with 2 h adsorption (V_2h), 22 days for granules with 0.5 h adsorption (V_0.5h) and 18 days for granules with 0.25 h adsorption (V_0.25h), with a limit of quantification of 9.11 µg/mL. Comparing the different adsorption times, V_2h and V_0.5h have a similar and higher release profile than V_0.25h, with the exception of day 11. Nevertheless, V_2h is able to release antibiotics for a prolonged period of time. No statistically significant differences were found between the different adsorption times for the same day.

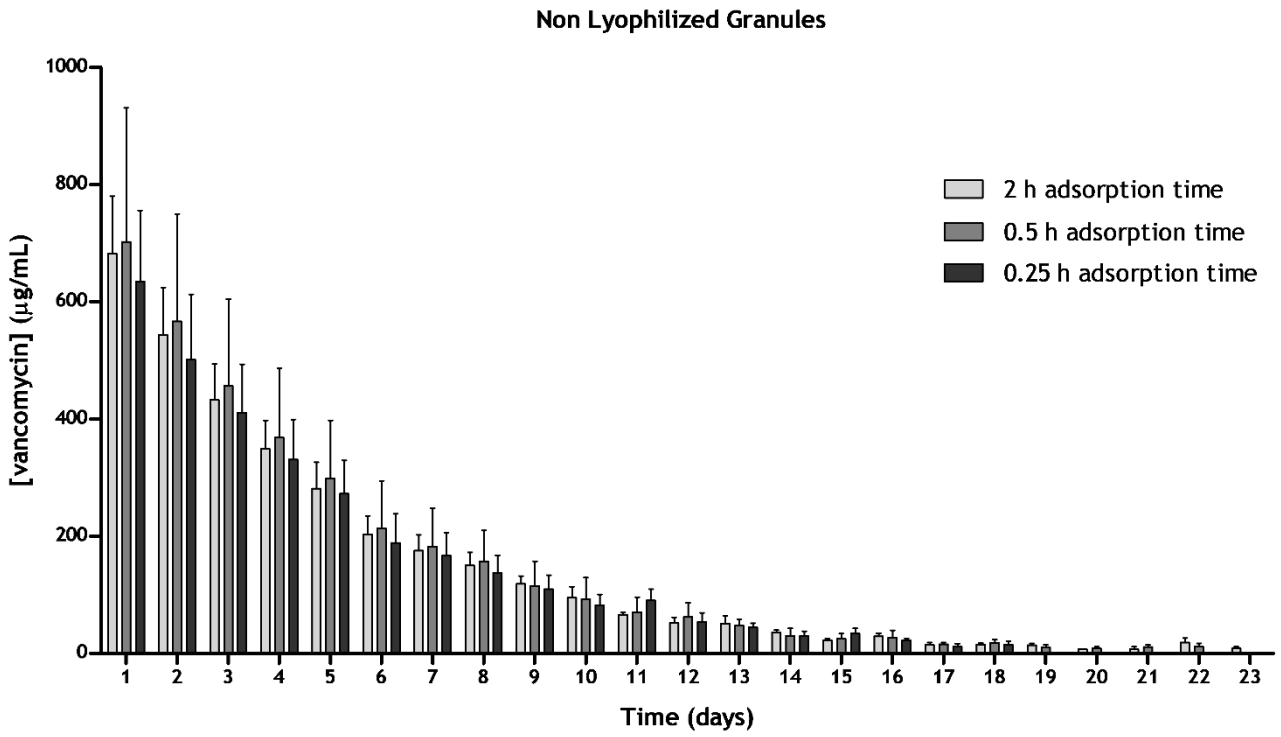

Figure 13 - Vancomycin release from nanoHA/collagen granules versus time, for different adsorption times.

Regarding lyophilized granules it was tested if by increasing the adsorption time, the amount of vancomycin released would be higher. For this purpose, adsorption times of 0.5, 2 and 24 h were used. In Figure 14, it is possible to observe that an antibiotic release was possible during 26 days for granules whose antibiotic adsorption was 24 h (VL_24h), 24 days for granules whose adsorption was 2 h (VL_2h) and 20 days for granules with 0.5 h adsorption (VL_0.5h). Comparing the different adsorption times, VL_24h releases a higher amount of antibiotic in the first 3 days, from the fourth day on VL_2h starts to release more. Statistically significant differences were found in most of the release profile, comparing 2 h with 24 h of antibiotic adsorption (days 5 - 10, 13 - 15, 17 and 19). Comparing adsorption times of 0.5 and 24 h, statistically significant differences were found near the end of the granule release profile with 0.5 h adsorption, and therefore on days 13 – 15 and 17 - 19. For adsorption times of 0.5 h and 2 h no statistically significant differences were found.

By comparing lyophilized and non-lyophilized granules (Figure A4, ANNEX), non-lyophilized granules show a higher initial antibiotic release, but lyophilized granules are able to release antibiotics for an extended time. For 0.5 h adsorption, statistically significant differences were found between lyophilized and non-lyophilized granules on day 20. For granules with 2 h adsorption, significant statistical differences were found for days 14, 15, 17 - 21 and 23.

The release of vancomycin results obtained show that the concentration of vancomycin in solution for each time point was always higher than the vancomycin minimum inhibitory concentration (MIC) for MRSA (MIC ≤ 2 μg/mL) [15, 110, 111].

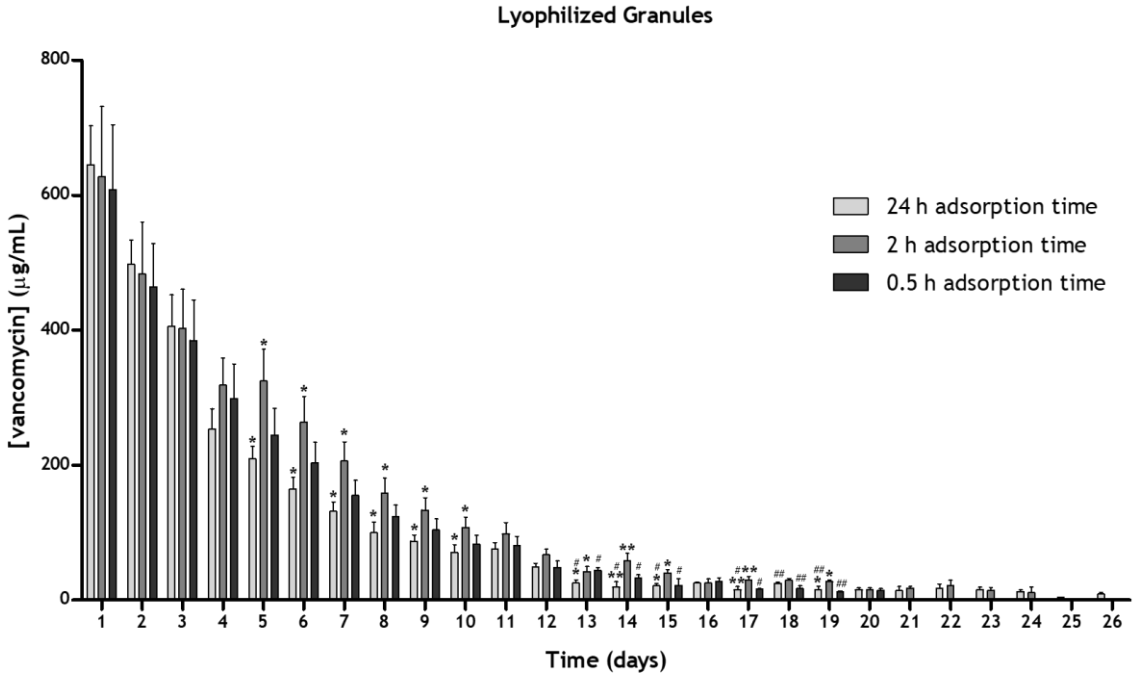

Figure 14 - Vancomycin release from lyophilized nanoHA/collagen granules versus time. Vancomycin adsorption occurred for 0.5, 2 and 24 h. *, ** Represents a statistically significant difference ($p<0.05$ and $p<0.01$, respectively) compared 24 h and 2 h adsorption for the same time point. #, ## Represents a statistically significant difference ($p<0.05$ and $p<0.01$, respectively) compared 24 h and 0.5 h adsorption for the same time point.

3.2.1. SEM Observation

The release of vancomycin from the granules was stopped when the values detected by spectrophotometry were no longer measurable. For granules that have been lyophilized with vancomycin adsorbed, in order to prove that there was no longer any antibiotic adsorbed to the surface, they were dried and prepared for SEM analysis, as described in Section 2.2.1. According to Figure 15, the antibiotic layer was no longer present on the surface of the material: the interconnected macroporosity was again evident (Figure 15 (A and B)), as well as the microporosity (Figure 15 (C and D)). It is also possible to observe in sections C and D that the collagen fibers are in the form of a network, apparently unaffected.

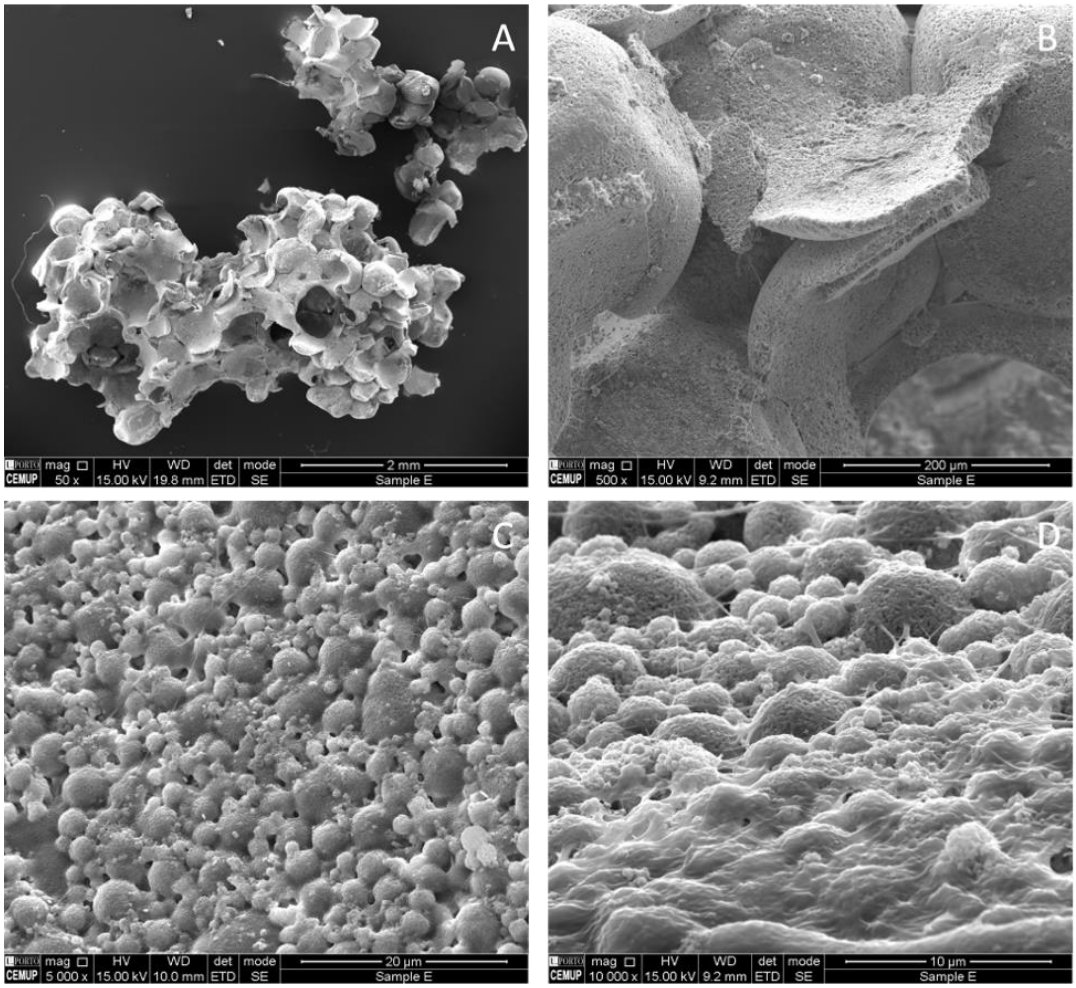

Figure 15 – Heparinized nanoHA/collagen granules with vancomycin adsorbed and lyophilized at the end of the antibiotic release. A and B: presence of interconnected macroporosity. C and D: presence of microporosity and collagen fibers.

3.2.2. FTIR Analysis

ATR-FTIR analysis was performed on the granules that have been lyophilized with vancomycin adsorbed after complete vancomycin release and in Figure 16, it is possible to visualize that the characteristic peaks of vancomycin are no longer present, showing only the characteristic peaks of HA, thus proving the absence of vancomycin in the material.

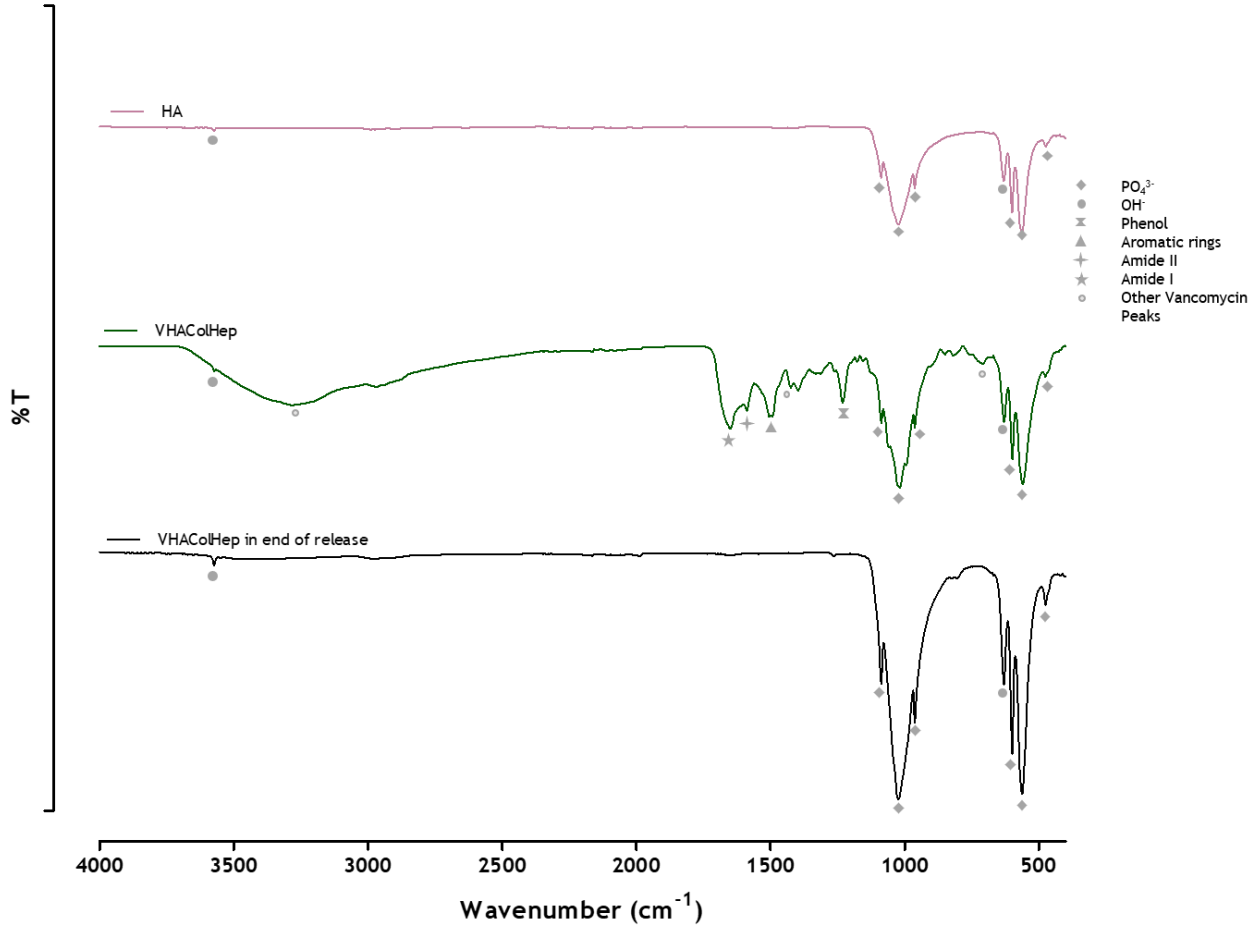

Figure 16 - ATR-FTIR spectra of HA, nanoHA/collagen with vancomycin lyophilized (VHAColHep) and VHAColHep in the end of the antibiotic release.

3.3 Mass Spectrometry

The LC-MS analysis was applied on samples of days 1,15 and 21 of the antibiotic release for both lyophilized and non-lyophilized samples with 2 h adsorption. First, a full scan MS analysis was performed on a vancomycin sample to determine the most intensive peaks and to trace the calibration curve in order to determine the amount of vancomycin present in the samples. The most intensive ion was at *m*/*z* 725, and corresponds to a doubly charged ion of vancomycin [112, 113, 114], and it was observed at a retention time of 4.40 min (Figure A6, ANNEX). The ion *m*/*z* 725 was scanned to determine the peak area of vancomycin in each sample. Figure 17 illustrates the use of this technique in the determination of the concentration of vancomycin in the several days.

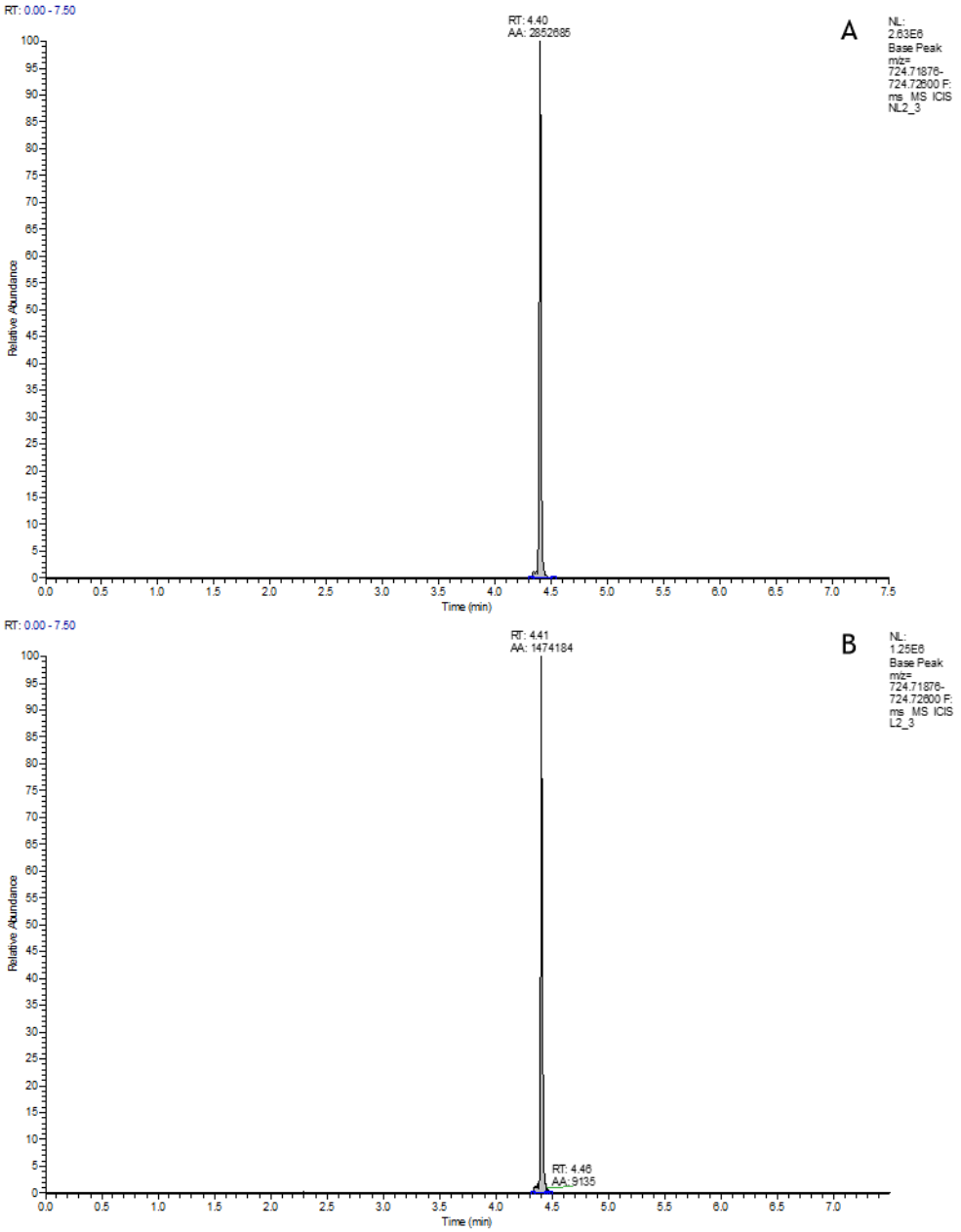

Figure 17 - Mass chromatograms of vancomycin samples with 2 h antibiotic adsorption. A: Sample of non-lyophilized nanoHA/collagen granules at day 1; B: Sample of lyophilized nanoHA/collagen granules at day 1.

The vancomycin concentration on each day is represented in Figure 18, where section B is a reduction of the x-axis for displaying the values of days 15 and 21. On day 1, we had a vancomycin quantification of about 1548 µg/mL for non-lyophilized nanoHA/collagen granules and 811 µg/mL for lyophilized. On day 15 the vancomycin values decreased to 23 µg/mL and 37 µg/mL, for lyophilized and non-lyophilized, respectively. On day 21, near the end of the antibiotic release, the values obtained were 4 µg/mL for non-lyophilized granules and 8 µg/mL for lyophilized. Statistically significant differences between lyophilized and non-lyophilized granules were found at the beginning (day 1) and near the end of antibiotic release (day 21).

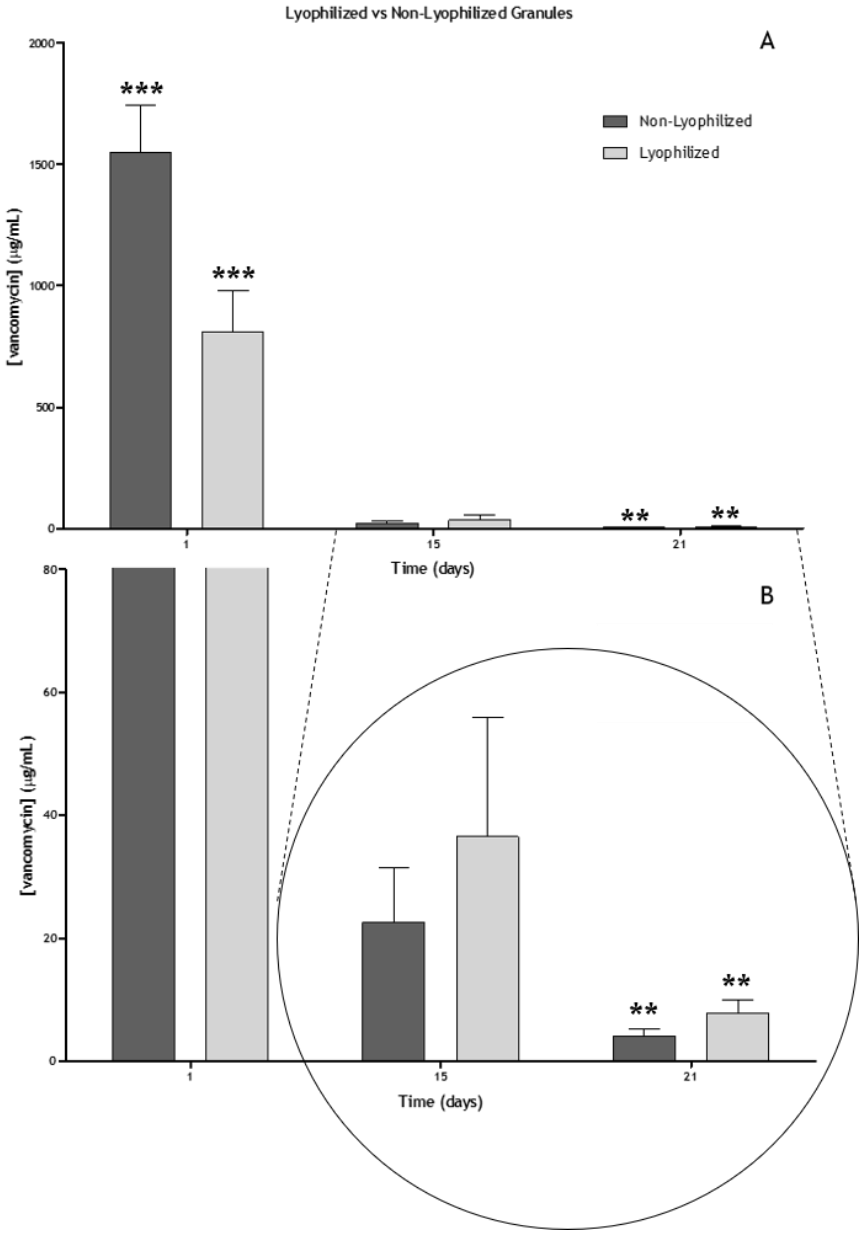

Figure 18 – A: Vancomycin quantification by LC-MS on days 1, 15 and 21 of the antibiotic release. B: Magnification of the x-axis for displaying the values of days 15 and 21. ** Represents a statistically significant difference ($p<0.01$) compared lyophilized with non-lyophilized granules with 2 h adsorption for the same time point. * Represents a statistically significant difference ($p<0.001$) compared lyophilized with non-lyophilized granules with 2 h adsorption for the same time point.**

Concerning the detection of vancomycin degradation products: a supernatant analysis of non-lyophilized (Figure 19 (A)) and lyophilized (Figure 19 (B)) nanoHA/collagen granules was performed in the last days of release (day 21) and no products resulting from vancomycin degradation were detected.

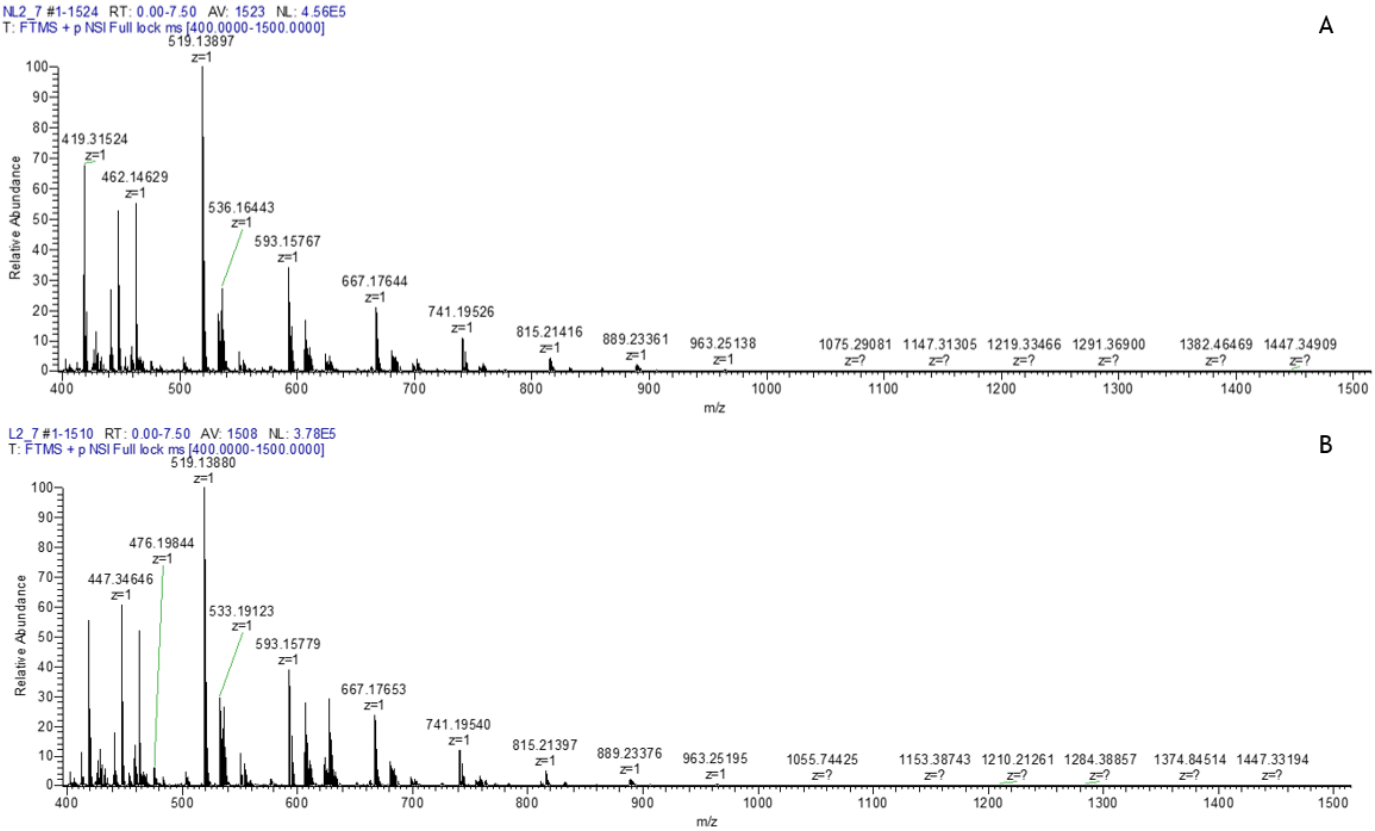

Figure 19 - Product scan of vancomycin in the supernatant of nanoHA/collagen granules. A: Scan from non-lyophilized granules at day 21; B: Scan from lyophilized granules at day 21.

3.4 Antibacterial Activity of Vancomycin

Results from bacterial adhesion studies with vancomycin are shown in Figure 20, and are expressed in Log_{10}(CFU/mL). After 24 h of incubation of the MRSA with granules, there is a 100 % reduction in the number of bacteria in suspension in the granules with vancomycin adsorbed, and 99.99 % reduction in the lyophilized granules, compared to granules without antibiotics.

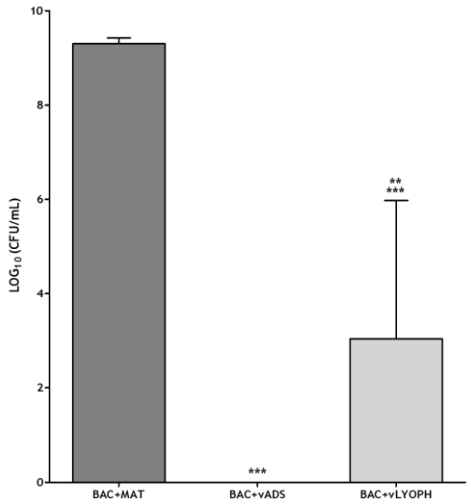

Figure 20 - Quantification of MRSA adhered onto granules expressed as Log10(CFU/mL) after incubation of the granules with vancomycin adsorbed and lyophilized, for 24 h. ** Represents a statistically significant difference (p<0.01) compared granules with vancomycin lyophilized (BAC +vLYOP) with non-lyophilized (BAC+vADS). * Represents a statistically significant difference (p<0.001) compared granules with (BAC+vADS and BAC+vLYOPH) and without vancomycin (BAC+MAT).**

3.5 *MRSA* adhesion to vancomycin granules

Figure 21 shows the results obtained from the bacterial adhesion studies. As it is possible to see in the images, the adsorption of vancomycin allowed a significant reduction in the number of bacteria adhered to the granules. This result corroborates the results obtained in the quantification of MRSA adhered: the use of antibiotics allows a reduction in the number of bacteria when compared to the material alone (A and B).

In images A and B, of the material without antibiotics, it is possible to verify that the bacteria have the characteristic spherical morphology, coccus, and that some are clustered. It is also possible to observe that in the samples that were in contact with the antibiotic, some bacteria suffer morphological alterations on the surface, and appear to be destroyed.

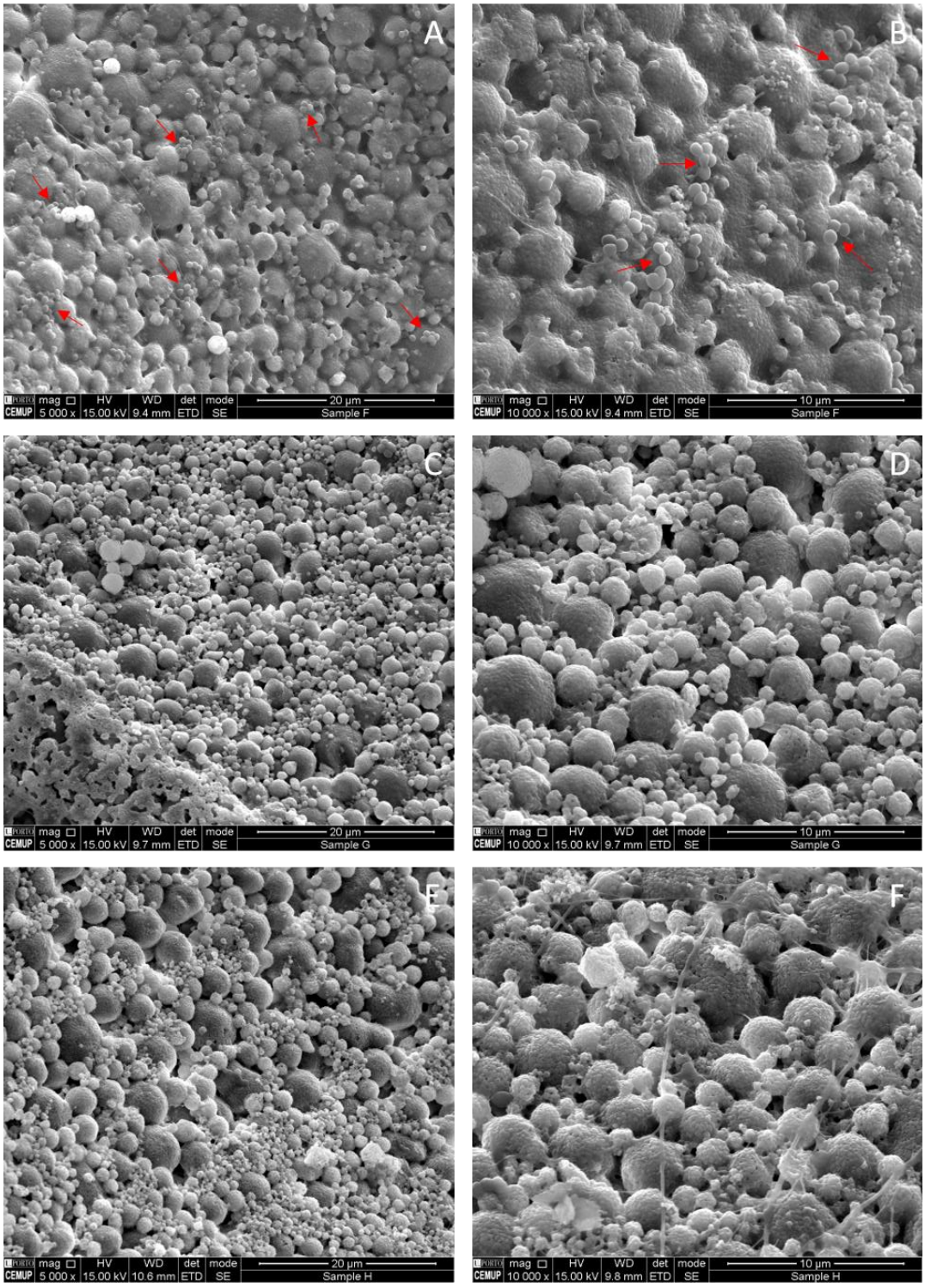

Figure 21 - SEM images of MRSA adhesion to granules. A and B: granules without vancomycin adsorption; C and D: granules with vancomycin adsorption; E and F: granules with vancomycin adsorption and lyophilization.

3.6 Gentamicin release kinetics

A preliminary study of gentamicin release from heparinized nanoHA/collagen granules was performed for 2 h adsorption, using 15 mg/mL and 40 mg/m of gentamicin. On Figure 22 it is possible to observe that an antibiotic release was possible during 15 days for granules with 15 mg/mL of gentamicin. For 40 mg/mL of gentamicin the quantity released on the first day increased to about 600 μg/mL (instead of 240 μg/mL when using 15 mg/mL), being possible to release antibiotic for 17 days.

The release of gentamicin results obtained show that the concentration of gentamicin in solution for each time point was always higher than the gentamicin minimum inhibitory concentration (MIC) for MRSA (MIC ≤ 1 μg/mL) [115].

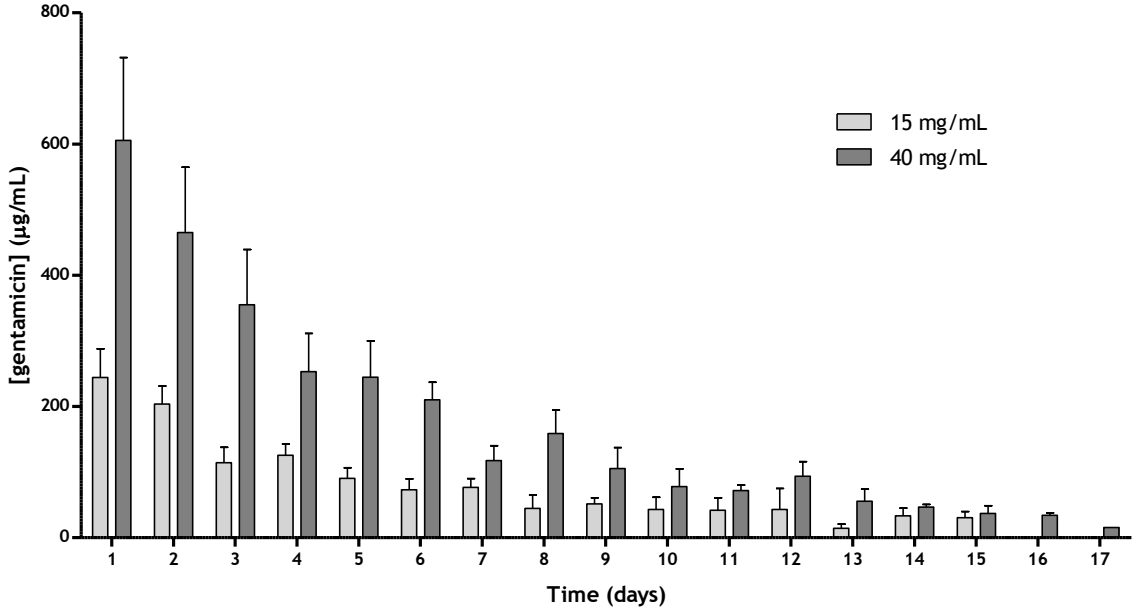

Figure 22 - Gentamicin release from heparinized nanoHA/collagen granules versus time, for different antibiotic concentrations adsorbed.

3.7 Antibacterial Activity of Gentamicin

Preliminary bacterial (MRSA) adhesion results using nanoHA/collagen granules with adsorbed gentamicin are showed in Figure 23. After 24 h of incubation of the MRSA with granules, it is possible to see that there was a 100 % reduction in the number of bacteria in suspension in the granules with gentamicin adsorbed compared to granules without antibiotics.

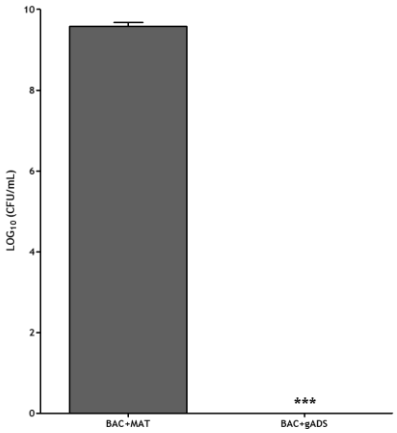

Figure 23 - Quantification of MRSA adhered in nanoHA/collagen granules expressed as Log_{10}(CFU/mL). Granules were incubated with gentamicin for 24h. * Represents a statistically significant difference ($p<0.001$) compared granules with (BAC+gADS) and without gentamicin (BAC+MAT).**

3.8 Effect of Gamma Sterilization

3.8.1. Granules Morphology

SEM analysis was performed to understand if the sterilization by gamma radiation affected the granules morphology, chemical composition or collagen distribution. On Figure 24 it is possible to observe that the morphology of biocomposite was maintained after sterilization showing the characteristic interconnective macroporosity (A and B), as well as microporosity (C and D). It is also possible to observe in Figure 25 that the collagen is still heterogeneously distributed after sterilization (C and D) and in a form of a grid when compared to the one on granules before sterilization (A and B).

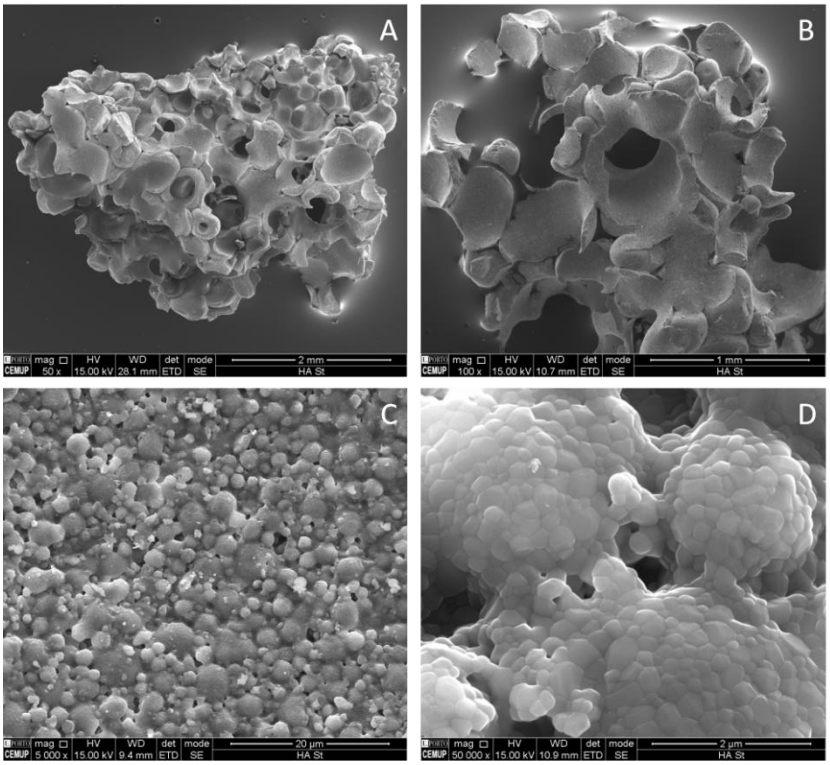

Figure 24 - NanoHA granules morphology after gamma sterilization. A, B: Presence of interconnective macroporosity. C, D: Presence of microporosity.

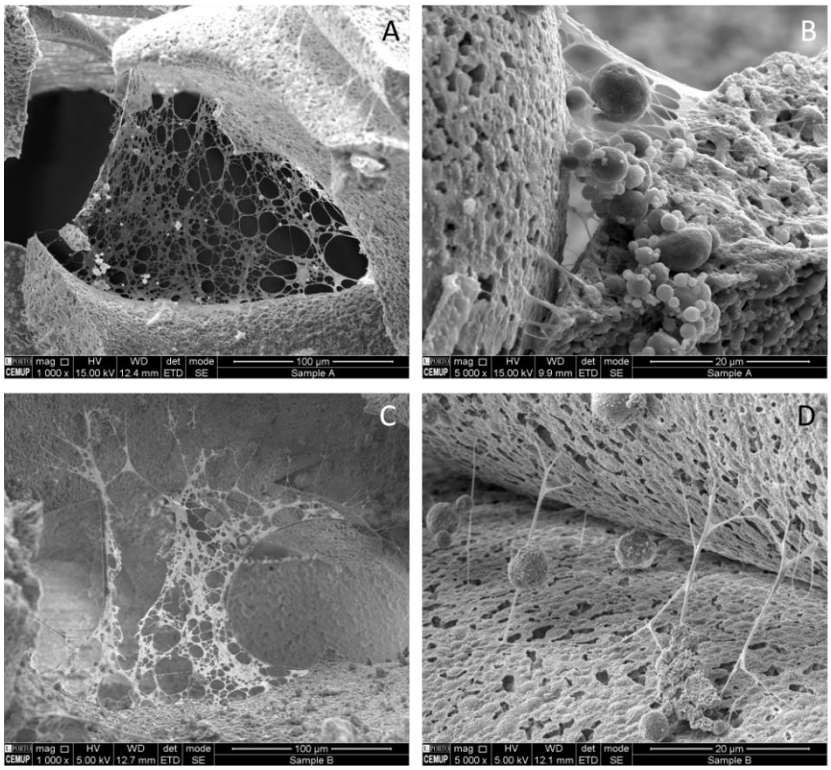

Figure 25 - Collagen distribution on heparinized nanoHA/collagen granules (A and B) and heparinized nanoHA/collagen granules sterilized with gamma radiation (C and D).

This way we can assume that the gamma sterilization does not seem to affect the granules morphology neither the collagen distribution, making it an efficient way to sterilize the material.

Similarly, an EDS analysis was performed to assess the semiquantitative elemental chemical composition. On Figure 26 it is possible to observe a SEM image of a gamma sterilized heparinized nanoHA/collagen granule. Z1 zone represents part of a broken collagen network, confirmed by the detection of the representative elements of its chemical composition: C, N and O; the presence of Ca and P from nanoHA is also detected.

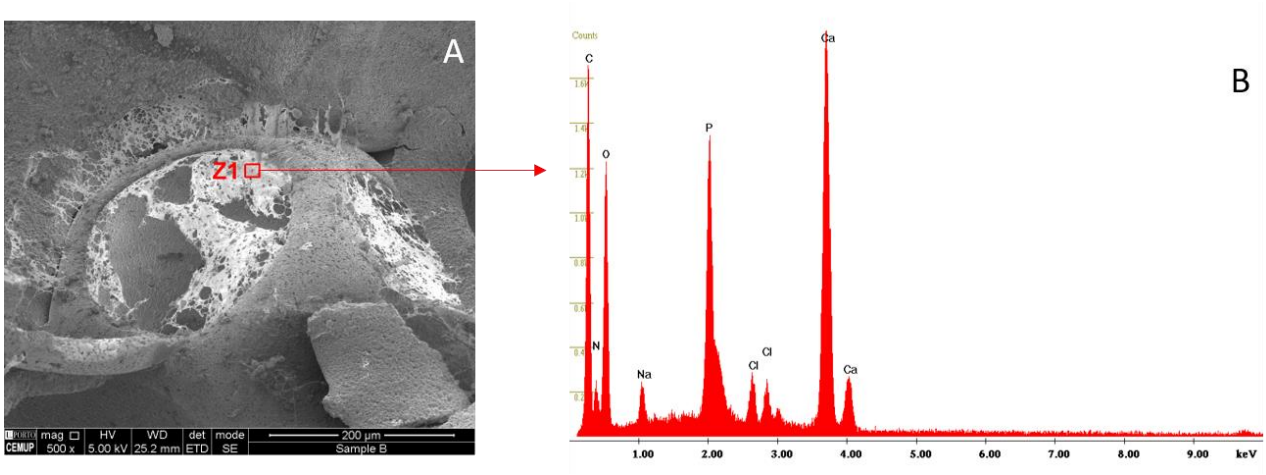

Figure 26 - EDS spectra of heparinized nanoHA/collagen granules sterilized with gamma radiation. Z1 corresponds to an area of a collagen network. B: Spectre of area Z1.

3.8.2. Granules Chemical Composition

The ATR-FTIR analysis was also performed on granules of HA, nanoHA/collagen, and HA and nanoHA/collagen that were sterilized with gamma radiation, revealing the spectra obtained in Figure 27. This analysis made it possible to determine whether the sterilization process affected the chemical composition not only of collagen, but also of nanoHA.

Considering the sample of HA lyophilized, the characteristic peaks of the phosphate and hydroxyl groups were obtained at locations previously described (473, 562, 599, 629, 961, 1023, 1087 and 3572 cm^{-1} [67, 68, 97, 98, 99]). This analysis confirmed that after gamma sterilization HA maintains its typical peaks, and no additional peaks corresponding to new functional groups were originated.

Regarding the samples with collagen, the characteristic peaks of collagen were not detected as the collagen quantity is below the detection limit of ATR-FTIR.

Raman Spectroscopy was additionally implemented on granules of HA and nanoHA/collagen sterilized and the spectra is presented in Figure 28. As is possible to observe, characteristic peaks of HA are present in all samples at locations described above (431, 447, 580, 592, 608, 616, 962, 1028, 1047, 1054, 1062 and 1076 cm^{-1} [105, 106]). No additional peaks were detected, and the presence of collagen was still not identified.

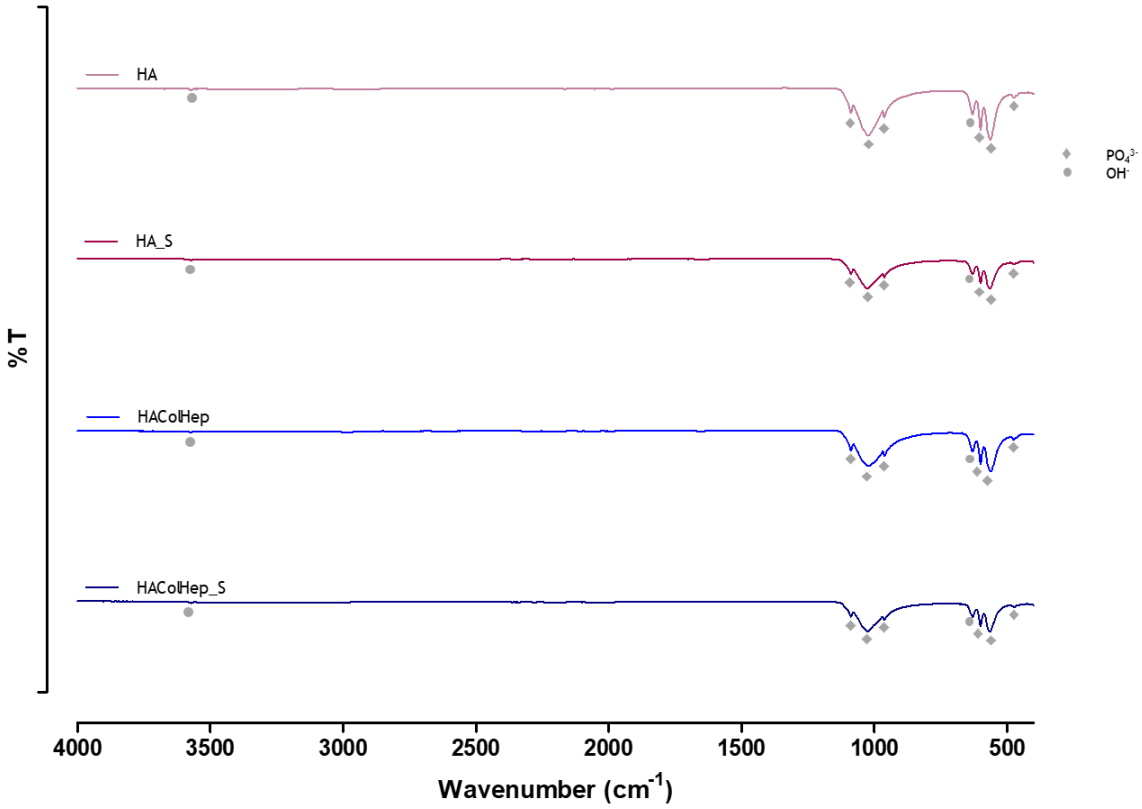

Figure 27 - ATR-FTIR spectra of HA, HA sterilized (HA_S), nanoHA/collagen (HAColHep) and HAColHep sterilized (HAColHep_S).

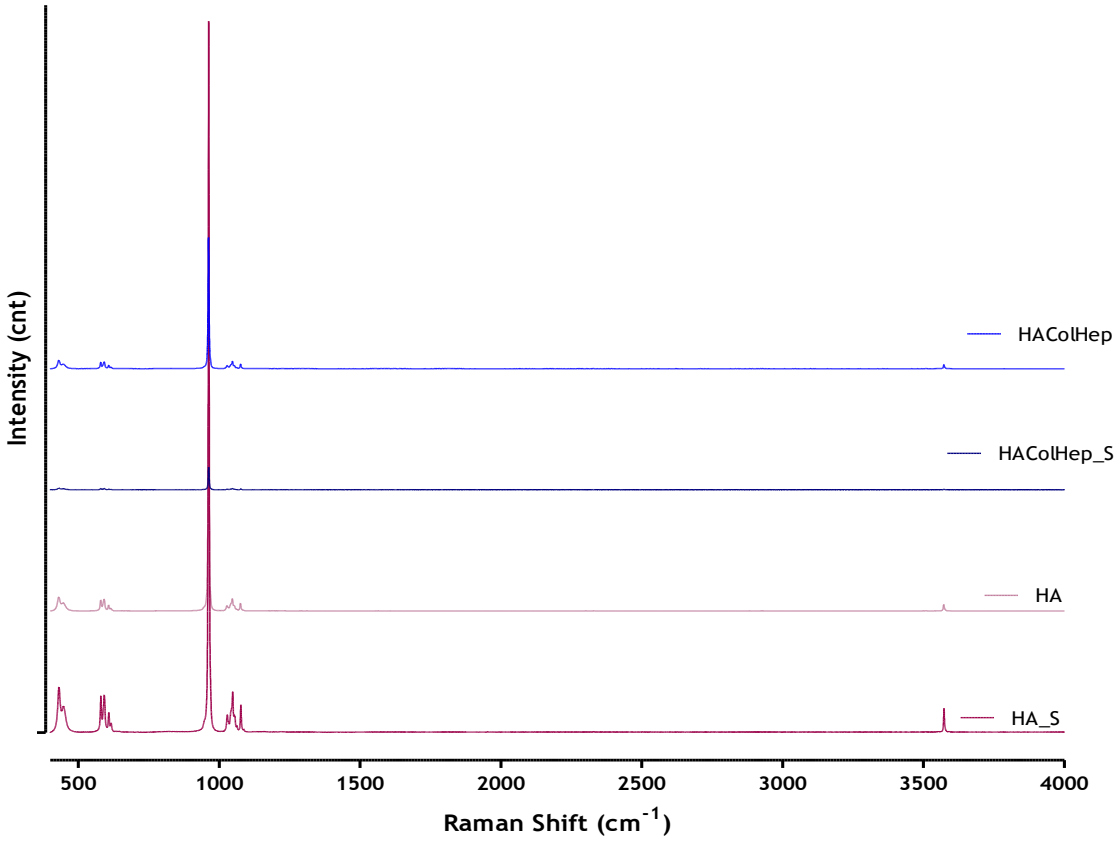

Figure 28 - Raman spectra of HA, HA sterilized, nanoHA/collagen (HAColHep), and HAColHep sterilized.

3.8.4. Antibiotic Release profile

A preliminary study of gentamicin release from heparinized nanoHA/collagen granules that were gamma irradiated was conducted using 2h adsorption and 40 mg/mL gentamicin. On Figure 29 it is possible to observe that antibiotic was released during 19 days, with an initial release of 820 µg/mL.

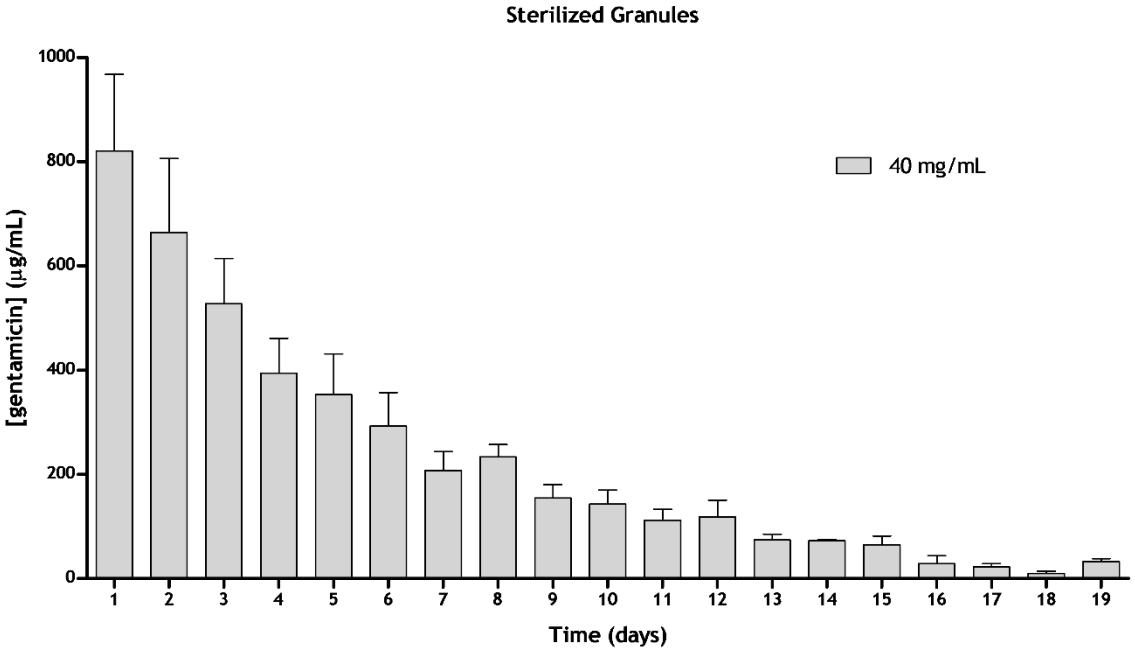

Figure 29 - Gentamicin release from gamma irradiated heparinized nanoHA/collagen granules versus time.

Chapter 4

Discussion

Osteomyelitis is an infection that can occur in bone or bone marrow. It can emerge from different mechanisms, being the most preeminent bacterial infection, caused by *Staphylococcus aureus*, with an increased incidence of methicillin-resistant *S. aureus*. A proper treatment is needed since osteomyelitis can become chronic. In cases of acute osteomyelitis, a treatment with systemic antibiotic administration is usually enough. Chronic osteomyelitis, on the other hand, requires surgical debridement associated with local and systemic administration of antibiotics like vancomycin and gentamicin [116]. Interest in reducing the number of surgical procedures required and making the treatment more patient friendly has been increasing. This implies the efficient removal of all dead tissue to eliminate the infection and prevent a second bone incision [51]. In cases where bone removal is required, the bone defect must be filled to prevent recurrence of infection and improve mechanical stability in a subsequent surgery [43].

Vancomycin and gentamicin are used in clinical practice to treat patients with infected open fractures, due to their combined efficacy against a broad range of Gram-positive and Gram-negative bacteria [22].

The systemic route of administration is sometimes ineffective and demands precise monitoring of serum drug concentrations to keep nontoxic levels: since the tissue surrounding the infected zone is altered, there is a low penetration rate, so high doses of therapeutic agents are needed, and this can lead to severe side effects.

It is possible to increase the local concentration of antibiotics at the site of the potential infection, without systemic toxicity, by using impregnating antibiotic carriers. They also allow a prolonged release of antibiotic in time, and depended on the material used, they avoid the need for further surgical procedures.

Previous studies carried out in the Biocomposites research group (i3S) allowed the development of nanohydroxyapatite and collagen biocomposite presented as granules, to act as a scaffold for antibiotic release and also bone regeneration. In order to make the technology more user friendly to orthopaedic surgeons, it was tested if, by being available on the scaffold surface in a lyophilized manner, vancomycin was equally effective at eradicating bacteria and with a similar release kinetics, when compared to not being lyophilized. The antibiotic release profile was evaluated as well as its antibacterial activity, for both vancomycin and gentamicin. Regarding vancomycin, MRSA adhesion was also performed. A sterilization procedure was additionally evaluated. All materials were submitted to morphological and chemical characterization.

The nanoHA scaffolds were produced by the method of replication of a polyurethane foam and subsequently sintered. A suitable granule size was used to effectively fill the bone defects [117].

The nanoHA granules, to the naked eye have a porous 3D structure. SEM images of nanoHA showed the presence of macroporosity, important for cell migration into material, improved nutrient and ion

transport [98] and invasion of vasculature [73]: these porous should have at least a size of 100 μm for *in vivo* ingrowth and to regenerate mineralized bone [68], [99]. They also promote the diffusion of drugs at a faster rate, compared to scaffolds with a smaller macropore size [118]. The presence of interconnective porosity promotes bone ingrowth, potentiates vascularization, provides higher surface area for a better interaction between the scaffold and the surrounding tissue, through nutrients and oxygen transfer and to waste products removal [98, 99, 118]. In Figure 5: A - D it is possible to observe that both lyophilized and non-lyophilized granules present this kind of porosity. The presence of microporosity is also notable (Figure 5 (E – H)). Microporosity (pore diameters lower than 10 μm) can improve cell-scaffold interaction due to a higher surface area, resulting in osteogenic effects [73]: it provides attachment locations for osteoblasts [98] inducing bone-like apatite formation [67] and allow the transfer of nutrients and metabolites [99]. Since both lyophilized and non-lyophilized granules present interconnected macroporosity and microporosity, the freeze-drying process did not alter the 3D conformation of granules.

The collagen incorporation was carried out as described by Coelho *et al.* [67], and provided similar results: the collagen is distributed heterogeneously and in a network shape, establishing bridges between sections of granules, without completely covering them (Figure 6). Similar to what was done, heparin was used to promote the interaction between the scaffold and vancomycin, increasing its adsorption and contributing to a more continuous and controlled release, for a longer period of time. These results were obtained for heparinized nanoHA/collagen granules (Figure 6 (A and C)) and heparinized granules that were lyophilized (Figure 6 (B and D)), proving that the freeze-drying process did not affect the collagen distribution. This collagen distribution allows for both hydroxyapatite and collagen are available to interact with the surrounding environment.

Vancomycin adsorption was performed on heparinized nanoHA/collagen granules. They were then frozen, freeze-dried, and ATR-FTIR and SEM analysed. The added vancomycin allowed the granules to be coated with an antibiotic layer (Figure 7, most evident in images D and F), regardless of the adsorption times. This layer of vancomycin covers the pores, making it impossible to visualize the interconnected macroporosity characteristic of the granules (Figure 7 (A)). In larger magnifications it is possible to notice that the vancomycin layer presents some discontinuities in its surface, probably due to the lyophilization process. These fissures allow us to observe the interior appearance of the vancomycin layer (Figure 7 (B)) and the characteristic appearance of the granules (Figure 7 (C, D and E)). The presence of microporosity is also noted (Figure 7 (E, F and G)). The porosity will be especially important after eradication of infection so the bone regeneration can take place.

The ATR-FTIR analysis showed that the lyophilization process did not affect the characteristic chemical composition of hydroxyapatite. Several studies have reported to lyophilized scaffolds impregnated with HA, and assumed that it did not affect its properties [66, 119, 120]. However, it was not possible to detect the characteristic peaks of collagen probably because of the lower sensibility of the equipment compared to the reduced amount present and the fact that it is heterogeneously distributed. Nevertheless, Popa *et al.* [105] studied the influence of collagen on the structure and morphology of hydroxyapatite, and it came to the conclusion that the addition of collagen induced a decrease of the peak intensities of hydroxyapatite, also observed in this study (Figure A2, ANNEX). The fact that there is a reduction in the intensity of HA peaks may be due to a layer formed by collagen on the granules. This layer may cause the laser not to penetrate as deeply during the analysis, so that the intensity with which it detects HA will be lower. Regarding heparinized nanoHA/collagen granules with vancomycin adsorption and lyophilization, besides the characteristic peaks of HA, the spectrum showed the representative peaks of vancomycin, thus confirming its presence.

In Raman spectroscopy, similarly to what was seen in FTIR analysis, the lyophilization process did not affect the chemical composition of hydroxyapatite, as all peaks were observed in the same position. This analysis also revealed the presence of vancomycin, but not collagen.

The antibiotic release from the granules was studied using vancomycin and gentamicin. Vancomycin is an antibiotic commonly prescribed for the treatment of osteomyelitis as it is effective against Gram-positive bacteria such as *S. aureus* and MRSA [111]. Previous studies within the Biocomposites research group used an initial vancomycin concentration of 50 mg/mL and an adsorption time of 2 hours. In order to make the material more useful to be used by surgeons, the adsorption time was reduced, and lyophilization was tested as a way to make the antibiotic available on the surface of the material. Reducing the adsorption time did not prove to be a viable option, since, although there were no statistically significant differences between the different adsorption times for the same day, the increased adsorption time allowed the antibiotic to be released for a longer period of time. Through the release profile presented in Figure 13, it is possible to verify that a release of vancomycin, with values above the MIC for MRSA ($MIC_{MRSA} \leq 2$ µg/mL), occurred during 23, 22 and 18 days for 2 h, 0.5 h and 0.25 h adsorption time, respectively. By making the antibiotic available on the surface of the material, the orthopaedic surgeons do not need to take any care to previously adsorb the antibiotic. For this reason, it was tested whether increasing the adsorption time of vancomycin would increase the amount of antibiotic release. Thus, the release profile presented in Figure 14 shows that it was possible to release the antibiotic for 26, 24 and 20 days, for adsorption times of 24 h, 2 h and 0.5 h, respectively. Using 0.5 h adsorption does not allow an increase in the release time, and between 2 h and 24 h, the amount of antibiotic released was statistically different, meaning that an increase in the adsorption time allows a higher release of antibiotic. For both studies, the quantity of granules used was the same (20 mg), however there were differences in the amount of antibiotic initially released and in the duration of the release time, indicating that the lyophilization process affects the antibiotic release. Comparing lyophilized material with non-lyophilized, lyophilized material releases antibiotics for longer, while non-lyophilized releases a higher initial amount of antibiotic. This rapid release of antibiotics may be related to the amount of antibiotic adsorbed immediately to the surface of the granule, followed by a slower releaser of the antibiotic that was dissolved more internally in the bulk of the granule [121], between the microporous: first there is a fast release due to a rapid water uptake of the granules and dissolution of the vancomycin at the surface, then the release rate decreases until the release is complete [122]. On lyophilized granules, since the granules were dry, by putting them on PBS they were first rehydrated, delaying the release process, and thus extending it.

Concerning the amount of antibiotic released, for non-lyophilized granules the maximum amount of vancomycin released was approximately 930 µg/mL (for 0.5 h adsorption) and for lyophilized granules was approximately 730 µg/mL (for 2 h adsorption) (Figure A4, ANNEX).

Gentamicin is an antibiotic effective against most Gram-negative and Gram-positive *Staphylococcus* and is mostly applied in combination with other antibiotics. Because it was the first study carried out in the research group that used gentamicin with nanoHA granules, we used two adsorbed concentrations. One lower concentration, 15 mg/mL, than that usually reported in the literature [24, 53, 95, 123]. The use of this concentration in the adsorption of the granules allowed an initial release of antibiotics of 240 µg/mL, and a controlled release for 15 days (Figure 22). Although the values released were higher than the MIC for MRSA ($MIC_{MRSA} \leq 1$ µg/mL) during the entire release time, the initial gentamicin concentration was increased in the expectation of obtaining a higher initial antibiotic release. Thus, the concentration was increased to 40 mg/mL and an initial

antibiotic release of 600 µg/mL was obtained, and it was possible to release the antibiotic for 17 days (Figure 22).

The interest in the use of local delivery systems has been increasing, since they provide a high concentration of antibiotics at the site of infection, without reaching systemic limits of toxicity, harmful to the organs. The use of local antibiotic carriers allows the amount of antibiotic provided to reach concentrations 10 - 100 times higher than the minimum inhibitory concentration and above the concentration needed to eradicate a biofilm [34]. Given that the initial antibiotic levels released are higher than 200 µg/mL and 100 µg/mL for vancomycin and gentamicin respectively, both lyophilized and non-lyophilized material and both gentamicin concentrations used are suitable for the treatment of MRSA-induced osteomyelitis. As regards toxicity levels, studies will have to be carried out to determine whether the quantities released reach toxicity levels.

Lian *et al*. [124] reported an antibiotic initial release of about 900 µg/mL from a vancomycin-loaded nano-hydroxyapatite/collagen/poly (lactic acid) bone substitute. They also seeded mesenchymal stem cells on the surface of the scaffold and no significant differences were observed, showing satisfied results for *in vivo* biocompatibility. Fleiter *et al*. [32] used calcium sulfate-based bone void filler beads with gentamicin as an antibiotic delivery system. They were able to delivery initial doses of gentamicin well above the minimal inhibitory concentration for relevant pathogens, with a concentration of gentamicin in wound exudate of about 700 µg/mL (after 24h implantation). They also did not reveal any nephrotoxic or hepatotoxic effects of gentamicin release. This study showed that the initial dose of gentamicin released did not cause toxicity when implanted in adults suffering from osteomyelitis.

The quantification of antibiotic release was also assessed by liquid chromatography – mass spectrometry. Samples of lyophilized and non-lyophilized nanoHA/collagen granules with 2 h of antibiotic adsorption were analysed for days 1, 15 and 21. The results show a higher initial release (day 1) of antibiotics for non-lyophilized granules, but closer to the end of release (day 21) the amount of antibiotic released is higher for lyophilized granules (Figure 18), in line with the results obtained from the measurement in the spectrophotometer UV-Vis NanoDrop. Comparing the values measured in NanoDrop with those obtained by mass spectrometry (Figure A6, ANNEX) we can verify that the release tendency is the same, as was to be expected. However, the discrepancy obtained in the values read for the same sample can be explained based on the sensitivity of the equipment and the ability to detect the molecules of interest. In the case of mass spectrometry, a specific search was made for the molecular mass of vancomycin, so that the probability of interference from other molecules is attenuated. In the case of the NanoDrop, it reads the complete sample, without distinguishing molecules of interest, so there may be interference from other molecules and decrease the capacity for detection of vancomycin. When analysing the mass spectrum of vancomycin, the parent mass spectrum was found at m/z 725, and not at m/z 1449.2 (which corresponds to the molecular mass of vancomycin). This outcome suggested that vancomycin was converted into diprotonated mass [112, 114]. This can be explained due to the fact that vancomycin has multiple acidic and basic ionizable groups [114]. The degradation products identified on Figure 19, corresponding to the end of the release, have an atomic charge of +1 (Z = 1), for both lyophilized and non-lyophilized samples. Since the identified vancomycin has an atomic charge of +2 (Z = 2), we can assume that the detected products do not correspond to degradation products of vancomycin. As no further degradation products were detected [125], we can presume that the lyophilization process does not induce alterations in the vancomycin molecule.

A study of the vancomycin bioactivity related to the MRSA strain was performed, as well as a preliminary study of the activity of gentamicin related to the same strain. The choice of this strain

was due to the fact that it is a resistant strain, with an increasing incidence in patients with osteomyelitis. Vancomycin bioactivity was studied for lyophilized granules with antibiotic adsorption and for granules with adsorption without lyophilization, and both proved to be effective in eradicating bacteria: after incubation for 24 hours with the bacteria, the number of bacteria in suspension with vancomycin adsorption was reduced by 100% and in lyophilized granules by 99.99%, compared to granules without antibiotic. A reduction of about 100% when using vancomycin to treat a *S. aureus* stain was also reported by Lian *et al.* [124]. The small difference in the results obtained may be due to one of the steps of preparing the material, before being incubated with bacteria: the disinfection of the materials in 70% ethanol. As the lyophilized materials already have vancomycin adsorbed on their surface, placing them in ethanol can hydrate the material and start the antibiotic release process. The amount of antibiotic that becomes available on the surface of the granules decreases, thus decreasing their antibacterial effect. This phenomenon does not occur in non-lyophilized granules, since the adsorption of vancomycin is carried out after disinfection with ethanol.

The preliminary study of the gentamicin bioactivity proved that after 24 hours of incubation of the bacteria with the granules with gentamicin, there was a 100% reduction in the number of bacteria in suspension when compared to the granules without antibiotics.

Adhesion of MRSA in granules was observed by SEM, but only for the vancomycin study, as the gentamicin study was only preliminary. Thus, in vancomycin granules it is possible to observe a significant decrease in the number of adherent bacteria, but it is not possible to see differences in the adhesion of bacteria in lyophilized and non-lyophilized granules. In granules without antibiotics, it is possible to verify that there is a greater adhesion of bacteria in areas that contain higher concentration of collagen, previously verified by Coelho *et al.* [67]. Bacteria bind to extracellular matrix proteins like collagen, but also because of heparin, since it is a glycosaminoglycan to which these bacteria can adhere.

Regarding the morphological aspect of the bacteria observed by SEM (Figure 21, but with more prominence in the Figure A7, ANNEX), the fact that some bacteria appear to be destroyed could be due to an effect of glutaraldehyde during the fixation process [126], but this condition was not found in samples not treated with antibiotics: in this case, bacteria have a characteristic spherical morphology and are clustered. Thus, another possible explanation is that the antibiotic may have disrupted the synthesis of peptidoglycan layer of the bacteria cell wall, leading to lysis [127, 128, 129]: previous studies said that an alteration in the Gram-positive cocci structure was due to vancomycin preventing the access of peptidoglycan hydrolases to their substrate and to vancomycin directly inhibition these hydrolases, thus acquiring a pseudomulticellular form [130]. Another explanation may be due to the dehydration procedure applied during the fixing method of the material for SEM observation: successive increasing concentrations of ethanol may have caused the dehydration of bacteria and the destruction of its cell membrane.

This study also evaluated the effect of gamma radiation sterilization on the structure and composition of granules, in particular on the distribution of the collagen network. SEM images show the presence of interconnective macroporosity (Figure 24 (A and B)) and also microporosity (Figure 24 (C and D)). Figure 25 shows that the collagen is heterogeneously distributed in a network shape, and forms fibers across the pores. Since these characteristics are also present in granules not gamma irradiated, it proves that the sterilization process does not seem to induce changes in granules morphology [83]. Through FTIR analysis we observed that the characteristic peaks of hydroxyapatite were identified, and collagen was still not detected. Raman spectroscopy analysis showed similar results: did not allow the detection of collagen, but the peaks of hydroxyapatite were distinguished. In the light of the results obtained, we can assume that the chemical composition of hydroxyapatite

and collagen remain unaffected. Regarding antibiotic release from sterilized granules, it was possible to obtain an initial release of 820 µg/mL of gentamicin, 220 µg/mL above the non-sterilized granules, but since it is only a preliminary study, further testing will need to be carried out in order to determine whether the effects of gamma radiation sterilization have an effect on the release of antibiotics. Faraj *et al*. [83] studied several methods to sterilize collagen scaffolds crosslinked with heparin and showed that the amount of heparin adhered to the scaffold did not change after being gamma sterilized and that sterilized materials do not affect cellular proliferation; however, they proved that sterilization by gamma irradiation induces collagen degradation. Despite this, several studies have reported the use of gamma irradiation of 25 kGy on collagenous scaffolds without damage to the material [98, 131]. Lian *et al*. [124] used a dose 15 kGy irradiation on scaffolds containing collagen, and did not address any effect. Bae *et al*. [132] used a dose of 25 kGy for both sterilization and crosslinking of collagen onto titanium surfaces.

Chapter 5

Conclusion

In this work, the versatility of the material produced was showed: it can efficiently and in a controlled manner release two antibiotic alternatives, it allows the antibiotic to be present on the surface in a lyophilized manner and to be released for a long time, and it is not affected by gamma radiation sterilization.

Using the lyophilization method to make the antibiotic available on the surface of the material has proven to be able to release antibiotics for a longer time than the material presenting the antibiotic in a non-lyophilized way: by lyophilizing the antibiotic on the surface of the material the initial amount of antibiotic released is slightly reduced, but this allows it to be released for a longer time when compared with material whose antibiotic has not been lyophilized. This method has proven to have no effect on the interconnected macroporosity or the microporosity typical of granules, which are important for cell adhesion and migration, nutrient flow and protein adsorption.

The incorporation of collagen in the material showed that collagen is distributed in a heterogenous manner, as a network, and establishing links between pores. This feature allows both nanoHA and collagen to be available to interact with the surrounding environment. It should be noted that this characteristic of the material remained present after suffering lyophilization, sterilization and at the end of the antibiotic release.

Both antibiotics used showed a high initial release, followed by a sustained release for more than 15 days, with values always higher than the MIC for MRSA. The release of antibiotic from granules was also able to inhibit the growth of MRSA, both for adsorbed vancomycin, adsorbed and lyophilized vancomycin and gentamicin, as demonstrated by antimicrobial activity assays.

The use of gamma radiation proves to be an efficient way to sterilize the heparinized granules, since it did not induce morphological changes in the material or in its chemical composition. In addition, the granules were also able to maintain a controlled and sustained release profile, with antibiotic release levels above the minimum inhibitory concentration for MRSA.

In vitro trials have not yet been performed, but the literature and studies conducted within the research group suggest that the presence of lyophilized vancomycin will not affect cell viability. Thus, it is possible to predict that the use of the material developed here, when implanted, first eradicates osteomyelitis and then promotes bone renewal.

Briefly, the material developed is biocompatible, with a geometry that allows the adjustment to the bone defect, has high porosity, it is possible to lyophilize without producing degradation products, it is adaptable to various antibiotics and allows the release of antibiotics in quantities sufficient to eradicate resistant bacteria, as is the case of MRSA. In addition, it is also possible to be sterilized by gamma radiation without suffering alterations.

Chapter 6

Further Work

As a proposal for future work it would be important to ensure that the gamma radiation sterilization process does not actually affect the material, mainly to ensure that it does not cause degradation of collagen. This can be evaluated by incubating the material in a buffer and analyse the hydroxyproline present in the supernatant, since it is an amino acid abundantly present in collagen. Additionally, given the results presented in this study, it would be interesting to study the sterilization of the material with antibiotic adsorbed and lyophilized.

In order to supplement the results obtained, it is necessary to perform *in vitro* assays on cell cultures and *in vivo* to confirm the absence of cytotoxicity of the material.

Mechanical tests, e.g. compression tests, would be interesting to test the mechanical strength of materials after lyophilization, as these granules at the end of their release appeared more brittle than the non-lyophilized.

Finally, in light of the increasing resistance of bacteria to antibiotics commonly used in the treatment of osteomyelitis, it would be interesting to study the effect of the combination of antibiotics, such as combining gentamicin with vancomycin.

References

[1] S. Preethi Soundarya, A. Haritha Menon, S. Viji Chandran, and N. Selvamurugan, “Bone tissue engineering: Scaffold preparation using chitosan and other biomaterials with different design and fabrication techniques,” *Int. J. Biol. Macromol.*, vol. 119, pp. 1228–1239, 2018.

[2] L. Polo-Corrales, M. Latorre-Esteves, and J. E. Ramirez-Vick, “Scaffold design for bone regeneration. Journal of nanoscience and nanotechnology,” vol. 14, no. 1, pp. 15–56, 2014.

[3] S. V. Dorozhkin, “Bioceramics of calcium orthophosphates,” *Biomaterials*, vol. 31, no. 7, pp. 1465–1485, 2010.

[4] M. C. Birt, D. W. Anderson, E. Bruce Toby, and J. Wang, “Osteomyelitis: Recent advances in pathophysiology and therapeutic strategies,” *J. Orthop.*, vol. 14, no. 1, pp. 45–52, 2017.

[5] G. Radcliffe, “(iii) Osteomyelitis - a historical and basic sciences review,” *Orthop. Trauma*, vol. 29, no. 4, pp. 243–252, 2015.

[6] D. P. Lew and F. A. Waldvogel, “Osteomyelitis,” *Lancet*, vol. 364, pp. 369–379, 2004.

[7] M. McNally and K. Nagarajah, “(iv) Osteomyelitis,” *Orthop. Trauma*, vol. 24, no. 6, pp. 416–429, 2010.

[8] J. C. Mandell, B. Khurana, J. T. Smith, G. J. Czuczman, V. Ghazikhanian, and S. E. Smith, “Osteomyelitis of the lower extremity: pathophysiology, imaging, and classification, with an emphasis on diabetic foot infection,” *Emerg. Radiol.*, vol. 25, no. 2, pp. 175–188, 2018.

[9] P. Dinh, B. Hutchinson, C. Zalavras, and M. Stevanovic, “Reconstruction of Osteomyelitis Defects,” *Semin. Plast. Surg.*, vol. 23, no. 02, pp. 108–118, 2009.

[10] R. M. Donlan, “Biofilms: microbial life on surfaces. Emerg Infect Diseases,” *Emerg Infect Dis.*, vol. 8, no. 9, pp. 881–890, 2002.

[11] E. Carretto, R. Visiello, and P. Nardini, “Methicillin Resistance in Staphylococcus aureus,” *Pet-to-Man Travel. Staphylococci A World Prog.*, vol. 4, no. May, pp. 225–235, 2018.

[12] J. Hatzenbuehler and T. J. Pulling, “Diagnosis and Management of Osteomyelitis,” *Am. Acad. Fam. Physicians*, vol. 84, no. 9, pp. 1027–1033, 2011.

[13] P. Anupama, “Review on Lyophilization of Anti-biotics,” vol. 5, no. 2, pp. 92–98, 2016.

[14] C. T. Walsh and T. A. Wencewicz, “Prospects for new antibiotics: A molecule-centered perspective,” *J. Antibiot. (Tokyo).*, vol. 67, no. 1, pp. 7–22, 2014.

[15] I. Hornyák *et al.*, “Increased Release Time of Antibiotics from Bone Allografts through a Novel Biodegradable Coating,” *Biomed Res. Int.*, vol. 2014, 2014.

[16] Y. Chang *et al.*, “In vitro activities of daptomycin-, vancomycin-, and teicoplanin-loaded polymethylmethacrylate against methicillin-susceptible, methicillin-resistant, and vancomycin-intermediate strains of Staphylococcus aureus,” *Antimicrob. Agents Chemother.*, vol. 55, no. 12, pp. 5480–5484, 2011.

[17] B. T. Tsuji, M. J. Rybak, C. M. Cheung, M. Amjad, and G. W. Kaatz, “Community- and health care-associated methicillin-resistant Staphylococcus aureus: a comparison of molecular epidemiology and antimicrobial activities of various agents,” *Diagn. Microbiol. Infect. Dis.*, vol. 58, no. 1, pp. 41–47, 2007.

[18] G. J. Moran *et al.*, “Methicillin-Resistant S. aureus Infections among Patients in the Emergency Department,” *N. Engl. J. Med.*, vol. 355, no. 7, pp. 666–674, 2006.

[19] F. R. DeLeo, M. Otto, B. N. Kreiswirth, and H. F. Chambers, “Community-associated meticillin-resistant Staphylococcus aureus,” *Lancet*, vol. 375, no. 9725, pp. 1557–1568, 2010.

[20] L. Mulazimoglu, S. D. Drenning, and R. R. Muder, “Vancomycin-gentamicin synergism

revisited: Effect of gentamicin susceptibility of methicillin-resistant Staphylococcus aureus," *Antimicrob. Agents Chemother.*, vol. 40, no. 6, pp. 1534–1535, 1996.

[21] S. W. Kim *et al.*, "Once-daily gentamicin administration for community-associated methicillin resistant Staphylococcus aureus in an in vitro pharmacodynamic model: Preliminary reports for the advantages for optimizing pharmacodynamic index," *Yonsei Med. J.*, vol. 51, no. 5, pp. 722–727, 2010.

[22] B. C. C. Rand, J. G. Penn-Barwell, and J. C. Wenke, "Combined local and systemic antibiotic delivery improves eradication of wound contamination: An animal experimental model of contaminated," *Bone Jt. J.*, vol. 97-B, no. 10, pp. 1423–1427, 2015.

[23] F. R. Bruniera *et al.*, "The use of vancomycin with its therapeutic and adverse effects: A review," *Eur. Rev. Med. Pharmacol. Sci.*, vol. 19, no. 4, pp. 694–700, 2015.

[24] R. B. Phinney, S. D. Schwartz, D. A. Lee, and B. J. Mondino, "Collagen-Shield Delivery of Gentamicin and Vancomycin," *Arch. Ophthalmol.*, vol. 106, no. 11, pp. 1599–1604, 1988.

[25] A. Gupta, M. Biyani, and A. Khaira, "Vancomycin nephrotoxicity: Myths and facts," *Neth. J. Med.*, vol. 69, no. 9, pp. 379–383, 2011.

[26] D. P. Levine, "Vancomycin : A History," vol. 42, no. Suppl 1, pp. 5–12, 2006.

[27] M. J. Weinstein *et al.*, "Gentamicin, a New Antibiotic Complex from Micromonospora," *J. Med. Chem.*, vol. 6, no. 4, pp. 463–464, 1963.

[28] G. B. Appel and H. C. Neu, "Gentamicin in 1978," *Ann. Intern. Med.*, vol. 89, no. 4, pp. 528–538, 1978.

[29] R. L. Jao and G. G. Jackson, "Gentamicin Sulfate , New Antibiotic Against Gram-Negative Bacilli," *Jama*, vol. 189, no. 11, pp. 817–822, 1964.

[30] J. H. Hull and F. A. Sarubbi, "Gentamicin serum concentrations: pharmacokinetic predictions," *Ann. Intern. Med.*, vol. 85, no. 2, pp. 183–189, 1976.

[31] F. G. Falco, H. M. Smith, and G. M. Arcieri, "Nephrotoxicity of aminoglycosides and gentamicin," *J. Infect. Dis.*, vol. 119, no. 4–5, pp. 406–409, 1969.

[32] N. Fleiter *et al.*, "Clinical use and safety of a novel gentamicin-releasing resorbable bone graft substitute in the treatment of osteomyelitis / osteitis," *Bone Jt. Surg.*, vol. 3, no. 7, pp. 223–229, 2014.

[33] Y. Yamashita, A. Uchida, T. Yamakawa, Y. Shinto, N. Araki, and K. Kato, "Treatment of chronic osteomyelitis using calcium hydroxyapatite ceramic implants impregnated with antibiotic," *Int. Orthop.*, vol. 22, no. 4, pp. 247–251, 1998.

[34] J. Ferguson, M. Diefenbeck, and M. McNally, "Ceramic Biocomposites as Biodegradable Antibiotic Carriers in the Treatment of Bone Infections," *J. Bone Jt. Infect.*, vol. 2, no. 1, pp. 38–51, 2017.

[35] J. A. Inzana, E. M. Schwarz, S. L. Kates, and H. A. Awad, "Biomaterials approaches to treating implant-associated osteomyelitis," *Biomaterials*, vol. 81, pp. 58–71, 2016.

[36] H. W. Kim, J. C. Knowles, and H. E. Kim, "Hydroxyapatite/poly(ε-caprolactone) composite coatings on hydroxyapatite porous bone scaffold for drug delivery," *Biomaterials*, vol. 25, no. 7–8, pp. 1279–1287, 2004.

[37] P. Panagopoulos, G. Drosos, E. Maltezos, and N. Papanas, "Local antibiotic delivery systems in diabetic foot osteomyelitis: Time for one step beyond?," *Int. J. Low. Extrem. Wounds*, vol. 14, no. 1, pp. 87–91, 2015.

[38] G. Fernandez de Grado *et al.*, "Bone substitutes: a review of their characteristics, clinical use, and perspectives for large bone defects management," *J. Tissue Eng.*, vol. 9, pp. 1–18, 2018.

[39] K. H. W, R. E. Galus, F. Katedra Zak, A. Histologii Embriologii, and T. Rehabilitacja, "Bioactive Composites for Bone Regeneration. Review," vol. 3, no. 10, pp. 201–210, 2008.

[40] C. R. Rathbone, J. D. Cross, K. V. Brown, C. K. Murray, and J. C. Wenke, "Effect of various concentrations of antibiotics on osteogenic cell viability and activity," *J. Orthop. Res.*, vol. 29, no. 7, pp. 1070–1074, 2011.

[41] M. El-Husseiny, S. Patel, R. J. MacFarlane, and F. S. Haddad, "Biodegradable antibiotic delivery systems," *J. Bone Jt. Surg. - Br. Vol.*, vol. 93-B, no. 2, pp. 151–157, 2011.

[42] S. J. Lee and A. Atala, "Engineering of tissues and organs," in *Tissue Engineering Using Ceramics and Polymers (Second Edition)*, 2014, pp. 347–386.

[43] A. Dvorzhinskiy, G. Perino, R. Chojnowski, and M. C. H. Van Der Meulen, "CERAMENT Bone Void Filler Impregnated with Gentamicin Increases Bone Formation and Decreases the Rate of Detectable Infection After Debridement in a Rat Model of Osteomyelitis," 2015.

[44] B. F. Ricciardi and M. P. Bostrom, “Bone graft substitutes: Claims and credibility,” *Semin. Arthroplasty*, vol. 24, no. 2, pp. 119–123, 2013.
[45] D. Pförringer *et al.*, “Antimicrobial Formulations of Absorbable Bone Substitute Materials,” *Antimicrob. Agents Chemother.*, vol. 60, no. 7, pp. 3897–3905, 2016.
[46] J. A. Leupold, W. R. Barfield, Y. H. An, and L. A. Hartsock, “A Comparison of ProOsteon, DBX, and Collagraft in a Rabbit Model,” *Wiley Period. Inc.*, vol. 79, no. B, pp. 292–297, 2006.
[47] Z. Biomet, “Equivabone Bone Graft Substitute.”
[48] J. Friesenbichler *et al.*, “Clinical experience with the artificial bone graft substitute Calcibon used following curettage of benign and low-grade malignant bone tumors,” *Sci. Rep.*, vol. 7, no. 1736, pp. 5–9, 2017.
[49] Q. Chen, S. Liang, and G. A. Thouas, “Elastomeric biomaterials for tissue engineering,” *Prog. Polym. Sci.*, vol. 38, no. 3–4, pp. 584–671, 2013.
[50] S. Estoril, “34 th Annual Meeting of the European Bone and Joint Infection Society (EBJIS) A COMPARATIVE STUDY OF THREE BIOABSORBABLE ANTIBIOTIC CARRIERS IN CHRONIC,” no. September, pp. 10–12, 2015.
[51] M. A. Mcnally, J. Y. Ferguson, A. C. K. Lau, M. Scarborough, and A. J. Ramsden, “Single-stage treatment of chronic osteomyelitis with a new absorbable , gentamicin-loaded , calcium sulphate / hydroxyapatite biocomposite,” vol. 98, no. 9, pp. 1289–1296, 2016.
[52] “Resorbable bone substitute / bone void filling material containing Gentamicin.”
[53] M. A. Rauschmann *et al.*, “Nanocrystalline hydroxyapatite and calcium sulphate as biodegradable composite carrier material for local delivery of antibiotics in bone infections,” *Biomaterials*, vol. 26, pp. 2677–2684, 2005.
[54] R. Dorati *et al.*, “Biodegradable scaffolds for bone regeneration combined with drug-delivery systems in osteomyelitis therapy,” *Pharmaceuticals*, vol. 10, no. 4, 2017.
[55] “Heraeus Medical operates in almost 60 countries*.”
[56] D. Neut, H. Van De Belt, J. R. Van Horn, H. C. Van Der Mei, and H. J. Busscher, “Residual gentamicin-release from antibiotic-loaded polymethylmethacrylate beads after 5 years of implantation,” *Biomaterials*, vol. 24, no. 10, pp. 1829–1831, 2003.
[57] Z. Biomet, “Septocoll ® E.”
[58] O. Kilian *et al.*, “Elution kinetics, antimicrobial efficacy, and degradation and microvasculature of a new gentamicin-loaded collagen fleece,” *J. Biomed. Mater. Res. - Part B Appl. Biomater.*, vol. 90 B, no. 1, pp. 210–222, 2009.
[59] J. Gallo, B. K. M. Siller, M. Svábová, J. Lost’ák, and M. KOLÁR, “Microbiological and pharmacological properties of bone cement VancogenX,” *Acta Chir. Orthop. Traumatol. Czechoslov.*, vol. 80, pp. 69–79, 2013.
[60] A. Barroug and M. J. Glimcher, “Hydroxyapatite crystals as a local delivery system for cisplatin: Adsorption and release of cisplatin in vitro,” *J. Orthop. Res.*, vol. 20, no. 2, pp. 274–280, 2002.
[61] I. Iacoboni, F. Perrozzi, L. Macera, G. Taglieri, L. Ottaviano, and G. Fioravanti, “In situ syntheses of hydroxyapatite-grafted graphene oxide composites,” *J. Biomed. Mater. Res. - Part A*, vol. 107, no. 9, pp. 2026–2039, 2019.
[62] Y. Zhang and J. Lu, “A simple method to tailor spherical nanocrystal hydroxyapatite at low temperature,” *J. Nanoparticle Res.*, vol. 9, no. 4, pp. 589–594, 2007.
[63] L. El Hammari, H. Merroun, T. Coradin, S. Cassaignon, A. Laghzizil, and A. Saoiabi, “Mesoporous hydroxyapatites prepared in ethanol-water media: Structure and surface properties,” *Mater. Chem. Phys.*, vol. 104, no. 2–3, pp. 448–453, 2007.
[64] W. W. Thein-Han and R. D. K. Misra, “Biomimetic chitosan-nanohydroxyapatite composite scaffolds for bone tissue engineering,” *Acta Biomater.*, vol. 5, no. 4, pp. 1182–1197, 2009.
[65] G. Wei and P. X. Ma, “Nanostructured Biomaterials for Regeneration,” *Adv. Funct. Mater.*, vol. 18, no. 22, pp. 3568–3582, 2008.
[66] M. Peter *et al.*, “Preparation and characterization of chitosan-gelatin/nanohydroxyapatite composite scaffolds for tissue engineering applications,” *Carbohydr. Polym.*, vol. 80, no. 3, pp. 687–694, 2010.
[67] C. C. Coelho, S. R. Sousa, and F. J. Monteiro, “Heparinized nanohydroxyapatite/collagen granules for controlled release of vancomycin,” *J. Biomed. Mater. Res. - Part A*, vol. 103, no. 10, pp. 3128–3138, 2015.
[68] M. S. Laranjeira, M. H. Fernandes, and F. J. Monteiro, “Innovative macroporous granules of nanostructured-hydroxyapatite agglomerates: Bioactivity and osteoblast-like cell behaviour,”

J. Biomed. Mater. Res. - Part A, vol. 95, no. 3 A, pp. 891–900, 2010.

[69] M. P. Ferraz *et al.*, "Nanohydroxyapatite microspheres as delivery system for antibiotics: Release kinetics, antimicrobial activity, and interaction with osteoblasts," *J. Biomed. Mater. Res. - Part A*, pp. 994–1004, 2007.

[70] M. G. Martinez, A. J. Bullock, S. MacNeil, and I. U. Rehman, "Characterisation of structural changes in collagen with Raman spectroscopy," *Appl. Spectrosc. Rev.*, vol. 0, no. 0, pp. 1–34, 2019.

[71] K. Belbachir, R. Noreen, G. Gouspillou, and C. Petibois, "Collagen types analysis and differentiation by FTIR spectroscopy," *Anal. Bioanal. Chem.*, vol. 395, no. 3, pp. 829–837, 2009.

[72] C. Lee, A. Singla, and Y. Lee, "Biomedical applications of collagen," *Int. J. Pharm.*, vol. 221, pp. 1–22, 2001.

[73] G. Turnbull *et al.*, "3D bioactive composite scaffolds for bone tissue engineering," *Bioact. Mater.*, vol. 3, no. 3, pp. 278–314, 2018.

[74] J.-C. Park *et al.*, "Type I atelocollagen grafting onto ozone-treated polyurethane films : Cell attachment , proliferation , and collagen synthesis," *J. Biomed. Mater. Res.*, vol. 52, pp. 669–677, 2000.

[75] G. R. Nireesha, L. Divya, C. Sowmya, N. Venkateshan, M. N. Babu, and V. Lavakumar, "Lyophilization / Freeze Drying," vol. 3, no. 4, pp. 87–98, 2013.

[76] X. C. Tang and M. J. Pikal, "Design of Freeze-Drying Processes for Pharmaceuticals: Practical Advice," *Pharm. Res.*, vol. 21, no. 2, 2004.

[77] J. D. Colandene, L. M. Maldonado, A. T. Creagh, J. S. Vrettos, K. G. Goad, and T. M. Spitznagel, "Lyophilization Cycle Development for a High-Concentration Monoclonal Antibody Formulation Lacking a Crystalline Bulking Agent," *J. Pharm. Sci.*, vol. 96, no. 6, pp. 1598–1608, 2007.

[78] G. Ozkan, P. Franco, I. De Marco, J. Xiao, and E. Capanoglu, "A review of microencapsulation methods for food antioxidants: Principles, advantages, drawbacks and applications," *Food Chem.*, vol. 272, no. February 2018, pp. 494–506, 2019.

[79] S. Raza, Y. Iqbal, I. Ullah, M. S. Mubarak, M. U. Hameed, and M. Raza, "Effects of gamma irradiation on the physico-chemical and biological properties of levofloxacin," *Pak. J. Pharm. Sci.*, vol. 31, no. 1, pp. 181–186, 2018.

[80] E. Sarıgöl, S. Bozdağ Pehlivan, M. Ekizoğlu, M. Sağıroğlu, and S. Çalış, "Design and evaluation of gamma-sterilized vancomycin hydrochloride-loaded poly(ε-caprolactone) microspheres for the treatment of biofilm-based medical device-related osteomyelitis," *Pharm. Dev. Technol.*, vol. 22, no. 6, pp. 706–714, 2017.

[81] A. Dziedzic-Goclawska, A. Kaminski, I. Uhrynowska-Tyszkiewicz, and W. Stachowicz, "Irradiation as a safety procedure in tissue banking," *Cell Tissue Bank.*, vol. 6, no. 3, pp. 201–219, 2005.

[82] H. D. Barth, E. A. Zimmermann, E. Schaible, S. Y. Tang, T. Alliston, and R. O. Ritchie, "Characterization of the effects of x-ray irradiation on the hierarchical structure and mechanical properties of human cortical bone," *Biomaterials*, vol. 32, no. 34, pp. 8892–8904, 2011.

[83] K. A. Faraj *et al.*, "The effect of ethylene oxide sterilisation, beta irradiation and gamma irradiation on collagen fibril-based scaffolds," *Tissue Eng. Regen. Med.*, vol. 8, no. 5, pp. 460–470, 2011.

[84] A. Villaret *et al.*, "Raman characterization of human skin aging," *Ski. Res. Technol.*, vol. 25, no. 3, pp. 270–276, 2019.

[85] A. Bartolotta *et al.*, "Effects of gamma-irradiation on trehalose-hydroxyethylcellulose microspheres loaded with vancomycin," *Eur. J. Pharm. Biopharm.*, vol. 59, no. 1, pp. 139–146, 2005.

[86] S. Bozdag *et al.*, "In vitro evaluation of gentamicin- and vancomycin-containing minitablets as a replacement for fortified eye drops," *Drug Dev. Ind. Pharm.*, vol. 36, no. 11, pp. 1259–1270, 2010.

[87] S. Teixeira, L. Yang, P. J. Dijkstra, M. P. Ferraz, and F. J. Monteiro, "Heparinized hydroxyapatite / collagen three-dimensional scaffolds for tissue engineering," *J. Mater. Sci. Mater. Med.*, vol. 21, pp. 2385–2392, 2010.

[88] M. A. Mosiewicki, N. E. Marcovich, and M. I. Aranguren, "Characterization of fiber surface treatments in natural fiber composites by infrared and Raman spectroscopy," *Interface Eng.*

Nat. Fibre Compos. Maximum Perform., pp. 117–145, 2011.
[89] J. V. Gulmine, P. R. Janissek, H. M. Heise, and L. Akcelrud, “Polyethylene characterization by FTIR,” *Polym. Test.*, vol. 21, no. 5, pp. 557–563, 2002.
[90] M. H. Tariq, H. Naureen, N. Abbas, and M. Akhlaq, “Development and validation of a method for the analysis of vancomycin in human serum using ultracentrifuge protein precipitation and UV spectroscopy,” *Lat. Am. J. Pharm.*, vol. 34, no. 8, pp. 1489–1496, 2015.
[91] V. E. Vandell and P. A. Limbach, *Overview of Biochemical Applications of Mass Spectrometry*, 3rd ed. Elsevier Ltd., 2016.
[92] F. A. Mellon, “Mass Spectrometry: Principles and Instrumentation,” *Encyclopedia of Food Sciences and Nutrition*. pp. 3739–3749, 2003.
[93] M. Liu, Z. Yang, and G. Li, “A Novel Method for the Determination of Vancomycin in Serum by High-Performance Liquid Chromatography-Tandem Mass Spectrometry and Its Application in Patients with Diabetic Foot Infections,” *Molecules*, vol. 23, no. 2939, pp. 1–12, 2018.
[94] O. A. Mamer, *Medical Applications of Mass Spectrometry*, 3rd ed. Elsevier Ltd., 2016.
[95] S. Channasanon, P. Udomkusonsri, S. Chantaweroad, P. Tesavibul, and S. Tanodekaew, “Gentamicin Released from Porous Scaffolds Fabricated by Stereolithography,” *J. Healthc. Eng.*, vol. 2017, 2017.
[96] Hospira UK Ltd, “Gentamicin 40 mg/ml Injection - Summary of Product Characteristics (SmPC) - (eMC).” [Online]. Available: https://www.medicines.org.uk/emc/medicine/21665/SPC/Gentamicin+40+mg+ml+Injection/. [Accessed: 31-Jan-2019].
[97] I. Rehman and W. Bonfield, “Characterization of hydroxyapatite and carbonated apatite by photo acoustic FTIR spectroscopy,” *J. Mater. Sci. Mater. Med.*, vol. 8, no. 1, pp. 1–4, 1997.
[98] S. Teixeira *et al.*, “In vivo evaluation of highly macroporous ceramic scaffolds for bone tissue engineering,” *J. Biomed. Mater. Res. - Part A*, vol. 93, no. 2, pp. 567–575, 2010.
[99] S. C. Rodrigues, C. L. Salgado, A. Sahu, M. P. Garcia, M. H. Fernandes, and F. J. Monteiro, “Preparation and characterization of collagen-nanohydroxyapatite biocomposite scaffolds by cryogelation method for bone tissue engineering applications,” *J. Biomed. Mater. Res. - Part A*, vol. 101 A, no. 4, pp. 1080–1094, 2013.
[100] B. González, M. Colilla, and M. Vallet-Regí, “Time-delayed release of bioencapsulates: A novel controlled delivery concept for bone implant technologies,” *Chem. Mater.*, vol. 20, no. 15, pp. 4826–4834, 2008.
[101] J. Zhou, T. Fang, Y. Wang, and J. Dong, “The controlled release of vancomycin in gelatin/β-TCP composite scaffolds,” *J. Biomed. Mater. Res. - Part A*, vol. 100 A, no. 9, pp. 2295–2301, 2012.
[102] Q. Yao, P. Nooeaid, J. A. Roether, Y. Dong, Q. Zhang, and A. R. Boccaccini, “Bioglass®-based scaffolds incorporating polycaprolactone and chitosan coatings for controlled vancomycin delivery,” *Ceram. Int.*, vol. 39, no. 7, pp. 7517–7522, 2013.
[103] M. Zarif, A. Afidah, J. Abdullah, and A. Shariza, “Physicochemical characterization of vancomycin and its complexes with β-cyclodextrin,” *Biomed. Res.*, vol. 23, no. 4, pp. 513–520, 2012.
[104] J. M. Unagolla and A. C. Jayasuriya, “Drug transport mechanisms and in vitro release kinetics of vancomycin encapsulated chitosan-alginate polyelectrolyte microparticles as a controlled drug delivery system,” *Eur. J. Pharm. Sci.*, vol. 114, no. September 2017, pp. 199–209, 2018.
[105] C. Popa, M. Albu, A. Costescu, C. Luculescu, R. Trusca, and S. Antohe, “Structural Characterization and Optical Properties of Hydroxyapatite/Collagen Matrix,” *Rom. Reports Phys.*, vol. 68, no. 3, pp. 1149–1158, 2016.
[106] S. Koutsopoulos, “Synthesis and characterization of hydroxyapatite crystals: A review study on the analytical methods,” *J. Biomed. Mater. Res.*, vol. 62, no. 4, pp. 600–612, 2002.
[107] Z. Movasaghi, S. Rehman, and I. U. Rehman, “Raman spectroscopy of biological tissues,” *Appl. Spectrosc. Rev.*, vol. 42, no. 5, pp. 493–541, 2007.
[108] C. Assmann *et al.*, “Identification of vancomycin interaction with Enterococcus faecalis within 30 min of interaction time using Raman spectroscopy,” *Anal. Bioanal. Chem.*, vol. 407, no. 27, pp. 8343–8352, 2015.
[109] A. Dion, B. Berno, G. Hall, and M. J. Filiaggi, “The effect of processing on the structural characteristics of vancomycin-loaded amorphous calcium phosphate matrices,” *Biomaterials*, vol. 26, no. 21, pp. 4486–4494, 2005.
[110] G. Sakoulas, P. A. Moise-Broder, J. Schentag, A. Forrest, R. C. Moellering, and G. M.

Eliopoulos, “Relationship of MIC and Bactericidal Activity to Efficacy of Vancomycin for Treatment of Methicillin-Resistant Staphylococcus aureus Bacteremia,” *J. Clin. Microbiol.*, vol. 42, no. 6, pp. 2398–2402, 2004.

[111] C. J. Phillips, N. A. Wells, M. Martinello, S. Smith, R. J. Woodman, and D. L. Gordon, “Optimizing the detection of methicillin-resistant staphylococcus aureus with elevated vancomycin minimum inhibitory concentrations within the susceptible range,” *Infect. Drug Resist.*, vol. 9, pp. 87–92, 2016.

[112] M. J. Bogusz, H. Hassan, and M. Al Tufail, “Comparative determination of various vancomycin preparations with positive ionization electrospray LC-MS-MS,” vol. 71, no. 1, pp. 2–9, 2004.

[113] S. L. Parker, J. Lipman, and J. A. Roberts, “An LC – MS / MS method to determine vancomycin in plasma (total and unbound), urine and renal replacement therapy effluent,” *Bioanalysis*, vol. 9, no. 12, pp. 911–924, 2017.

[114] N. Shibata *et al.*, “Highly sensitive quantification of vancomycin in plasma samples using liquid chromatography – tandem mass spectrometry and oral bioavailability in rats,” *J. Chromatogr. B*, vol. 789, pp. 211–218, 2003.

[115] Infectious Disease and Antimicrobial Agents, “Staphylococcus aureus Tables.” [Online]. Available: http://www.antimicrobe.org/b237tabrev.htm. [Accessed: 04-Sep-2019].

[116] T. A. G. Van Vugt, J. Geurts, and J. J. Arts, “Clinical Application of Antimicrobial Bone Graft Substitute in Osteomyelitis Treatment: A Systematic Review of Different Bone Graft Substitutes Available in Clinical Treatment of Osteomyelitis,” *Biomed Res. Int.*, 2016.

[117] S. Sangeetha and A. R. Jain, “Current bone substitutes for implant dentistry,” *J. Prosthodont. Res.*, vol. 62, pp. 152–161, 2018.

[118] S. Bose and S. Tarafder, “Calcium phosphate ceramic systems in growth factor and drug delivery for bone tissue engineering: A review,” *Acta Biomater.*, vol. 8, no. 4, pp. 1401–1421, 2012.

[119] O. Baniukaitiene *et al.*, “Impact of cellulose/hydroxyapatite composites on liver cells and skeletal muscle,” *Cellul. Chem. Technol.*, vol. 52, no. 5–6, pp. 441–448, 2018.

[120] E. Díaz, M. B. Valle, and J. M. Barandiarán, “Magnetic composite scaffolds of polycaprolactone/nFeHA, for bone-tissue engineering,” *Int. J. Polym. Mater. Polym. Biomater.*, vol. 65, no. 12, pp. 593–600, 2016.

[121] T. Govender, S. Stolnik, M. C. Garnett, L. Illum, and S. S. Davis, “PLGA nanoparticles prepared by nanoprecipitation: Drug loading and release studies of a water soluble drug,” *J. Control. Release*, vol. 57, no. 2, pp. 171–185, 1999.

[122] Y. Zhang and M. Zhang, “Calcium phosphate/chitosan composite scaffolds for controlled in vitro antibiotic drug release,” *J. Biomed. Mater. Res.*, vol. 62, no. 3, pp. 378–386, 2002.

[123] M. Uchino *et al.*, “Elution Characteristics of Vancomycin, Gentamicin, and Vancomycin/Gentamicin Combination from Calcium Phosphate Cement,” *Adv. Orthop. Surg.*, vol. 2015, no. Vcm, pp. 1–5, 2015.

[124] X. Lian, H. Liu, X. Wang, S. Xu, F. Cui, and X. Bai, “Antibacterial and biocompatible properties of vancomycin-loaded nano-hydroxyapatite/collagen/poly (lactic acid) bone substitute,” *Prog. Nat. Sci. Mater. Int.*, vol. 23, no. 6, pp. 549–556, 2013.

[125] M. Cao, Y. Feng, Y. Zhang, W. Kang, K. Lian, and L. Ai, “Studies on the metabolism and degradation of vancomycin in simulated in vitro and aquatic environment by UHPLC-Triple-TOF-MS/MS,” *Sci. Rep.*, vol. 8, no. 15471, pp. 1–13, 2018.

[126] B. Y. Liu, G. M. Zhang, X. L. Li, and H. Chen, “Effect of Glutaraldehyde Fixation on Bacterial Cells Observed by Atomic Force Microscopy,” *Scanning*, vol. 34, no. 1, pp. 6–11, 2012.

[127] R. L. Perkins and A. S. Klainer, “Antibiotic-Induced Alterations in the Surface Morphology of Bacterial Cells: A Scanning-Beam Electron Microscope Study,” *J. Infect. Dis.*, vol. 122, no. 4, pp. 323–328, 1970.

[128] C. Spalding, E. Keen, D. J. Smith, A. M. Krachler, and S. Jabbari, “Mathematical modelling of the antibiotic-induced morphological transition of Pseudomonas aeruginosa,” *PLoS Comput. Biol.*, vol. 14, no. 2, pp. 1–28, 2018.

[129] W. Hachicha *et al.*, “In vitro efficacy of newly designed vancomycin-based microparticles,” *J. Cataract Refract. Surg.*, vol. 33, no. 4, pp. 702–708, 2007.

[130] T. P. T. Cushnie, N. H. O’Driscoll, and A. J. Lamb, “Morphological and ultrastructural changes in bacterial cells as an indicator of antibacterial mechanism of action,” *Cell. Mol. Life Sci.*, vol. 73, no. 23, pp. 4471–4492, 2016.

[131] Z. Wachol-Drewek, M. Pfeiffer, and E. Scholl, “Comparative investigation of drug delivery of

collagen implants saturated in antibiotic solutions and a sponge containing gentamicin," *Biomaterials*, vol. 17, no. 17, pp. 1733–1738, 1996.

[132] E. Bin Bae *et al.*, "Effect of Titanium Omplants Coated with Radiation- Crosslinked Collagen on Stability and Osseointegration in Rat Tibia," *Materials (Basel).*, vol. 11, no. 2520, pp. 1–17, 2018.

ANNEX

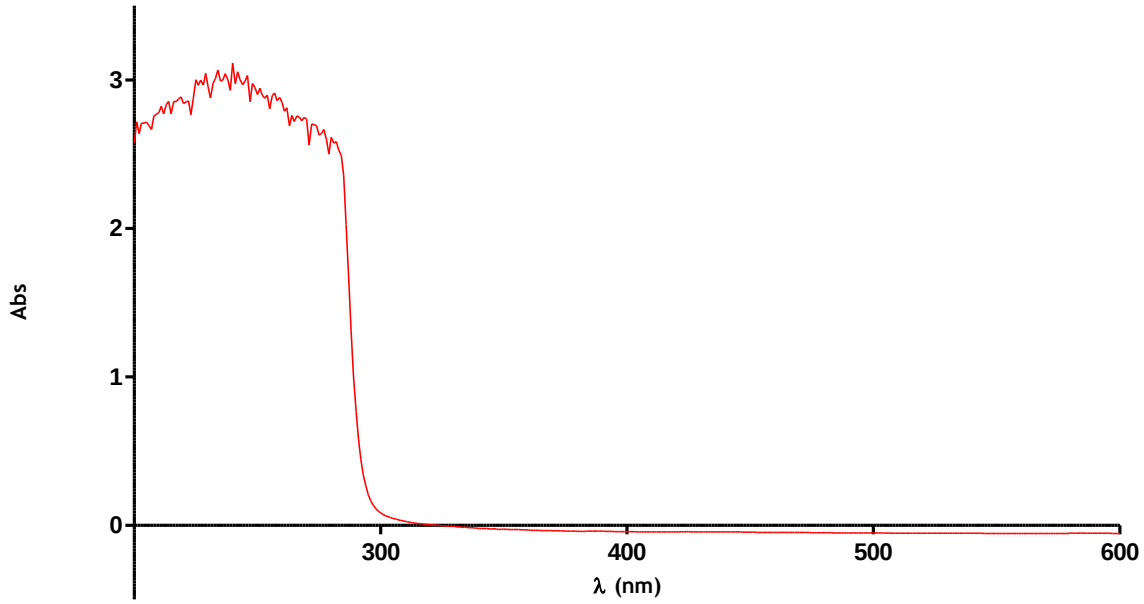

Figure A1 - Gentamicin spectrum, showing the absorbance as a function of wavelength.

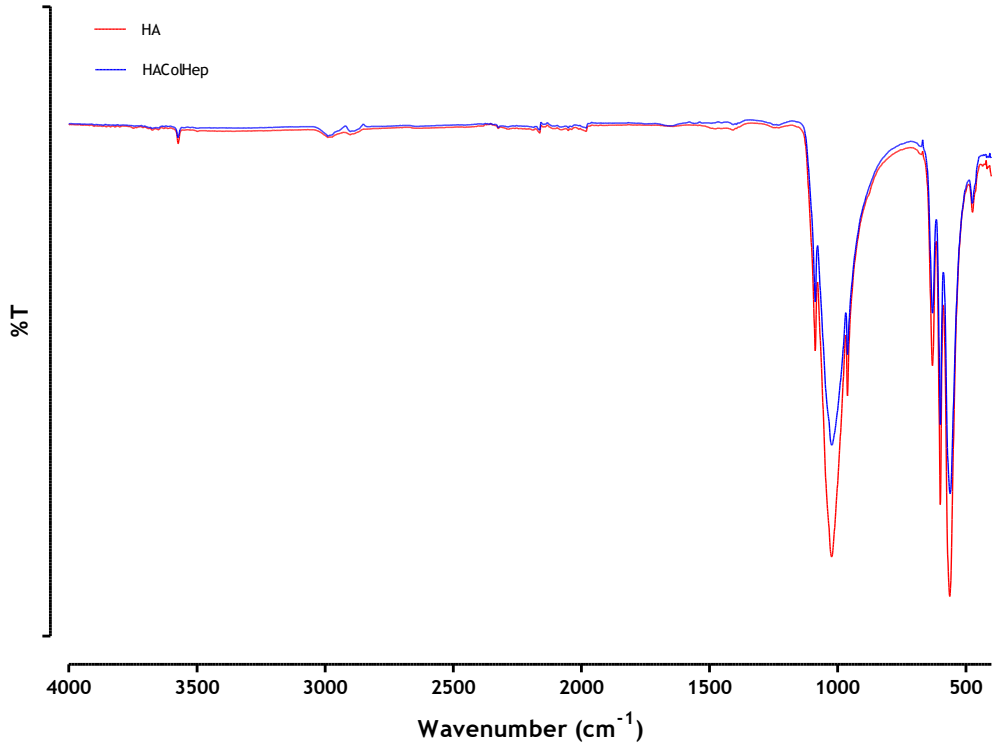

Figure A2 – ATR-FTIR spectra of HA and nanoHA/collagen (HAColHep). It is not possible to identify the characteristic peaks of collagen, but it is visible that in granules containing collagen, the intensity of the HA peaks is attenuated.

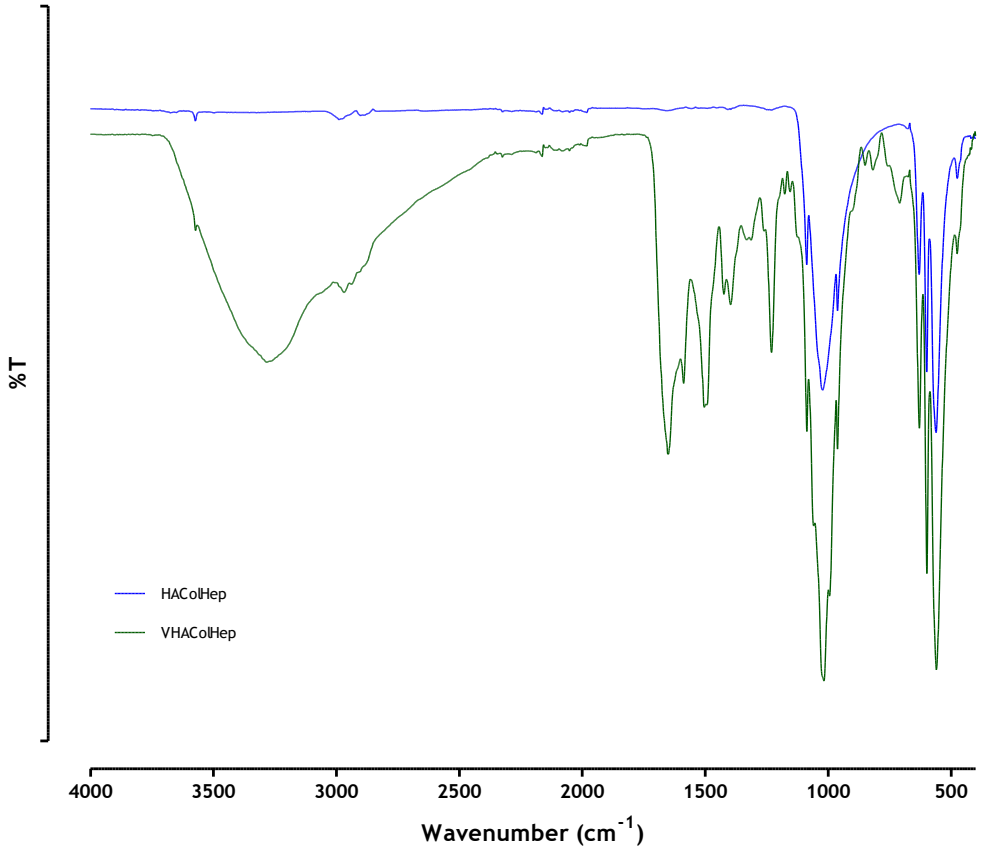

Figure A3 – ATR-FTIR spectra of nanoHA/collagen (HAColHep) and HAColHep with vancomycin lyophilized (VHAColHep).

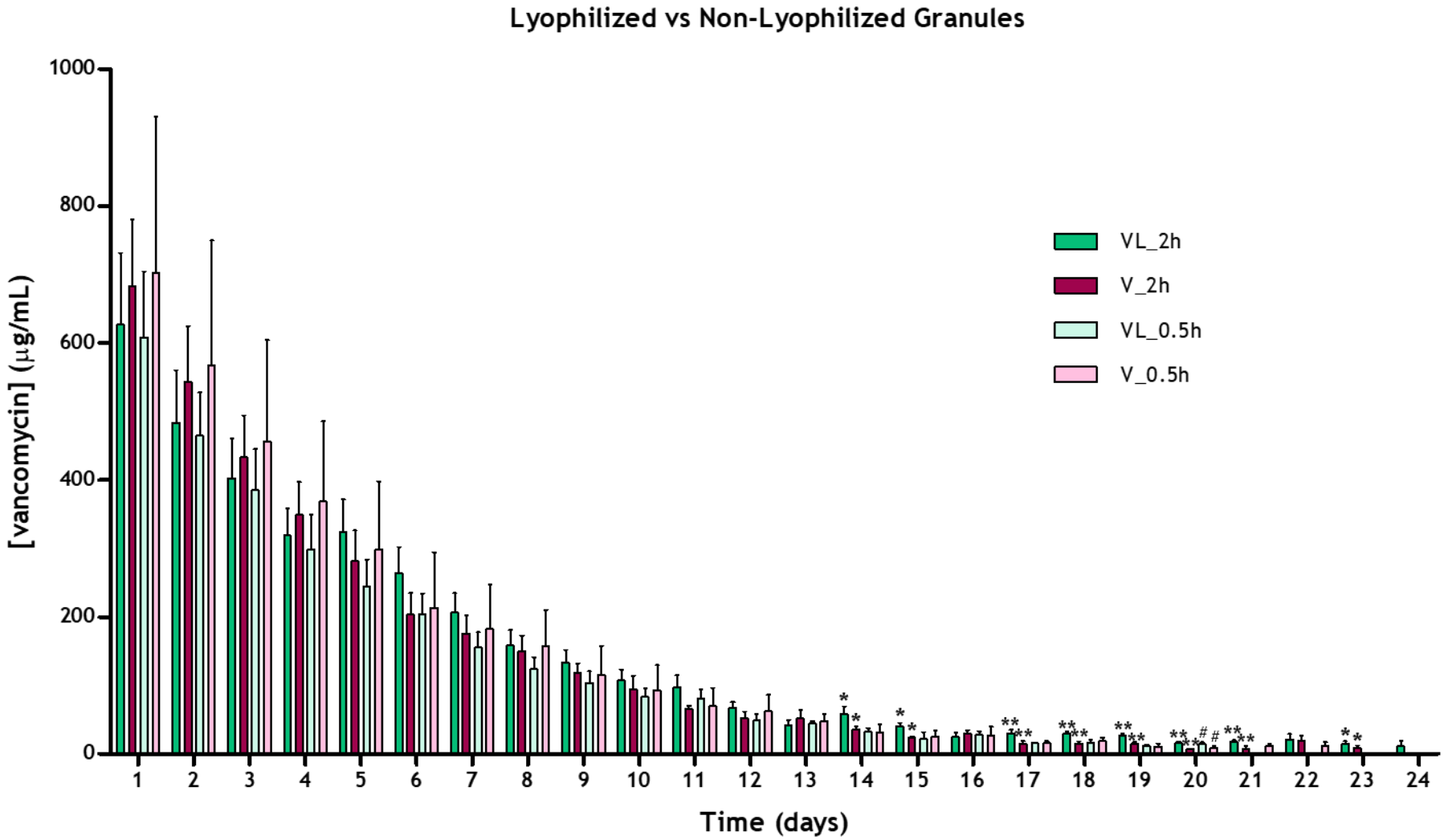

Figure A4 - Vancomycin release from nanoHA/collagen granules and from lyophilized nanoHA/collagen versus time, for comparison of adsorption times (2h and 0.5h). * Represents a statistically significant difference ($p<0.05$) compared lyophilized with non-lyophilized granules with 2 h antibiotic adsorption for the same time point. # Represents a statistically significant difference ($p<0.05$) compared lyophilized with non-lyophilized granules with 0.5 h adsorption for the same time point.

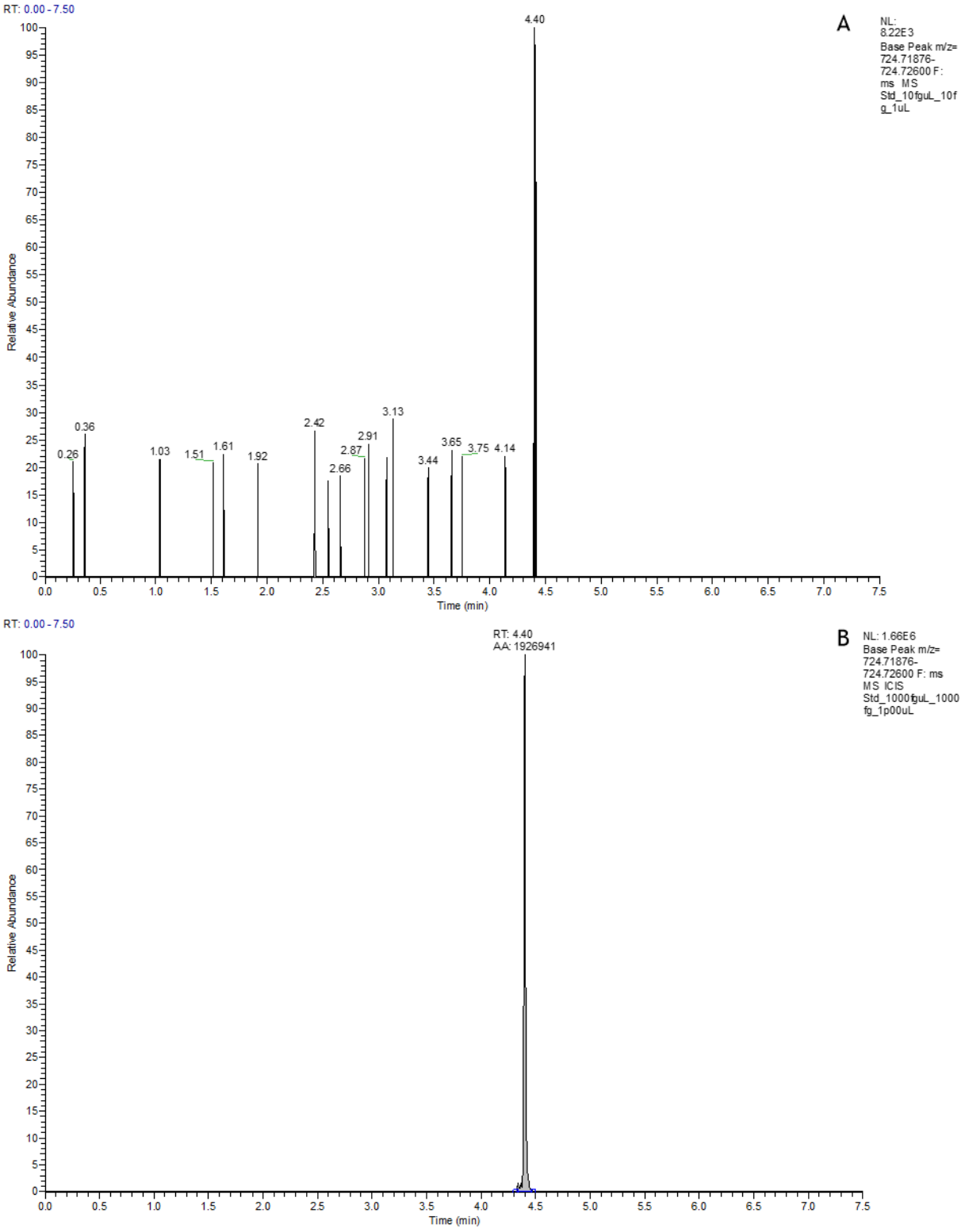

Figure A5 - Full scan LC-MS analysis of vancomycin, with different concentrations injected. A: concentration of 10 fg/µL, B: concentration of 1000 fg/µL.

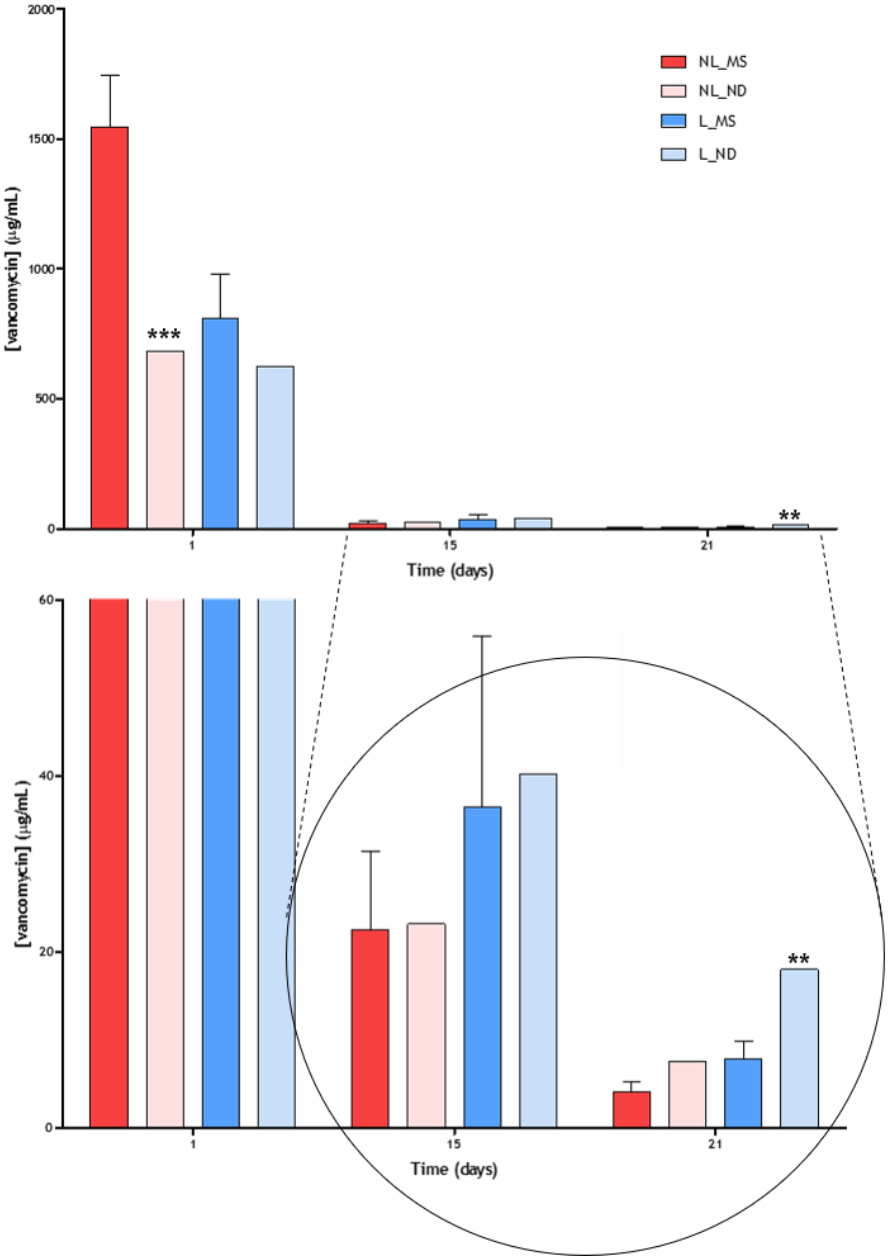

Figure A6 - A: Vancomycin quantification on days 1, 15 and 21, for nanoHA/collagen granules (NL) and nanoHA/collagen granules that were lyophilized (L) using nanodrop (ND) and Mass Spectrometry (MS); B: Magnification of the x-axis for displaying the values of days 15 and 21. ** Represents a statistically significant difference ($p<0.01$) compared lyophilization results read from nanoDrop with Mass Spectrometry for day 21. * Represents a statistically significant difference ($p<0.001$) compared lyophilization results read from nanoDrop with Mass Spectrometry for day 1.**

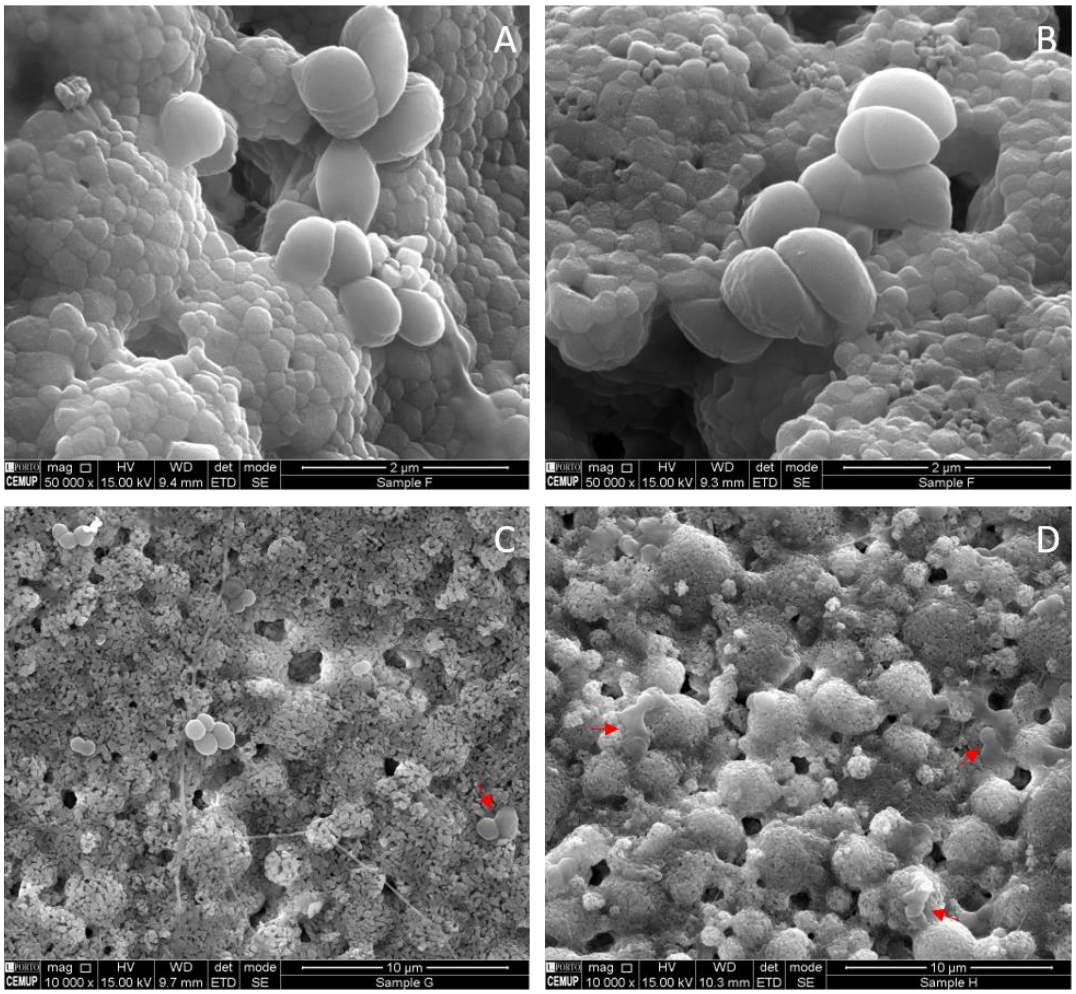

Figure A7 - SEM images of MRSA adhesion to granules, where it is possible to see that the bacteria cell wall seems to be destroyed. A and B: Granules without vancomycin adsorption; C: Granules with vancomycin adsorption; D: Granules with vancomycin adsorption and lyophilization.